

Review Article

Review of the Mechanistic and Structural Assessment of Binders in Electrodes for Lithium-Ion Batteries

Hyungsub Yoon,¹ Promoda Behera ,^{2,3} Sooman Lim,⁴ Tae Gwang Yun ,⁵ Byungil Hwang ,⁶ and Jun Young Cheong ²

¹Department of Intelligent Semiconductor Engineering, Chung-Ang University, Seoul 06974, Republic of Korea

²Bavarian Center for Battery Technology (BayBatt) and Department of Chemistry, University of Bayreuth, Universitätsstraße 30, 95447 Bayreuth, Germany

³Department of Design of Machine Elements & Mechanism (KST), Technical University of Liberec (TUL), Studentská 1402/2, Liberec 1 461 17, Czech Republic

⁴Department of Flexible and Printable Electronics, LANL-JBNU Engineering Institute-Korea, Jeonbuk National University, Jeonju 54896, Republic of Korea

⁵Department of Molecular Science and Technology, Ajou University, Suwon 16499, Republic of Korea

⁶School of Integrative Engineering, Chung-Ang University, Seoul 06974, Republic of Korea

Correspondence should be addressed to Tae Gwang Yun; ytk0402@ajou.ac.kr, Byungil Hwang; bihwang@cau.ac.kr, and Jun Young Cheong; jun.cheong@uni-bayreuth.de

Received 27 June 2023; Revised 19 January 2024; Accepted 27 February 2024; Published 20 April 2024

Academic Editor: Ahmad Azmin Mohamad

Copyright © 2024 Hyungsub Yoon et al. This is an open access article distributed under the Creative Commons Attribution License, which permits unrestricted use, distribution, and reproduction in any medium, provided the original work is properly cited.

With the continual increase in CO₂ levels and toward a sustainable society, developing high-performance lithium-ion batteries (LIBs) is crucial. A suitable electrode design is the key to enhancing the quality of battery cells (e.g., cycle retention characteristics and rate capabilities), and the binder plays an important role in providing sufficient adhesion between the active material, conductive agent, and current collector. Despite significant advances in the development of novel binder materials and solutions that can be employed as anode and cathode materials, careful investigations and summaries of the assessment methods for binder materials remain lacking. In this review, we examine the different analyses used to assess the quality of binder materials and how they help in assessing the quality of the electrode design. In addition, future perspectives on binder assessment are presented, which can be applied to future research directed toward binder development for advanced LIBs or post-LIBs.

1. Introduction

Lithium-ion batteries (LIBs) have dominated the market for consumer electronic power sources for decades because of their high energy density, high efficiency, light weight, and portability [1–3]. There are still significant efforts by academia and industry to enhance LIB performance to support the large-scale energy storage requirements in applications like all-electric vehicles, the military, and aerospace [4–6]. LIBs have become ubiquitous in the energy storage industry because they can be used to power handheld devices, automobiles, and power grids. The efficiency of LIBs is deter-

mined by the strength and consistency of the electrode components, including the active materials, conductive additives, and binders. The binder is one of these components, and preserving the mechanical stability and structural integrity of the electrode during repeated charge-discharge cycles is extremely important [7, 8].

Considering they significantly influence the overall battery performance, understanding the structural and mechanistic characteristics of binders in LIB electrodes has garnered considerable attention in recent years. The binder material, which acts as a glue to hold the active material and conductive additive, can affect the electrochemical

performance, cycling stability, and safety of batteries. LIB electrode creation has frequently utilized various binder substances, including sodium alginate, carboxymethyl cellulose, polyacrylic acid (PAA), and polyvinylidene fluoride (PVDF) [9–11]. However, choosing and optimizing a suitable binder material requires a thorough knowledge of its mechanical and structural characteristics.

Battery performance is significantly influenced by the binder materials used, especially when the battery operates at high cut-off voltages [12]. The stability of the electrode structures and the overall battery efficiency can be significantly influenced by the binder choice. If an incorrect binder is used under high-voltage conditions, the electrode materials may degrade, reducing their capacity and ability to store energy and ultimately shortening the lifespan of the battery [13]. A decrease in battery performance can result from the degradation of the binder, which can harm the electrodes and compromise their structural integrity, thus making it crucial to choose an appropriate binder material to ensure a stable electrode structure, reduce potential negative effects on battery performance, and ultimately increase the overall dependability and longevity of the battery [14].

Wang et al. [15] studied the adhesive properties of organic polyvinylidene fluoride (PVDF) binders and the electrochemical performance of CuO electrodes handled with various binders. Shi et al. [16] discussed the progress in novel binder systems in terms of material and structural design. Owing to their potent ability to bind to active particles, non-conductive polymers with abundant carboxylic groups have been used as binders to stabilize ultrahigh-capacity inorganic electrodes that undergo significant volume or structural changes during charging/discharging.

Recent research on binders has provided insight into how lithium alloying reactions improve the reversibility of composite electrodes. The cycling stability of the Si electrodes was significantly enhanced by a binder made of carboxymethyl cellulose (CMC). According to Hochgatterer et al., effective binding and improved performance are significantly aided by the covalent chemical bonds that form between the CMC and Si particles [17–20]. Moreover, various analytical techniques have been utilized to evaluate the properties and behavior of binders in LIB electrodes, such as nuclear magnetic resonance spectroscopy (NMR) [21–24], X-ray diffraction (XRD) [25–28], and scanning electron microscopy (SEM) [29–32]. Additionally, molecular dynamics simulations have been used to investigate the binding-ion interactions in LIB electrodes [33].

This review is aimed at presenting a thorough overview of the function of binders in improving the performance of LIBs, specifically in the context of electrode materials. This study explores the mechanical, compositional, and structural characteristics of the binders used in LIB electrodes. The increasing need for reliable LIBs—widely used in various applications, including portable electronics, electric vehicles, and renewable energy storage—is the main driving force for undertaking this review. Binders are essential to the performance of LIBs to maintain the integrity of the electrode structure, prevent electrolyte leakage, and ensure good adhesion between the active material and the current collector.

Hence, a deeper understanding of the mechanical, compositional, and structural aspects of binders in electrode materials is crucial to developing more effective and long-lasting LIBs. Hence, this article aims to present a thorough understanding of the role of binders in LIB performance, including their influence on mechanical and electrochemical stability, adhesion to active materials, resistance to electrolyte degradation, and overall battery durability. By providing a deeper understanding of the crucial role of binders in electrode performance, this study is aimed at contributing to the development of more effective and long-lasting LIBs.

2. Role of Binder in LIBs

Binders play a significant role in binding active materials, conductive agents, and current collectors together in an electrode. Particularly for LIBs, the presence of a binder is necessary for the wet-coating process; as a result, significant work has focused on resolving some of the production issues that arise from the use of binders [34]. In general, binders can be divided into two categories: 1-methyl-2-pyrrolidone- (NMP-) soluble and water-soluble. The former refers to the conventional binder system initially employed together with polyvinylidene difluoride (PVDF) [35–37], whereas the latter refers to recent research attempts to replace toxic, environmentally unfriendly, and high-cost NMP with green, environmentally friendly, and low-cost water. In some studies [38–40], water-soluble binders exhibited enhanced electrochemical performance compared to NMP-PVdF-based systems. Previous studies have demonstrated that water-soluble binders exhibit superior electrochemical performances compared to systems based on NMP-PVdF. Salian et al. [41] investigated the effect of water-soluble binders, CMC, and sodium alginate (SA) on the electrochemical performance of a high-voltage lithium nickel manganese oxide (LNMO) cathode and found that LNMO cathodes prepared with aqueous binders exhibited greater cycling stability. Li et al. [42] successfully synthesized a water-soluble bifunctional binder by combining a conductive polythiophene polymer (PED) with the highly adhesive PAA. This novel binder formulation demonstrated remarkable performance in Si-based anodes, exhibiting high reversible capacity, excellent cycle stability, and impressive high-rate capacity. Li et al. [43] conducted an experiment in which they established that using a water-soluble polyamide acid (WS-PAA) binder featuring ionic bonds yielded satisfactory mechanical strength for SiO_x anodes, which, in turn, leads to enhanced cycling performance and rate capability. Zheng et al. [44] synthesized a water-soluble PAAS-CDP-PAA binder with enhanced adhesion, Li⁺ diffusion, and structural integrity, resulting in increased specific capacity and capacity retention for Si electrodes. Jang et al. [45] investigated whether water-soluble lambda carrageenan (CGN) could be used as a binder for SiNPs. They discovered that CGN binders exhibited excellent mechanical characteristics and improved the cycling and rate performances of the silicon anodes. The electrochemical performance and stability of a silicon (Si) anode were significantly enhanced by utilizing a water-soluble conductive binder, specifically a polyvinyl pyrrolidone/polyaniline (PVP/PANI)

copolymer, as demonstrated in a study conducted by Zheng et al. [46]. This improvement was observed in comparison to conventional binders such as polyvinylidene fluoride (PVDF). A separate investigation conducted by Yang et al. [47] examined a hybrid water-soluble binder composed of humic substances and CMC. This study revealed that this binder exhibited the ability to improve the electrochemical performance and cycling stability of cathode materials for LIBs, specifically LiFePO_4 . To improve the electrochemical stability of Sb_2O_3 anodes, Liu et al. [48] developed a cross-linked polymeric binder via an esterification reaction between sodium CMC and fumaric acid (FA). Li et al. [49] studied $\text{ZnMn}_2\text{O}_4/\text{C}$ microsphere anodes using a water-soluble sodium carboxymethyl cellulose binder. The results of their investigation demonstrated notable characteristics, such as a high reversible capacity and extended cycle life.

Figure 1(a) shows the chemical structure of the PVDF binder. PVDF, a synthetic and organic-soluble binder, is widely used in the LIB industry owing to its good binding ability and chemical and electrochemical stability [50–53]. NMP is generally used as an organic solvent to dissolve PVDF binders. In combination with the search for new polymers that can be employed as water-soluble binders, more analytical/evaluation tools have been developed to further understand the role of binders in the electrode, even after the charge-discharge process. The following sections provide detailed information on different aspects of the binder in electrodes and the importance of defining the role of the binder in the electrode.

To address the issue of using toxic and volatile solvents and replacing PVDF with weak van der Waals, aqueous-based binders have been investigated because water-soluble binders are more cost-effective and harmless than PVDF binders. Furthermore, LIBs using water-soluble binders exhibit outstanding performance compared to batteries with PVDF because most water-soluble binders have functional groups such as hydroxyl groups (OH) and carboxylic acid groups (COOH), which can connect the components via hydrogen and chemical bonding [54–56]. There are various types of water-soluble binders, including CMC [57], PAA [57], chitosan [58], and alginate [58], among others [53, 59–62]. CMC is a water-soluble and biodegradable binder from cellulose. As CMC is a natural binder, it is more biodegradable and cost-effective than PVDF. Moreover, CMC is considered an alternative candidate for PVDF binders because of its solubility in water. In general, CMC is used in the sodium salt form [63–65]. Figure 1(b) shows the chemical structure of CMC, which contains carboxymethyl and hydroxyl groups. As such, CMC has good mechanical and adhesive properties, leading to strong interactions with the active material and current collector [51].

PAA is a widely used synthetic binder with many carboxylic acid groups on its backbone, as shown in Figure 1(c). Compared to the PVDF system, the high density of carboxylic acid groups in the PAA backbone indicates the possibility of strong interactions between the active materials and the current collector. In addition to PVDF, CMC, and PAA, other types of water-soluble binders exist, such as chitosan-based binders [33] (Figure 1(d)) and alginate-based binders

[33] (Figure 1(e)), among others [32, 50–54], which also have attractive options for enhancing the mechanical properties of electrodes in LIB.

When assessing the suitability of binders, particularly alternative polymers such as alginate and chitosan, for battery applications, functional groups must be carefully considered. The functional groups of these polymers determine whether they are compatible with the materials used for the electrodes, electrolyte, and overall electrochemical performance of the battery. The following analysis provides an overview of the functional groups found in alginate and chitosan and their significance in battery applications. Alginate, a polysaccharide obtained from brown algae, is biocompatible and can undergo gelation. Incorporating carboxylic acid functional groups into batteries has been reported to positively affect multiple aspects of battery performance, such as ion conductivity, adhesion, and compatibility with electrolytes. The carboxylic acid groups present in alginate facilitate strong interactions with active materials, current collectors, and electrolyte components. This results in improved structural integrity and reduced formation of passivation layers [66–68]. Chitosan, a biopolymer made from chitin, has shown promise in the field of battery technology. The amino groups of the material improve the ionic interaction, adhesive strength, and flexibility, which enhances lithium-ion mobility and protects the integrity of the electrode while reducing the rate at which the electrolyte degrades. As a result, these advancements have aided in improving the overall battery stability [69–71]. In Table 1, we summarized the key parameters of LIBs employing water-based and nonwater-based binders during electrode fabrication.

3. Assessment of Binder in Electrode

3.1. Structural/Morphological Assessment. The structural or morphological evaluation of various binders in electrodes for LIBs is an essential consideration that must be considered when developing high-performance batteries. Anodes, cathodes, electrolytes, and binders are the various components that have entered the construction of LIBs. The binder, an essential component, is responsible for enhancing the adhesion of the electrode materials to the current collector and for holding the mixture together. During the charging and discharging cycles, the binder helps maintain the structural integrity of the electrode.

By holding the active components and conductive additives together, upholding their structural integrity, and enhancing the mechanical strength of the electrodes, binders play a significant role in the production of electrodes. The performance of LIBs, including their capacity, cycling stability, and rate capability, can be significantly affected by the choice of the binder, thus making it crucial to assess the structural and morphological traits of various binders and their impact on electrode properties.

Kim et al. [97] synthesized highly interconnected Si nanoparticles using extremely thin cellulose nanofibers as a carbon source to enhance the cycling and rate performance of Si anodes in LIBs. After 500 cycles at a high current

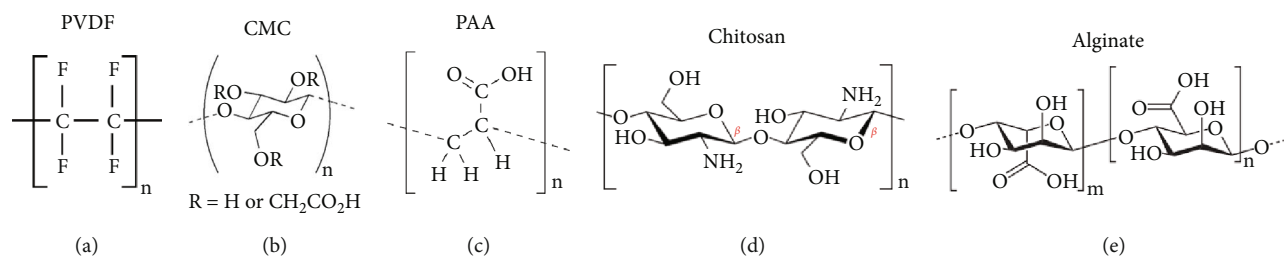


FIGURE 1: Chemical structure of (a) PVDF, (b) CMC, (c) PAA, (d) chitosan, and (e) alginate.

TABLE 1: Concise tabular representation comparing key parameters of LIBs employing water-based and nonwater-based binders during electrode fabrication.

Parameter	Water-based binder	Nonwater-based binder
Binder type	Water-based binder [72–75]	Nonwater-based binder [76, 77]
Advantages	(i) Environmentally friendly [78] (ii) Better compatibility with some electrode materials [80]	(i) Enhanced mechanical strength [79] (ii) Improved electrochemical performance [81] (iii) Wide range of material compatibility [82]
Disadvantages	(i) Lower mechanical strength compared to nonwater-based binders [83] (ii) Limited compatibility with some electrode materials [80]	(i) Potential solvent compatibility issues [84] (ii) Higher cost [83] (iii) Potential environmental concerns [77]
Mechanical properties	Moderate mechanical strength [85]	Improved mechanical stability [79]
Electrochemical	(i) Slightly lower capacity [86]	(i) Potential for higher capacity [87]
Performance	(i) Good cycle life [88] (ii) Moderate rate capability [89]	(i) Improved cycle life [88] (ii) Enhanced rate capability [90]
Compatibility	Works well with specific electrode materials and electrolytes [91]	Versatile compatibility with various electrode materials and electrolytes [92]
Cost	Generally lower cost [93]	Generally higher cost [94]
Environmental impact	Generally lower environmental impact [95]	Potential environmental impact related to solvent use [96]

density of 2 Ag⁻¹, the material produced exhibited a reversible capacity of 808 mAhg⁻¹ with a coulombic efficiency of 99.8% and a high reversible discharge capacity of 464 mAhg⁻¹ even at a high current density of 8 Ag⁻¹. As a promising material for LIB applications, the highly interconnected carbon network prevents the formation of brittle electrodes with water-based binders. They postulated that ultrathin cellulose nanofibers serve as a binder to connect the silicon nanoparticles. Binders, such as those made of silicon nanoparticles, are only useful if they interact with the host material [98, 99].

The direct analysis of CMC and styrene-butadiene rubber (SBR), two binders that play crucial roles in graphite electrodes for Li-ion batteries, remains challenging, especially at very low concentrations, such as those found in actual graphite anodes. The behaviors of CMC and SBR binders and their distributions in graphite electrodes were examined by Chang et al. [100] using various analytical techniques. They discovered that the amount of crosslinking in the binder-graphite networks, influenced by the surface characteristics of the graphite and CMC materials, determines how much CMC migrates toward the surface during the drying process. This study also showed that the SBR

and CMC have different vertical distributions. Binder migration in the electrode films is common.

Further analysis of the cross-section is required to understand how this occurs and how the gradient between the potential extrema changes. We examined thicker cross-sections of approximately 400 nm because the standard thickness of an electrode film is relatively thin compared with the graphite particle size. Figure 2 displays the findings for samples A400-94-C (high drying rate) and A400-73-C (low drying rate). The copper foil was removed before ion milling to prevent the cross-section from being coated with copper. For thicker samples, the size of the energy-dispersive X-ray spectroscopy (EDS) maps increases [101].

SEM and EDS evaluations, as depicted in Figure 3, provide insights into the distribution and interaction of materials in various anodes. In the Si/HBPEI anode, the Si nanoparticles and HBPEI were unevenly dispersed, leading to regions where these elements did not overlap well, as shown by EDX mapping, indicating a tendency for HBPEI, with its low viscosity, to self-aggregate, thus failing to completely cover the Si nanoparticles. In contrast, the anodes with the Alg or Alg-Ca binders showed no significant

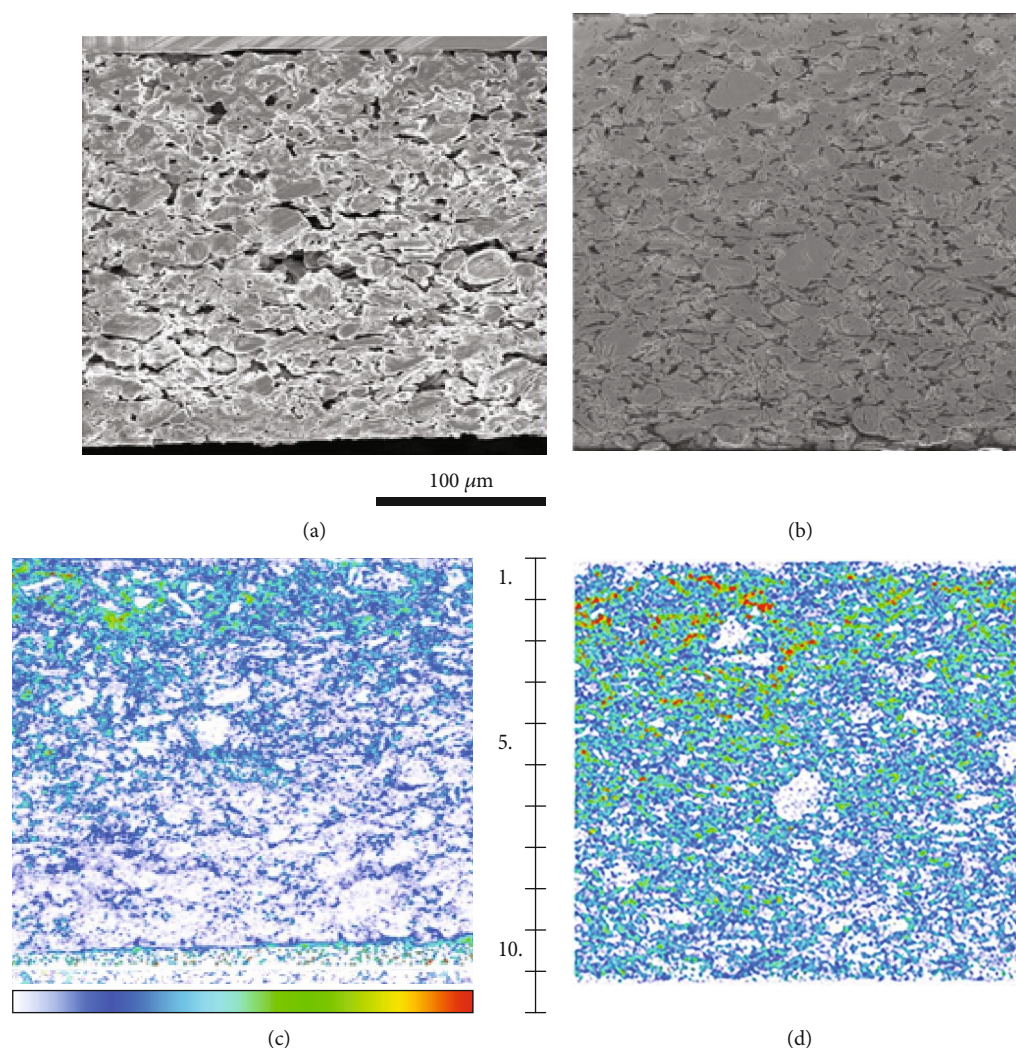


FIGURE 2: (a–d) Cross-sectional SEM images and F-concentration maps of HDR and LDR samples (A400-94-C and A400-73-C) [101].

aggregation of Si or Alg, and the distributions of Si and Na were more congruent. However, some regions were predominantly Na, indicating only rough coverage of Si nanoparticles by Alg. The Si/Alg-HBPEI anode exhibited a network structure, with the distributions of Si, Na, and N mainly overlapping, suggesting that free HBPEI chains diffused and gathered in the Alg-rich regions owing to strong electrostatic attraction and hydrogen bonding. A more uniform and denser 3D network structure was observed for the Si/Alg-Ca-HBPEI anode, where the addition of Ca^{2+} led to rapid ionic crosslinking with Alg, forming a network that restricted the migration of HBPEI, thus resulting in a more homogeneous distribution of N, Na, and Ca, with HBPEI anchored more evenly on the Alg-Ca frame owing to the interaction of its amino-rich hyperbranched chains with the nearby Alg chains [102].

The SEM and EDS evaluations (Figure 4) revealed significant insights into the distribution and interaction of the components in the different anode samples. In the Si/HBPEI anode, the Si nanoparticles and HBPEI were unevenly dispersed, and the elements Si and N from HBPEI did not over-

lap well, indicating that the low-viscosity HBPEI tended to self-aggregate and failed to completely cover the Si nanoparticles. Conversely, in the Si/CMC anode, no significant aggregation of Si or CMC was observed. While the distributions of Si and O largely overlapped, there were areas containing only O, suggesting that CMC could only roughly cover the Si nanoparticles. The most notable observation was made for the Si/CMC-HBPEI sample: the FE-SEM image showed a uniform and dense 3D network structure. This anode exhibited a more even distribution of Si, O, and N than the other samples, indicating effective interactions such as hydrogen bonds, ion bonds, and covalent bonds between CMC and HBPEI, which improved their compatibility and coverage with the Si nanoparticles. In this matrix, the Si nanoparticles were well dispersed and effectively covered with HBPEI [103].

Hu et al. [104] studied the surface morphologies of Si@CGG and Si@SA electrodes using scanning electron microscopy (SEM) before and after 200 cycles (Figure 5). While both electrodes had smooth surfaces before cycling, the SEM images revealed that the Si@SA electrode developed

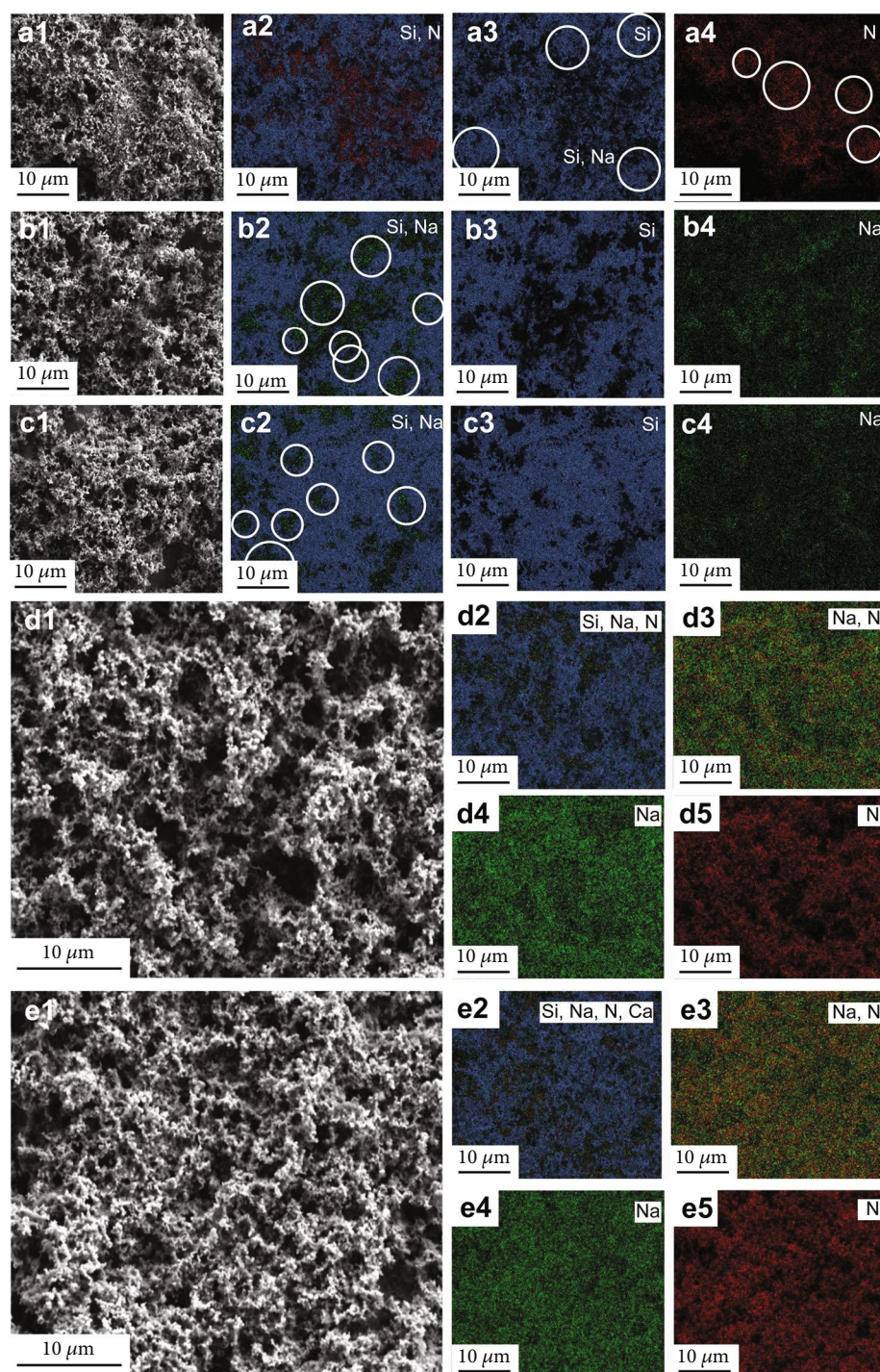


FIGURE 3: FESEM and EDX mapping images of (a1–a4) Si/HBPEI, (b1–b4) Si/Alg, (c1–c4) Si/Alg-Ca, (d1–d5) Si/HBPEI, and (e1–e5) Si/Alg-Ca-HBPEI anodes [102].

significant cracks, as opposed to the Si@CGG electrode, which had microcracks and integrated surface morphology. The stress caused by the volume expansion of Si materials during charge-discharge cycling is attributed to cracks. According to the study, the CGG binder outperformed the SA binder in maintaining mechanical integrity and accommodating changes in the Si electrode volume.

To improve battery performance, Wang et al. [105] discuss how crucial the importance of creating advanced lithium batteries and comprehending the basic mechanisms of electrode deterioration. Atomic force microscopy (AFM), a perfect tool for providing localized morphological, chemical, and physical information at the nanoscale, has been used among other advanced material characterization techniques.

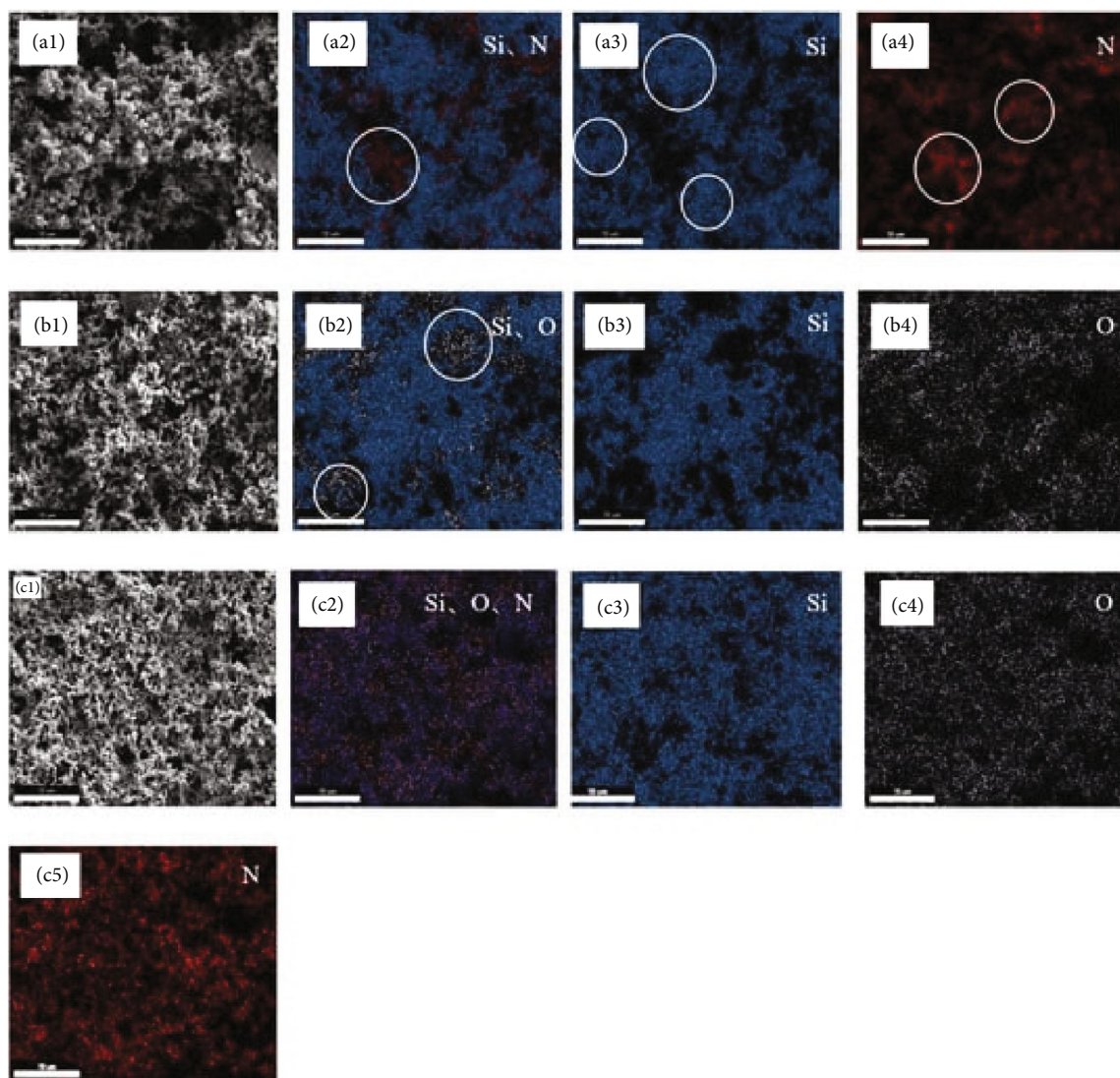


FIGURE 4: FESEM and element mapping images of Si/HBPEI (a1–a4), Si/CMC (b1–b4), and Si/CMC-HBPEI (c1–c5) anodes [103].

Atomic force microscopy was used to analyze graphite, silicon, layered metal oxides, and other representative electrode materials. We also reviewed the recent developments in the development and application of AFM in high-performance LIBs. Along with the remaining difficulties and potential solutions for future growth, the significance of AFM in studying the Li-S and Li-O₂ systems of the next generation is also emphasized. They examined the use of AFM to understand the components of LIBs and other types of LIBs. Several modes of atomic force microscopy (AFM) have been used to ascertain the morphology and the mechanical and electrical properties of electrodes, including a variety of anodes and cathodes. They can also monitor the evolution of real-time interfaces. This new understanding can be applied to failure, ion transport, and electrode material phase transformations.

In addition, they help optimize the electrolyte, guide the structural modification of electrode materials, discuss the importance of creating advanced lithium batteries, and

understand the mechanisms of electrode deterioration to improve battery performance. Atomic force microscopy (AFM) is a valuable tool for studying electrode materials, and recent developments in AFM have been reviewed for their use in LIBs. This article emphasizes the significance of AFM in learning about the next generation of Li-S and Li-O₂ batteries. AFM can be used to examine the morphology and properties of electrodes and monitor the real-time interface evolution. This understanding can be applied to failure, ion transport, electrode material phase transformation, electrolyte optimization, and guiding the structural modification of electrode materials [105].

According to Oishi et al. [106], Figure 6 presents scanning transmission electron microscopy (STEM) images and EDS elemental mappings of LiNi_{0.5}Mn_{1.5}O₄ (LNMO) electrodes after 50 cycles using different binders, including sulfated alginate (SO₃-ALG). The STEM images show that the lattice fringes on the surface of the LNMO particles are less distinct than those in the bulk, indicating structural

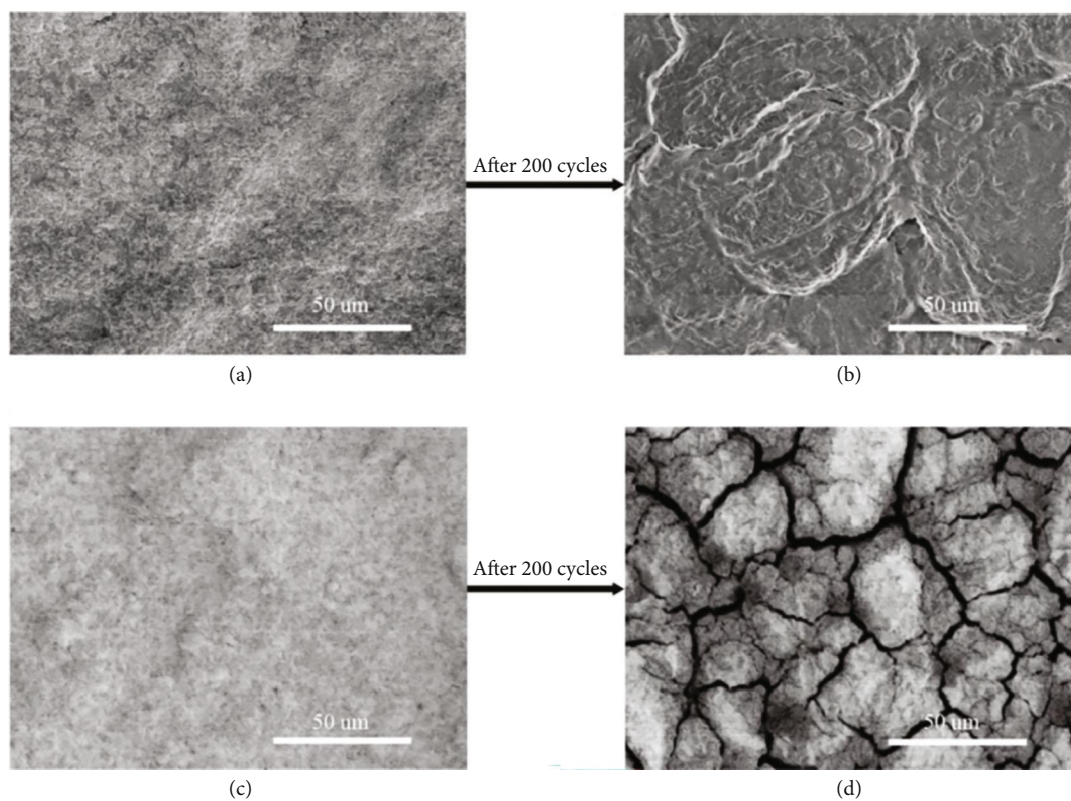


FIGURE 5: SEM images of Si electrodes treated with CGG (a, b) and SA (c, d) before (left) and after 200 cycles [104].

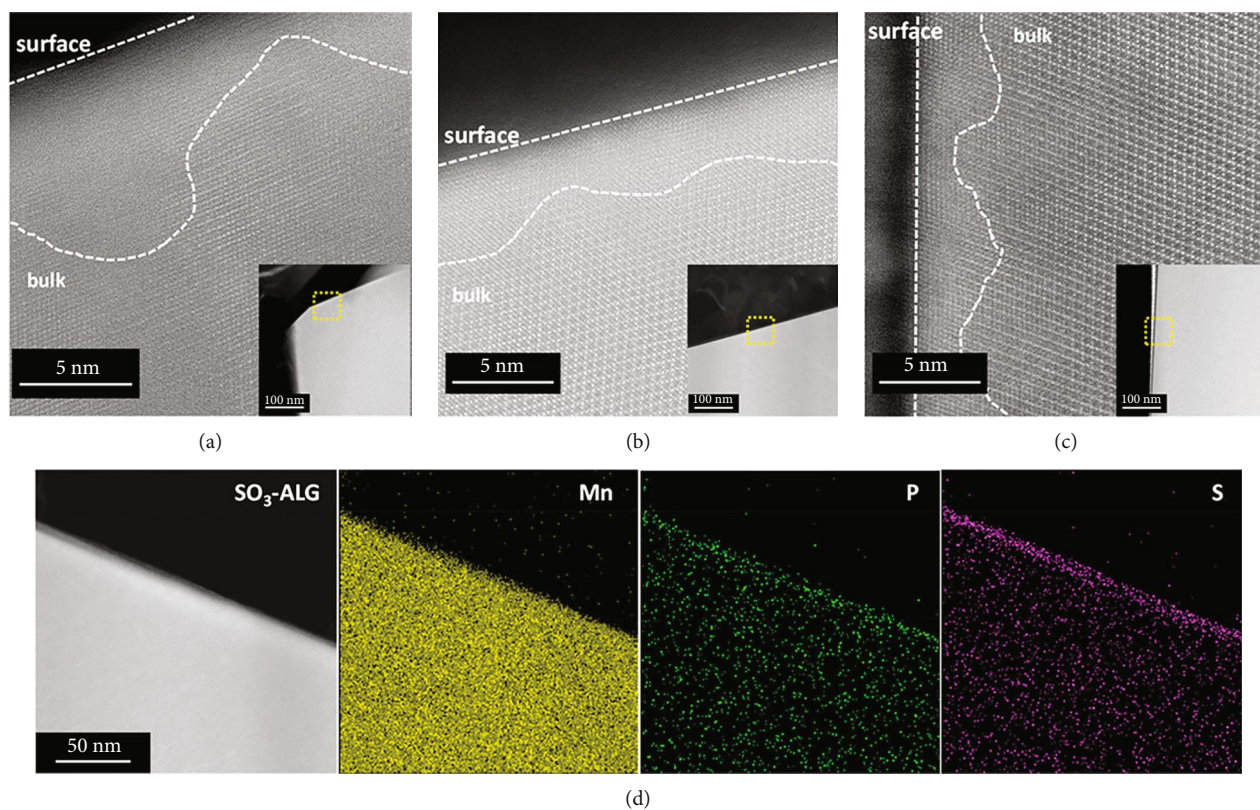


FIGURE 6: LNMO particles in 50-fold cycled electrodes with (a) PVdF, (b) ALG, and (c) SO₃-ALG are shown in FIB-STEM images. (d) EDS mappings for Mn, P, and S of the SO₃-ALG electrode after 50 cycles [106].

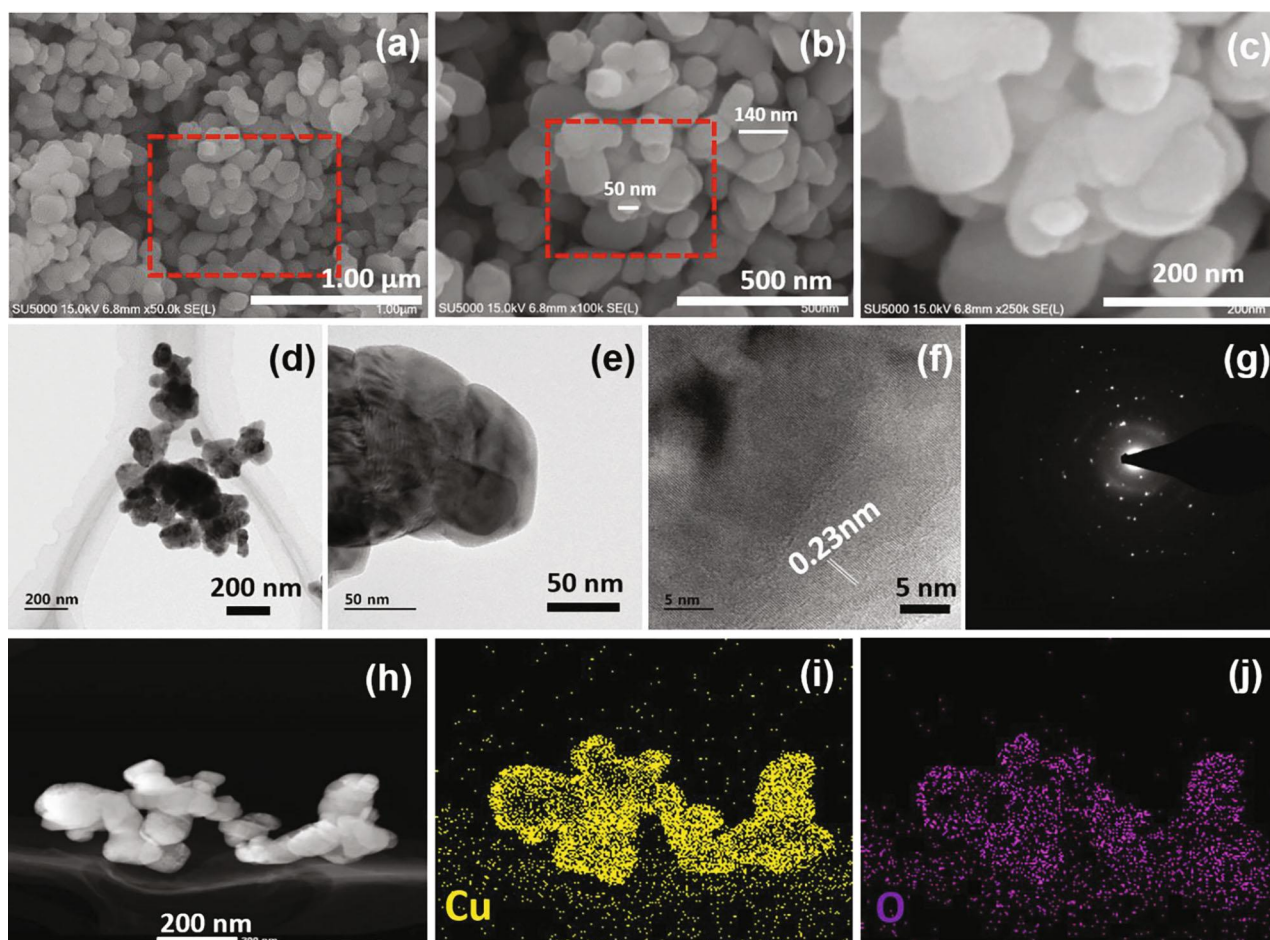


FIGURE 7: (a–c) Field-emission scanning electron microscope (FE-SEM) images of r-CuO at different magnifications, (d, e) TEM images at two magnifications, (f) HR-TEM image, (g) SAED pattern, (h) HAADF image, and (i, j) EDS elemental mapping [107].

degradation at the electrode/electrolyte interface, attributed to the reaction of the electrolyte's LiPF_6 component with water, leading to the leaching of Mn^{2+} and Ni^{2+} from LNMO, causing surface degradation. The thickness of the degraded area exceeded 10 nm for the poly(vinylidene fluoride) (PVDF) electrode. However, it was approximately 5 nm for the ALG and SO_3 -ALG electrodes, suggesting that the alginate binders better preserved the electrode structure near the surface. In particular, the SO_3 -ALG electrode, which shows the best cycling performance, is uniformly coated with a sulfur-containing layer approximately 10 nm thick, indicating adequate coverage of the LNMO particles by the SO_3 -ALG binder, which acts as a protective layer [106].

Akshay et al. [107] included Figure 7, which illustrates the TEM analysis. The TEM images at different magnifications (Figures 7(d) and 7(e)) confirm the size and morphology of the r-CuO particles. High-resolution TEM (HR-TEM) images distinctly display lattice fringes with a spacing of 0.23 nm, correlating to the (111) plane of r-CuO (Figure 7(f)). The selected area electron diffraction (SAED) pattern indicated the polycrystalline nature of the r-CuO particles (Figure 7(g)), and the STEM image, along with EDS mapping (Figures 7(h)–7(j)), illustrated the elemental distribution within the r-CuO particles. This comprehensive

TEM analysis is critical for understanding the microstructural characteristics of r-CuO particles—vital for developing efficient Li-ion capacitors [107].

3.2. Mechanical Assessment. The outstanding mechanical properties of the electrodes for LIBs are an essential factor in maintaining the performance of the battery without rapid capacity loss during the charge/discharge procedure owing to the repeated intercalation and deintercalation of lithium ions, which causes volume expansion, cracks, and pulverization [16, 52, 53, 59, 108–110]. Furthermore, in the manufacturing process, external stress is applied to the electrode, resulting in delamination of the main components from the current collector. Therefore, the binder is a key candidate for achieving excellent electrode mechanical properties because the fundamental role of the binder is to tightly adhere to the active material, conductive additive, and current collector [56, 111–114]. Therefore, in this section, owing to the importance of the electrode's integrity, we focus on the effect of binders on the mechanical properties of the electrode and the correlation between the mechanical properties and the electrochemical performance stability of LIBs and review various strategies to enhance the integrity. First, we introduce an analytical method for

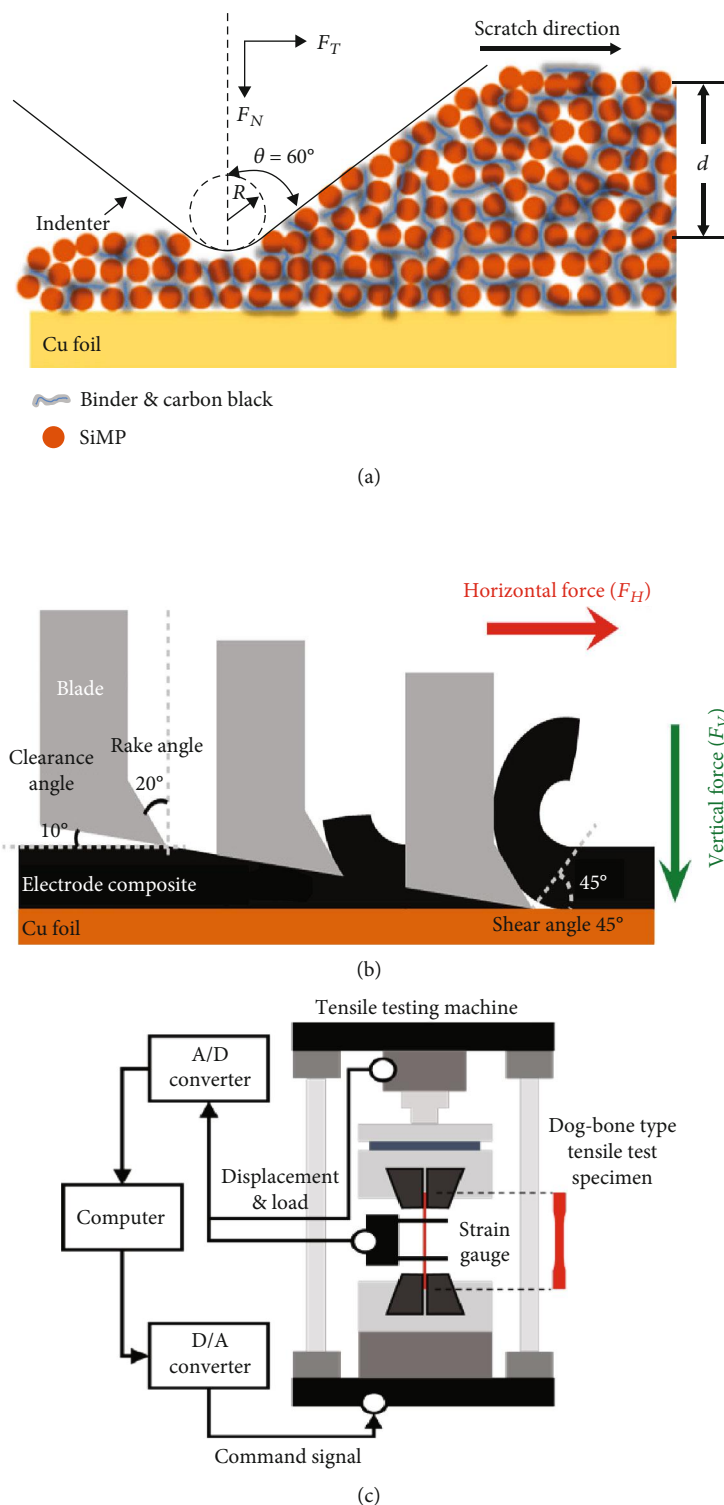
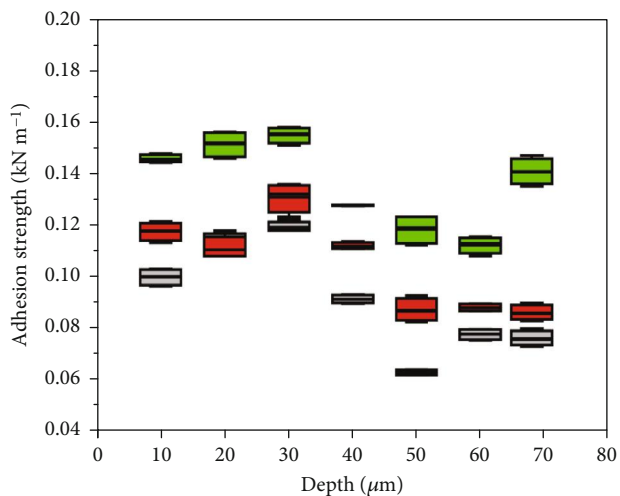


FIGURE 8: Schematic of the tests for the adhesive property of the electrodes: (a) scratch test [138], (b) SAICAS method [123], and (c) tensile test [139].

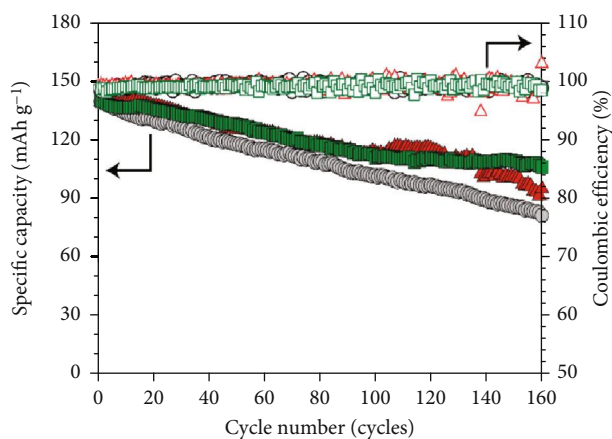
investigating the mechanical strength of the electrode. The evaluation methods for a binder system include the peeling-off test [114–117], scratch test [118–121], surface and interfacial cutting analysis system (SAICAS) [122–124], and tensile test [125–128]. The peeling-off test has been widely used to analyze the adhesion strength between the electrode material

and current collector because this method is simple and convenient. After attaching the adhesive tape to the fabricated electrode, the adhesion strength is the force required to peel off the tape from the electrode at a constant rate and angle. In the widely used scratch test, the tip or indenter scratches the surface of the electrode, and the load



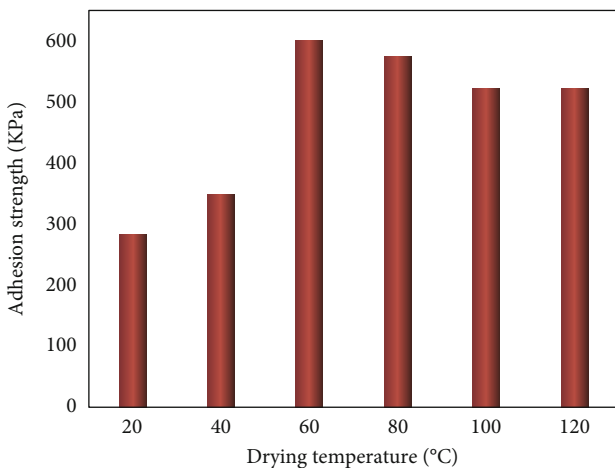
■ PVdF 500 k
■ PVdF 630 k
■ PVdF 1000 k

(a)

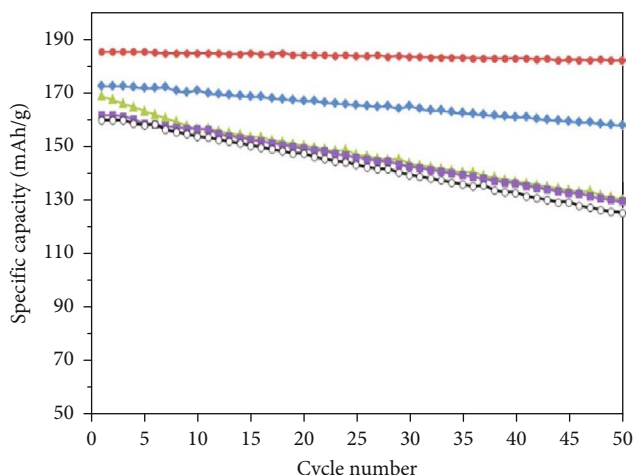


● PVdF 500 k
▲ PVdF 630 k
■ PVdF 1000 k

(b)



(c)



◆ 40 °C
● 60 °C
▲ 80 °C
■ 100 °C
○ 120 °C

(d)

FIGURE 9: Continued.

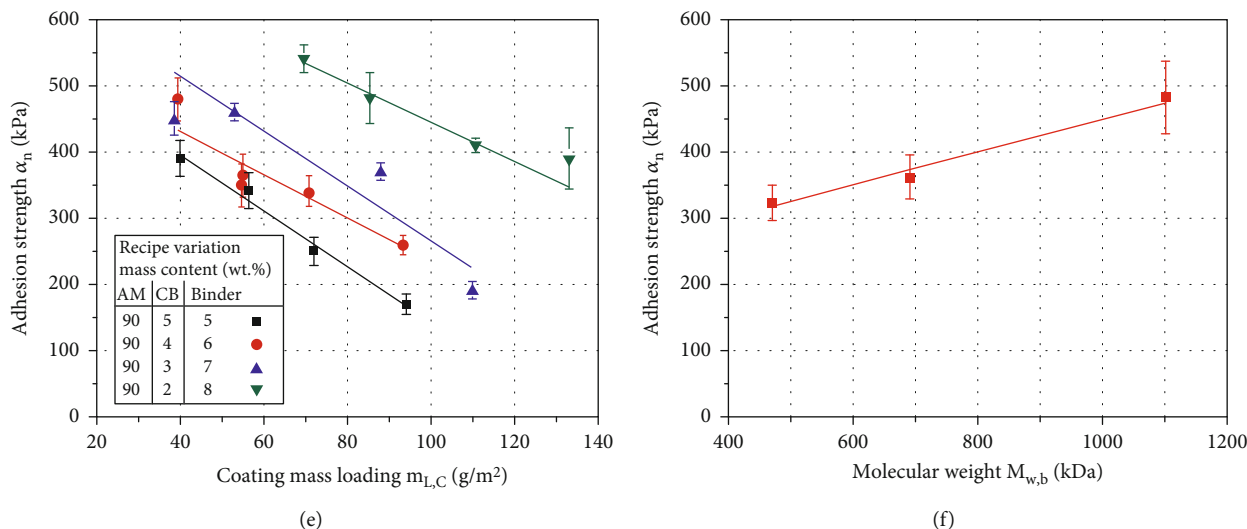


FIGURE 9: (a) Adhesion strength of LiCoO₂-based electrodes, according to the molecular weight of PVDF, and (b) cycling performance, depending on the molecular weight of PVDF [122]; (c) adhesion strength of LiNi_{0.8}Co_{0.15}Al_{0.05}O₂-based electrodes, as a function of preparation temperatures, and (d) cycle stability of the electrodes with various drying temperature [151], and the adhesion strength of the electrodes, according to the PVDF with different (e) contents and (f) molecular weight [154].

applied to the indenter increases gradually until the electrode material is delaminated from the current collector (Figure 8(a)). In addition to the two commonly used methods for studying the adhesive strength of binders, a new technique called SAICAS was used to analyze the adhesion force of electrodes. As shown in Figure 8(b), the adhesion force of the electrodes was simultaneously investigated in the horizontal and vertical directions using a V-shaped microblade [123]. There were two modes of action: cutting and peeling. The depth of the interface between the electrode materials and the current collector can be determined through the cutting mode, and the adhesion force at the interface can be measured through the peeling mode. Therefore, the adhesion force between interfaces can be measured more accurately than in the conventional peeling-off test. Furthermore, the adhesion properties at a specific depth could be evaluated because the blade position could be adjusted. Therefore, SAICAS is a more accurate analysis method for the battery industry. In addition to the adhesion property of the electrode, a flexible and stretchable binder has been researched to deal with repeated volume variations of active materials during the charge-discharge process [129–131]. Moreover, with the advent of wearable devices, LIBs must maintain their integrity even under various deformations [51, 132, 133]. In general, the flexibility or stretchability of a binder is investigated via tensile tests, widely used to determine the tensile strength and elongation of materials, including films and composites [134–137]. Figure 8(c) shows the tensile test machine. Through tensile tests, we determined the strength required to break or strain a material under a tension-based force. The mechanical properties of the binder film and electrode were determined using this method. In this section, we discuss the literature on the improvement in the integrity of the electrode depending on the type of binder.

In LIBs, various types of binders have been used to enhance the mechanical properties of electrodes, including PVDF [140–143], CMC [99, 144–146], and PAA [98, 147, 148], among others [58, 60, 134, 149, 150]. Polyvinylidene fluoride (PVDF) is the most widely used traditional binder, and various studies have been conducted on the strength of the electrode based on the molecular weight or amount of PVDF. Byun et al. [122] investigated the effect of the molecular weight of PVDF on the adhesion strength of LIB electrodes using SAICAS to analyze the adhesion properties of the electrodes. They utilized three types of PVDF with different molecular weights (500 k, 630 k, and 1,000 k) and cast the slurry onto an Al foil as a current collector. The adhesion strengths of the electrodes with different PVDF binders were proportional to the molecular weight of PVDF at all depths. Especially at a depth of 10 μ m, the LiCoO₂-based electrode with a molecular weight of 1,000 k showed the highest adhesion strength (0.1469 kN/m). In contrast, those of the electrodes with molecular weights of 500 k and 630 k were 0.0998 and 0.1175 kN/m, respectively, as shown in Figure 9(a). Figure 9(b) shows the cycle stability at 60°C, depending on the molecular weight of PVDF. The electrode with 1,000 k PVDF retained approximately 80% of its initial capacity after 160 cycles, followed by the electrode with 630 k and 500 k PVDF. These results indicate that the use of higher-molecular-weight PVDF has a positive effect on the adhesion properties and cycle stability because of the higher degree of chain entanglement and higher crystallinity. Loghavi et al. [151] reported on the effect of the crystalline microstructure of PVDF as a cathode binder on the mechanical properties and electrochemical properties of LiNi_{0.8}Co_{0.15}Al_{0.05}O₂-based electrode. After casting the slurry onto the Al foil, the cast foil was dried for 24 h at different temperatures (20, 40, 60, 80, 100, and 120°C), influencing the crystalline structure of PVDF.

Generally, PVDF has different physical and electrical properties depending on its crystalline phase [152, 153]. The XRD patterns of the samples were measured at various drying temperatures to evaluate the crystalline structure of PVDF. PVDF prepared at 20°C did not exhibit any specific phase. However, the PVDF dried at 60 and 120°C showed β phase and α phase, respectively. They utilized double-sided adhesive tape to measure the adhesion strength of the electrodes. The electrode prepared at 60°C showed the highest adhesion strength (599 kPa), followed by the electrodes dried at 120 and 20°C (Figure 9(c)). They indicated the PVDF with β phase was the most stable and had a most polar nature, leading to the strongest intermolecular interactions between the PVDF chains. Furthermore, they investigated the electrochemical properties, including cycle stability, rate capability, and EIS measurements. As shown in Figure 9(d), the electrode with 60°C showed the highest initial specific capacity (185 mAh/g) and most stable cycle retention (93%), compared to others. Although there are many factors that enhance the electrochemical performance, outstanding mechanical integrity is important for achieving desirable LIBs. Haselrieder et al. [154] utilized PVDF with different contents and molecular weights for graphite-based anodes of LIBs. A pull-off test machine was used to determine the adhesion strengths of the electrodes. In the pull-off test machine, an electrode was placed between two plane plates and fixed using double-sided adhesive tape. The plate on one side was moved upward at a defined velocity, and the maximum tensile strength was characterized at the point of adhesion failure. Figures 9(e) and 9(f) show the adhesion strength of the electrode as a function of the PVDF content and molecular weight, respectively. In Figure 9(e), the adhesion strength of the electrodes is proportional to the PVDF content because an increased amount of PVDF can interact with the components of the electrode. Furthermore, the adhesion strength of the electrode increased with increasing PVDF molecular weight (Figure 9(f)). They attributed the enhanced adhesion strength to the uniform binder distribution during the drying process because of the lower trend for migration, leading to a higher binder content in the anode and a higher possibility of interactions among the components.

Although PVDF has been widely used as a binder for both the cathode and anode in LIB, some limitations remain, including a restricted soluble solvent and weak van der Waals forces—inappropriate for ecofriendly aspects, even for electrochemical aspects (such as high voltage and large volume expansion system). In addition, PVDF can react with lithium metal or lithiated graphite during the charge/discharge process, resulting in stable lithium fluoride (LiF) [52]. As a result, lithium ions were consumed, and the amount of intercalated and deintercalated lithium ions was reduced. Therefore, novel binders with strong bonding strength are required to maintain electrode integrity and maximize the performance of LIB.

To solve the problems associated with PVDF, CMC has been considered as an alternative candidate owing to its water solubility and functional groups, such as carboxymethyl and hydroxyl groups, which can enhance strong

adhesion with active materials and current collectors via hydrogen bonding. Zhang et al. [155] compared the adhesive properties of a $\text{Li}_{1.2}\text{Ni}_{0.13}\text{Co}_{0.13}\text{Mn}_{0.54}\text{O}_2$ cathode for LIBs based on the type of binder, including PVDF, CMC, and polyacrylonitrile (PAN), which is a synthetic binder. To evaluate the adhesion properties of the electrode, a peeling test was performed at an angle of 90° with a constant 50 mm/min. As shown in Figure 10(a), regardless of the CMC content, the electrodes with CMC as the binder exhibited enhanced adhesion strength compared to the electrodes using PVDF and PAN. Furthermore, the strength of the electrodes increased with increasing CMC content. To investigate the effect of the binder type on the electrochemical stability of the electrode, the cycle performance and mid-point discharge voltage (MPV) fading were investigated, as shown in Figures 10(b) and 10(c), respectively. The cycling stability and MPV fading of the electrodes exhibited the same trend as the mechanical strength of the electrodes in the order of CMC, PAN, and PVDF. The cycle retentions of the electrodes with CMC, PAN, and PVDF were 109%, 62%, and 57%, respectively. Moreover, for MPV fading, the electrode with CMC showed 88% of the initial value, representing the most stable result compared with those of PAN (76%) and PVDF (74%). In the case of electrodes using CMC, the electrode material was tightly attached to the current collector, positively affecting the mechanical strength and electrochemical stability of the electrodes. Gordon et al. [156] utilized CMC for graphite-based anodes and measured the mechanical properties of electrodes with different binder contents, molecular weights, and degrees of substitution (DS), i.e., the average number of hydroxyl groups substituted by carboxymethyl groups. For the adhesive strength of the electrode, a 90° peeling-off test was conducted at a constant peeling rate of 5 mm/s. Figures 10(d) and 10(e) show the adhesive strength profiles with different concentrations of CMC as a function of DS at the same molecular weight (250 kDa) and as a function of molecular weight at the same DS (0.9). As shown in Figures 10(d) and 10(e), although the adhesion strength of the electrode seemed to increase with increasing binder content, there were large error bars and negligible differences in the adhesion strength regardless of the factors. All the investigated samples showed adhesion strength between 0.6 and 1.8 N/m. Thus, in their experiment, they explained that the adhesive strength of the graphite-based anode with CMC was not significantly dependent on the molecular weight and DS; thus, stronger types of binders were required to enhance the integrity of the electrode. In order to enhance the adhesion strength, they added an elastomeric styrene-butadiene rubber (SBR) as a secondary binder, a synthetic rubber with high binding ability, mechanical property, and flexibility [157, 158]. They investigated the effect of SBR on the anode with fixed CMC contents (2.5 vol%), molecular weight (700 kDa), and DS (0.9). As shown in Figure 10(f), the adhesion strength of the electrode increased significantly with the addition of SBR, and the strength of the electrode increased with increasing SBR concentration, thus indicating that the use of SBR and CMC together is an attractive combination for enhancing adhesion to the current collector. Although the

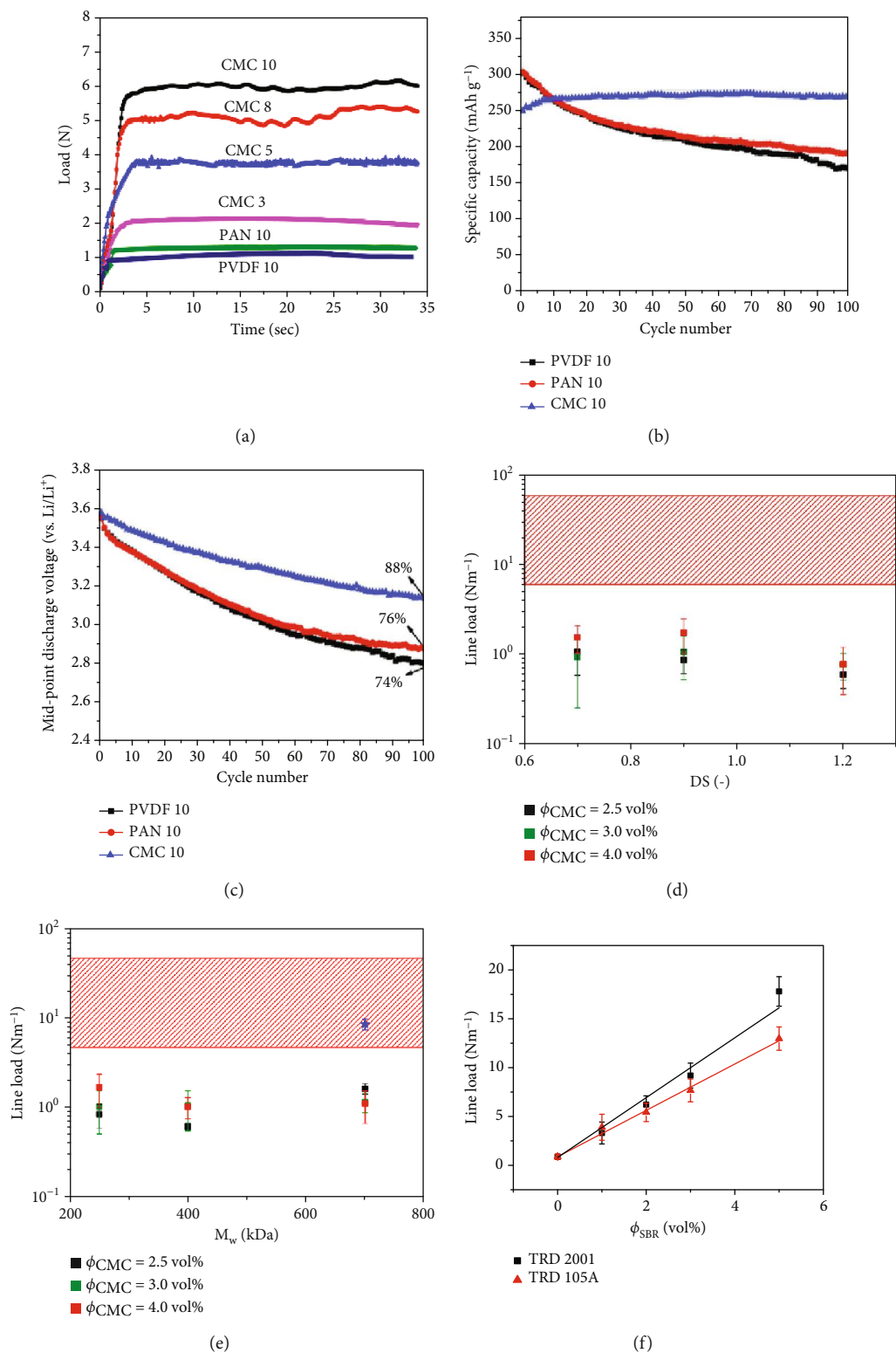


FIGURE 10: Continued.

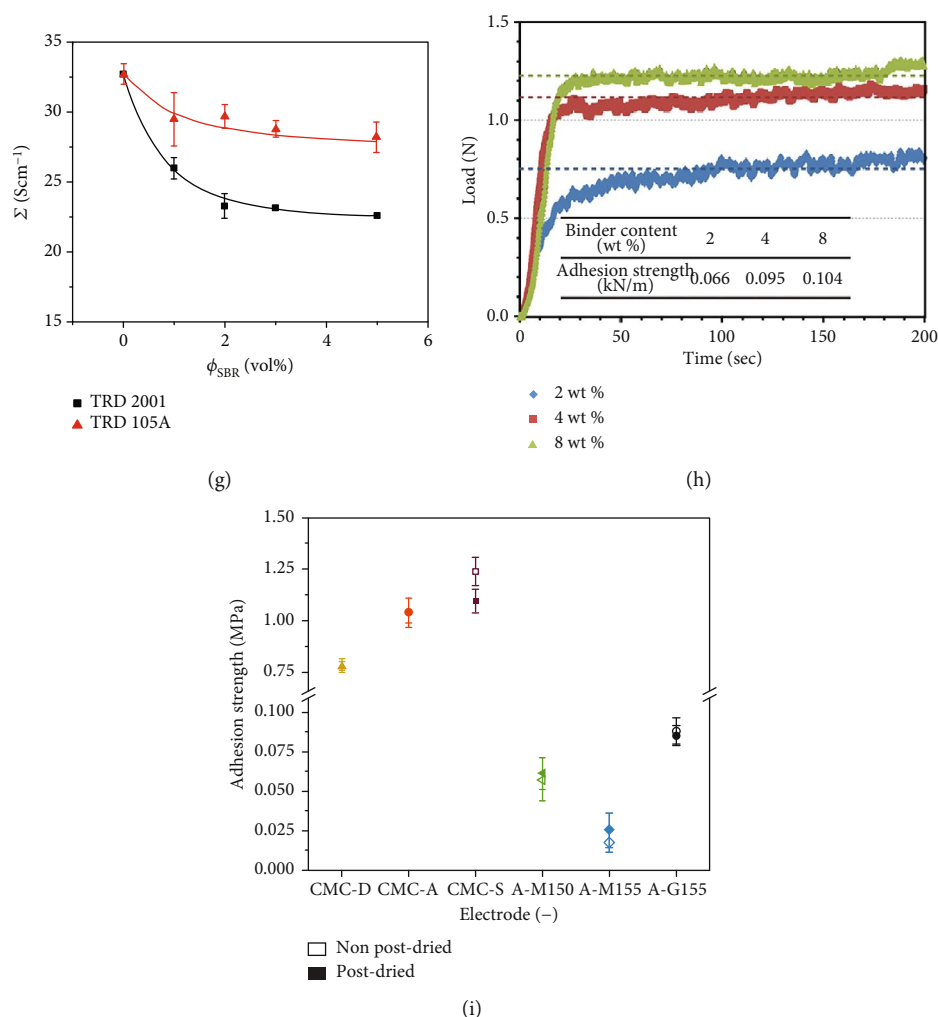


FIGURE 10: (a) Results of the peeling-off test, depending on the electrodes with different binders, and the electrochemical stability of the electrodes with different binders: (b) cycling stability and (c) MPV fading curves [155]. An adhesive strength of the electrodes with different contents of CMC, according to the (d) DS with constant molecular weight and (e) molecular weight with constant DS and an (f) adhesive strength of electrodes with CMC/SBR as binder, as a function of contents of SBR, and as fixed CMC contents (2.5 vol%). (g) Electrical conductivity variation as the contents and types of SBR [156]. (h) The peeling-off test profiles of the electrode with CMC/SBR as binder with different contents of the binder [123] and (i) comparison of the adhesion strength of the electrodes with different types of binders [159].

electrode integrity increased with the addition of SBR, the electrical conductivity decreased with increasing SBR content owing to the insulating property of SBR. Considering this situation is inevitable, an effort to optimize the tradeoff is required (Figure 10(g)). Son et al. [123] analyzed the adhesion properties of a graphite-based anode using a combination of CMC and SBR as binders. The binder content was varied with fixed ratios of SBR and CMC of 40 wt% and 2 wt%, respectively. As the result of the 180° peeling off test with a rate of 100 $\mu\text{m/s}$, the adhesion properties of the electrode with 2 wt%, 4 wt%, and 6 wt% of the binder increased and the values were 0.066, 0.095, and 0.104 kN/m, respectively (Figure 10(h)). Jagau et al. [159] investigated the adhesion strength of a graphite-based anode with the same SBR and several types of CMC with different molecu-

lar weights and DS. CMC-D, CMC-A, and CMC-S are CMC with molecular weights of 224, 700, and 355 kg/mol, respectively, and DS of 0.9, 0.9, and 0.67, respectively. As shown in Figure 10(i), the adhesion strength of the anode increased with increasing molecular weight and decreasing DS of the CMC because of the increased binder entanglements [160, 161].

In addition to the SBR binder, other types of polymers have been utilized to achieve a synergistic effect through combination with CMC for applications in Si-based anodes [23, 125, 162–164]. The Si-based anode has been investigated exclusively because the Si has a higher theoretical lithium storage capacity than the graphite-based anode [165–168]. However, the large volume expansion of Si during the charge/discharge process is a critical issue that can destroy

the electrode and cause electrical contact loss between active materials, leading to poor cycling stability [169–172]. Research has proceeded dramatically to buffer and deal with repeated volume changes in Si and to enhance the mechanical properties of the electrode. Ma et al. [162] reported the synergistic effect of polydopamine (PDA) and CMC as a binder, and the synthesized CMC-PDA binder showed strong interactions between each Si particle and the interface of the active materials and current collector via hydrogen and covalent bonding (Figure 11(a)). PDA is widely used to enhance the adhesive strength of composites. Thus, in the peeling-off test, the electrode with the CMC-PDA binder showed a higher and more uniform adhesion strength than the electrode with only CMC as a binder, as shown in Figure 11(b). Figure 11(c) shows the cycle performance of the electrode with CMC and CMC-PDA as binders at 1 C. Because of the higher adhesion ability of CMC-PDA, the electrode with CMC-PDA showed a more stable cycle performance than the electrode with only CMC. Tang et al. [125] also prepared a CMC-PDA (CP) binder for application to a Si-based anode and investigated the mechanical properties of the electrode and the effect of the binder type on the electrochemical performance. As shown in Figure 11(d), the adhesion strength of the electrode with CP increased dramatically from 1.6 N (only CMC) to 10.5 N. Because of the increased electrode integrity, a higher cycling stability of the electrode with CP (80%) was achieved compared to that with only CMC (58.9%) (Figures 11(e) and 11(f)). These results show that adding PDA to CMC is an effective method to enhance the adhesion properties of the electrode and the stretchability of the binder, implying that the volume expansion of Si is well suppressed. Lee et al. [163] synthesized a CMC-polyethylene glycol (CMC-PEG) binder and applied it to a Si-based anode. The chemical structure of the cross-linked CMC-PEG is shown in Figure 11(g). PEG is an eco-friendly and water-soluble material. For the fabrication of anodes, they prepared a slurry with Si powder, a conducting agent, SBR, and different binders (CMC or CMC-PEG binder) and then cast the obtained slurry onto a copper current collector. As shown in Figure 11(h), because the functional groups of the CMC-PEG binder were abundant, the electrode with CMC-PEG showed a higher peeling strength (~2 gf/mm) than the electrode with CMC (~1.1 gf/mm). Furthermore, the PEG had a positive effect on the cycling performance of the electrode, as shown in Figure 11(i).

In addition to CMC as an alternative candidate for PVDF, PAA is an excellent candidate because it is water soluble and enhances the ability of CMC to interact with active materials and current collectors through carboxylic acid groups. Unlike natural binders such as CMC, PAA is a synthetic binder that is beneficial for large-scale production and is easy to design depending on the requirements of the electrodes. Therefore, synthetic and water-soluble PAA with high adhesion properties have been extensively investigated. Zhang et al. [173] investigated the effect of a PAA binder on a LiFePO_4 cathode and compared the strength and electrochemical performance of the electrode with those of a PVDF binder. The average strength of the electrode with the PAA binder was 5.6 N/cm, higher than that of the electrode with

PVDF (0.2 N/cm). The cycling performances of both electrodes are shown in Figure 12(a). PAA exhibited better cycling stability than PVDF. Although NMP was used as the solvent in this study, a positive effect was observed when PAA was used as the binder. In addition to its solubility in NMP, PAA is soluble in water and ethanol—an attractive advantage for ecofriendly systems. Zhang et al. [174] used a peeling-off test to compare the adhesion strengths of LiMn_2O_4 electrodes with PVDF, CMC, and PAA as binders. The adhesion properties of PVDF and PAA were compared in an NMP solvent system, and those of CMC and PAA were compared in a water solvent system. The LiMn_2O_4 cathode with PVDF and CMC showed an adhesion strength of 0.32 N/cm and 1.5 N/cm, respectively. However, the adhesion strength of the electrode with PAA was 3.26 N/cm in the NMP solvent system and 1.57 N/cm in the water solvent system. These results prove that the PAA binder has a positive effect on both the NMP and water systems, enhancing the adhesion properties. Therefore, PAA is widely used as an LIB binder. Sun et al. [175] compared the adhesion properties of a LiFePO_4/C cathode using PAA or poly(vinyl alcohol) (PVA) as the binder. Figures 12(b) and 12(c) show images of the electrodes after the peeling-off test. Although the adhesion properties were compared, the electrode with PAA clearly showed a smaller amount of delaminated electrode material than the electrode with PVA. Shin et al. [176] investigated the effect of PAA on the adhesion strength and electrochemical performance of a graphite-based electrode by comparing an electrode with only CMC and one with cross-linked PAA-CMC as a binder. The slurry was prepared with a ratio of 97.5:1.0:1.5, corresponding to graphite, binder, and SBR. They fixed the weight of the binder and changed only the types, such as CMC and PAA-CMC. The fabricated electrodes were then subjected to a peeling-off test. Consequently, the adhesion strength of the electrode with PAA-CMC (~2.86 gf/mm) was almost twice that of the electrode with CMC, as shown in Figure 12(d). Figure 12(e) shows the cycling stabilities of the PAA-CMC and CMC, respectively. PAA-CMC showed a more stable electrochemical performance than CMC. Lee et al. [177] also analyzed the adhesion strength of a graphite-based anode in the presence of PAA in a CMC/SBR system. The strength values were ~14.496 mN/mm and ~4.705 mN/mm for the electrodes with and without PAA, respectively. Niu et al. [178] fixed the CMC content of graphite-based anodes and investigated the effect of the type of binder added, such as PAA or SBR, on the adhesion strength. As shown in Figure 12(f), for the electrode with natural graphite (NG) as the active material, the electrode with PAA showed a much higher adhesion strength than the electrode with SBR. They explained that the reason for the enhanced strength of the electrode was that aqueous-based PAA can cover a larger area of the electrode than an emulsion-type SBR.

With lithium hydroxide (LiOH) or sodium hydroxide (NaOH), PAA becomes neutral, further enhancing its adhesion ability [50, 53, 138, 179, 180]. In general, PAA is weakly acidic. In water, undissociated carboxylic groups bind to each other via hydrogen bonding, resulting in the aggregation of

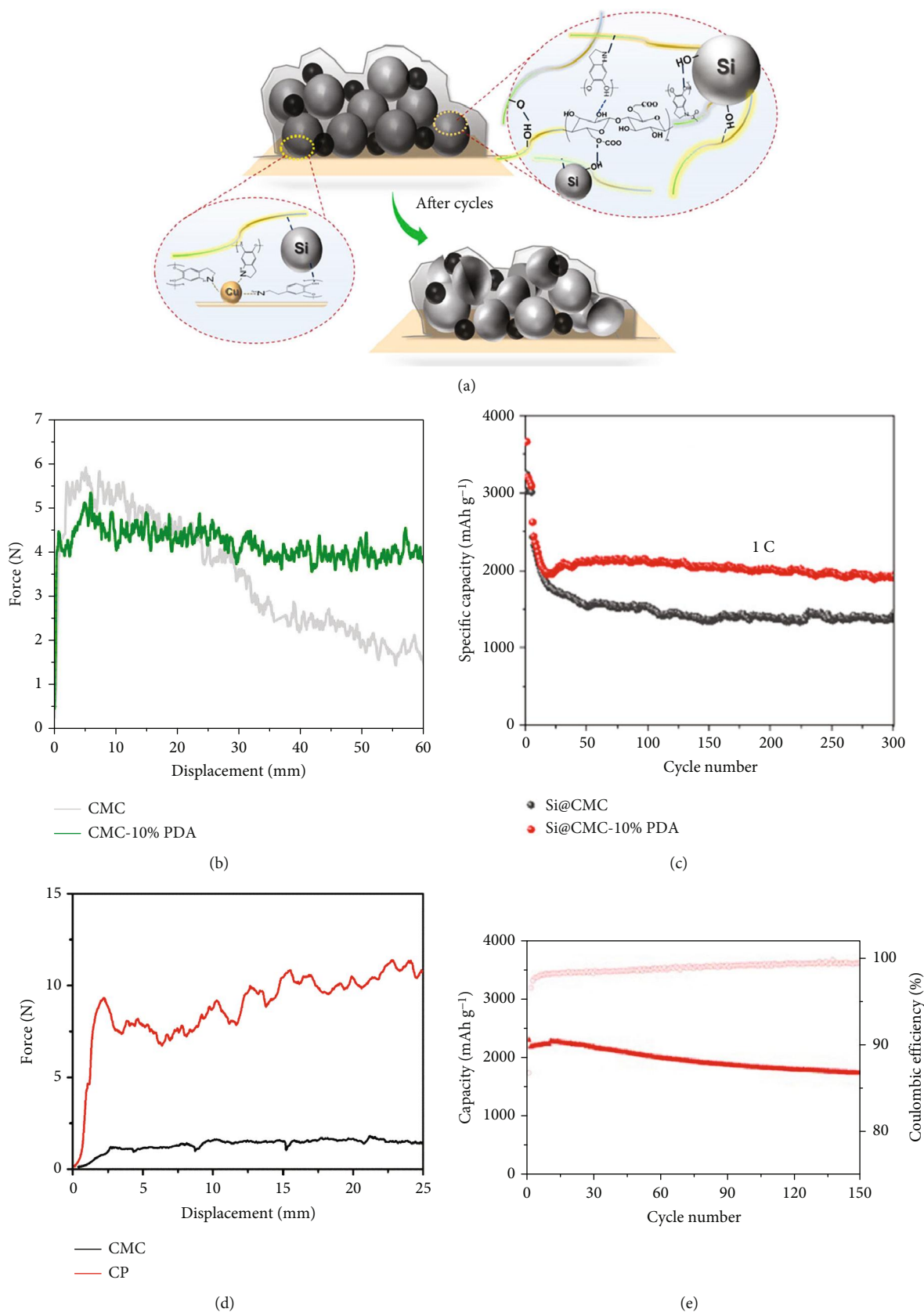


FIGURE 11: Continued.

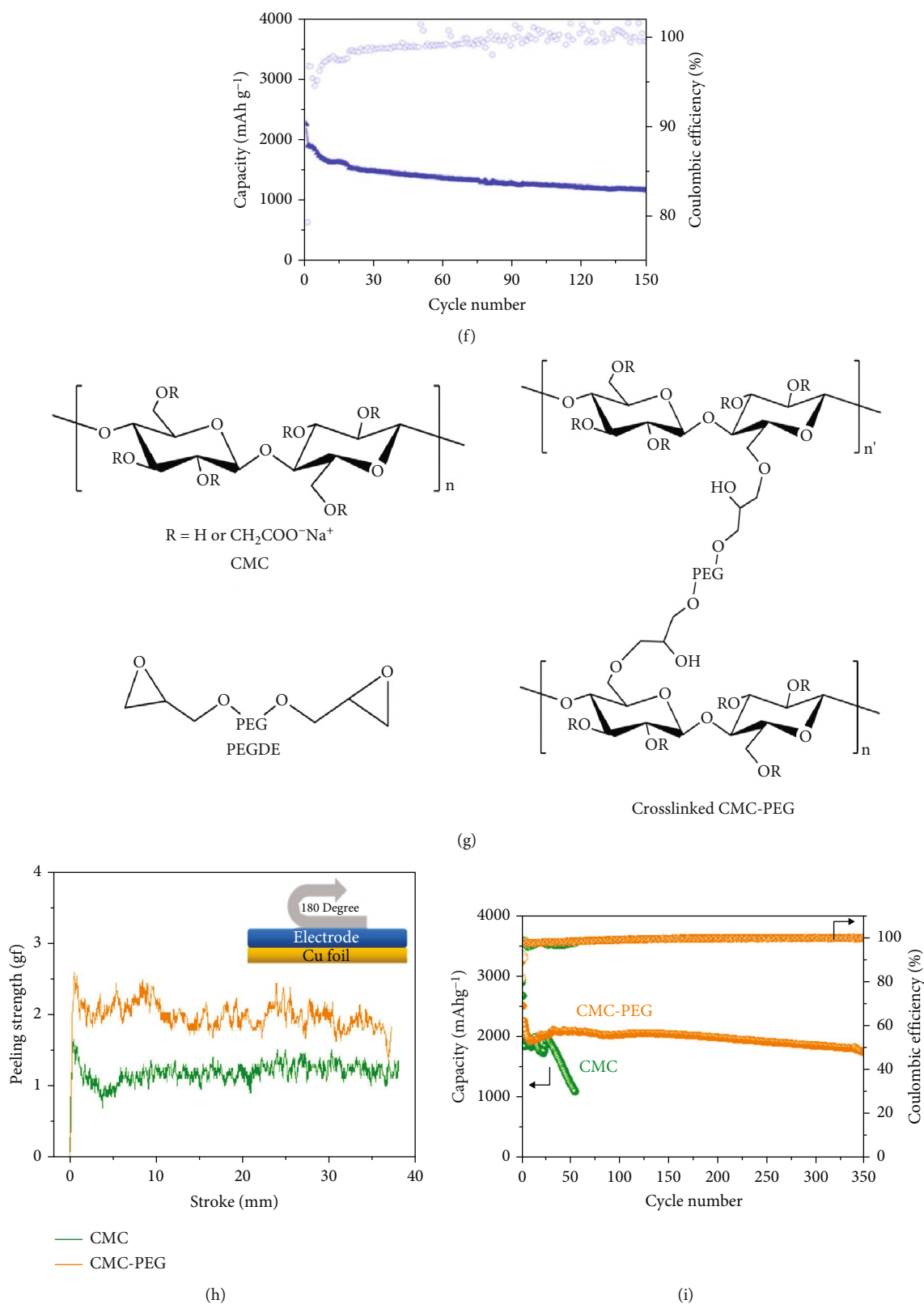


FIGURE 11: (a) Schematic of interactions between CMC-PDA as a binder and Si particles for Si-based anode. (b) The results of the peeling-off test of the electrodes with CMC and CMC-PDA. (c) Cycling stability of the electrodes with CMC and CMC-PDA [162]. (d) Profile of the adhesion test of the electrodes with CP and CMC and cycling performance of the electrodes with (e) CP and (f) CMC [125]. (g) The chemical structure of the CMC-PEG, (h) the adhesion strength of the electrodes with CMC and CMC-PEG, and (i) the cycling performance of the electrodes, depending on the binder types [163].

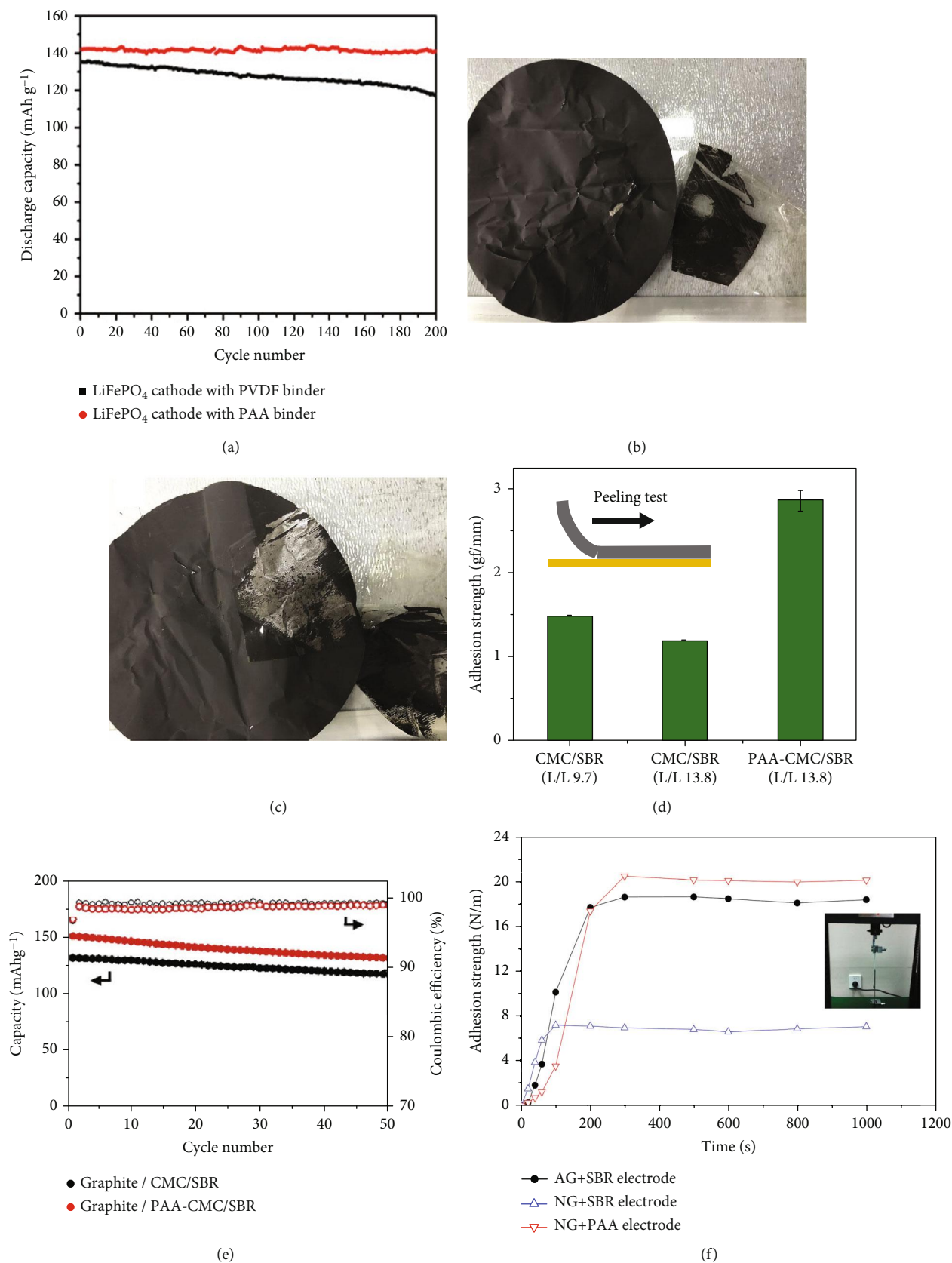


FIGURE 12: (a) Cycling performance of the electrodes with PVDF and PAA binder [173]. Images of the electrode with (b) PAA and (c) PVA after the peeling-off test [175]. (d) Adhesion strength and (e) cycling performance of the electrodes, according to the addition of PAA [176]. (f) Adhesion profiles of the electrode with different types of graphite and binder [178].

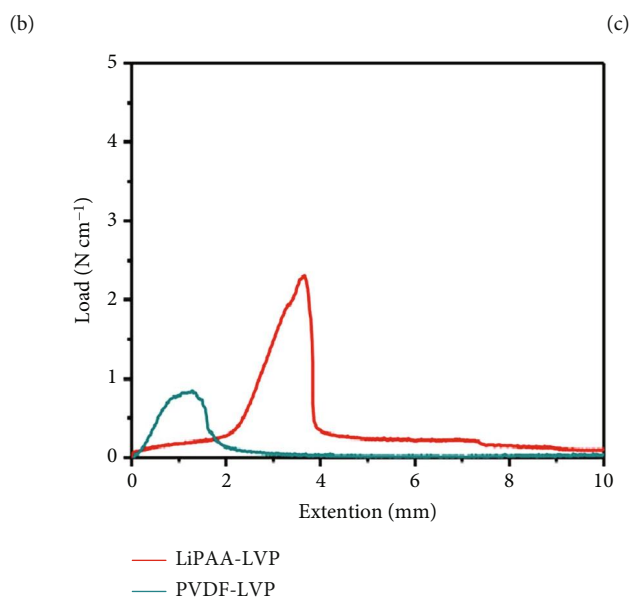
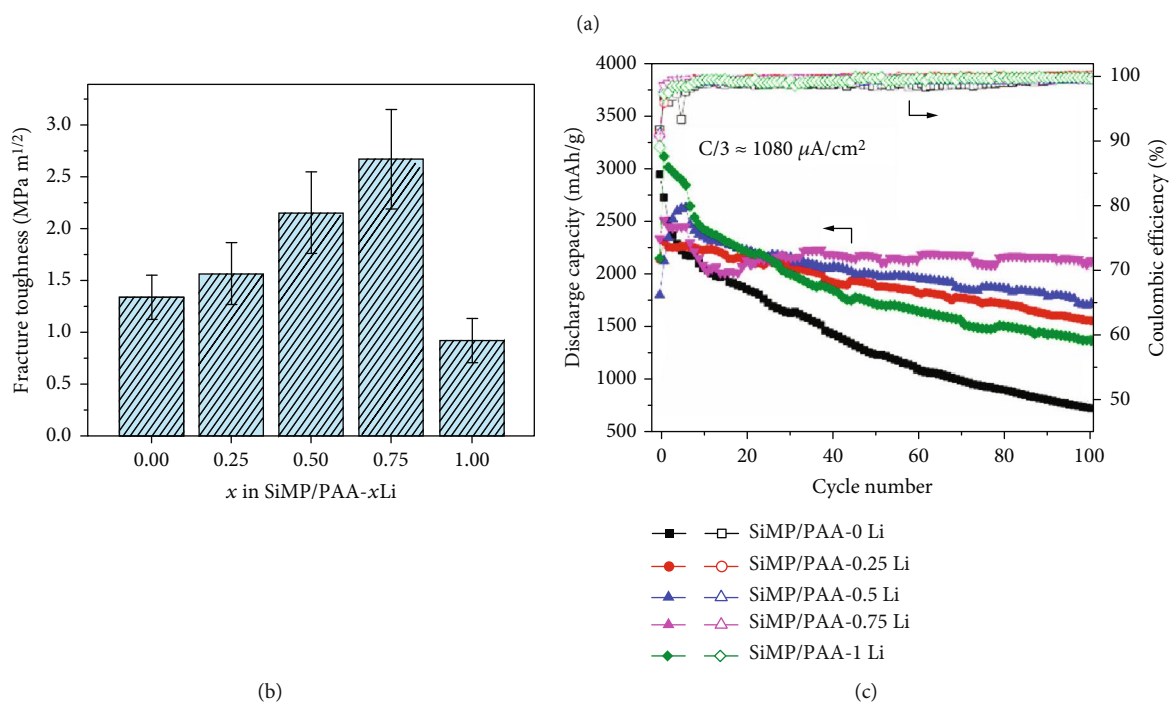
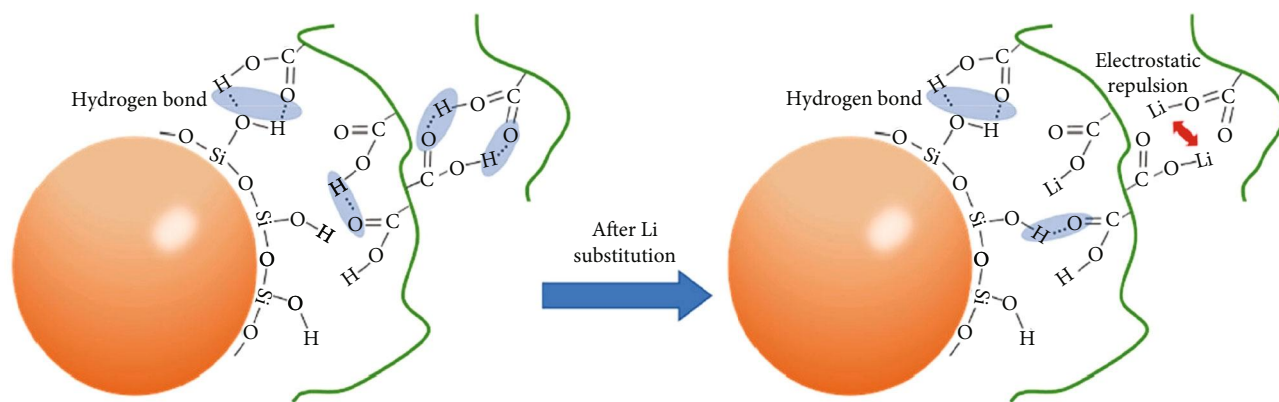


FIGURE 13: Continued.

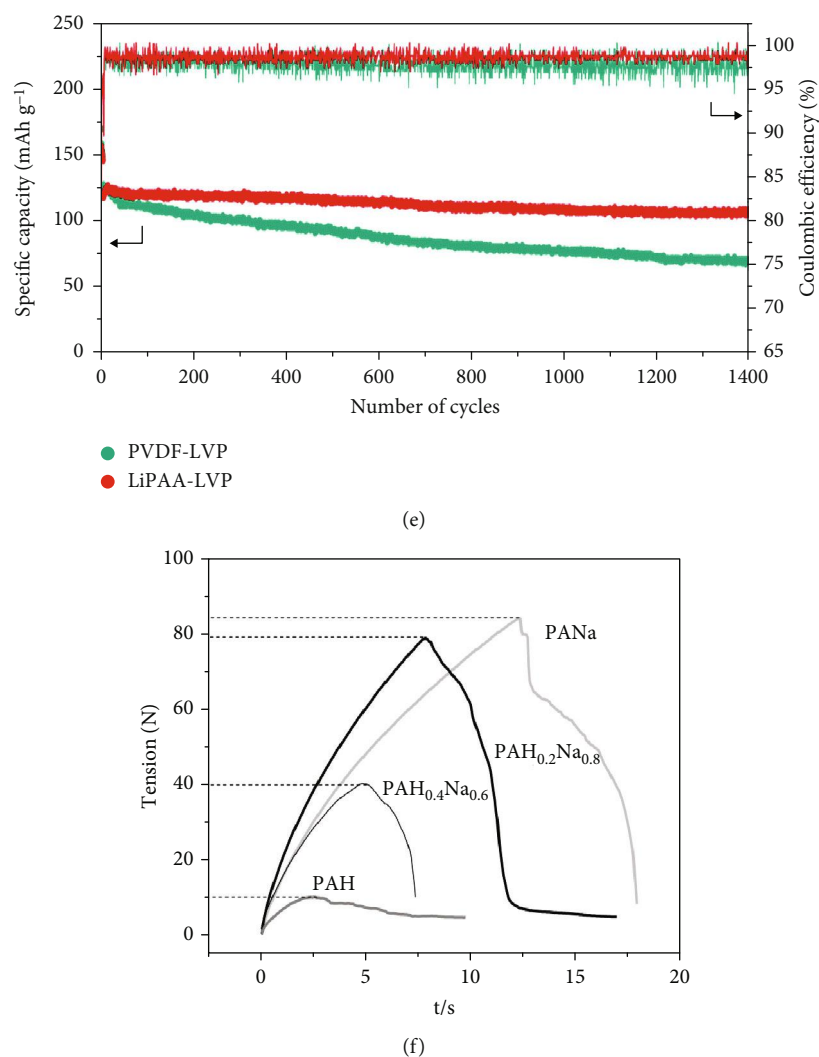


FIGURE 13: (a) Schematic illustration of interactions between PAA-Li and Si particles, (b) comparison of the fracture toughness of electrodes with different types of binder, and (c) cycling stability of the electrodes, according to the neutralization degree of PAA-Li [138]. (d) The peeling-off test profile and (e) cycling stability of electrodes with LiPAA and PVDF [180]. (f) Adhesion strengths of the electrode with PAH with different neutralization degrees [181].

PAA. However, upon neutralization of PAA, the carboxylic groups become fully dissociated, resulting in electrostatic repulsion between the carboxylic groups, which blocks the aggregation of each PAA and enhances its adhesion ability with active materials. Dang et al. [138] utilized LiOH as the neutralization agent of PAA and analyzed the adhesion properties of Si-based anodes with different degrees of PAA neutralization (Figure 13(a)). The samples were named PAA-0Li, PAA-0.25Li, PAA-0.75Li, and PAA-1Li according to the degree of neutralization. They conducted the scratch test with a scratch distance of 2500 μm , scratch rate of 10 $\mu\text{m/s}$, maximum normal load of 100 mN, and loading rate of 0.5 mN/s. In the range of the scratch distance between 1500 and 2000 μm , they calculated the average fracture toughness [138]. As shown in Figure 13(b), the calculated fracture toughness of the electrodes was ~ 0.91 , ~ 1.33 , ~ 1.56 , ~ 2.15 , and $\sim 2.67 \text{ MPa m}^{1/2}$, corresponding to the PAA-1Li, PAA-0Li, PAA-0.25Li, PAA-0.5Li, and PAA-0.75Li, respectively.

The average fracture toughness increased with an increase in the degree of neutralization of PAA, except for PAA-1Li, because PAA-1Li could not cover the Si-based active material, and there were a number of cracks in the electrode even without the scratch test. The cycling performance of the electrodes was measured over 100 cycles to investigate the effect of PAA neutralization on the electrochemical stability. As shown in Figure 13(c), similar to the trend in the mechanical properties, the cycling stability also increased with increasing neutralization degree of PAA-Li, indicating that the neutralization of PAA with LiOH had a positive effect on the mechanical and electrochemical properties. In a study by Su et al. [180], they also used lithium polyacrylic acid (LiPAA) as a binder for the $\text{Li}_3\text{V}_2(\text{PO}_4)_3$ cathode to improve the mechanical properties and electrochemical stability of the battery. To dissolve LiPAA, water was used, and NMP was utilized as the solvent for the PVDF binder. As shown in Figure 13(d), the strength of the electrode with LiPAA

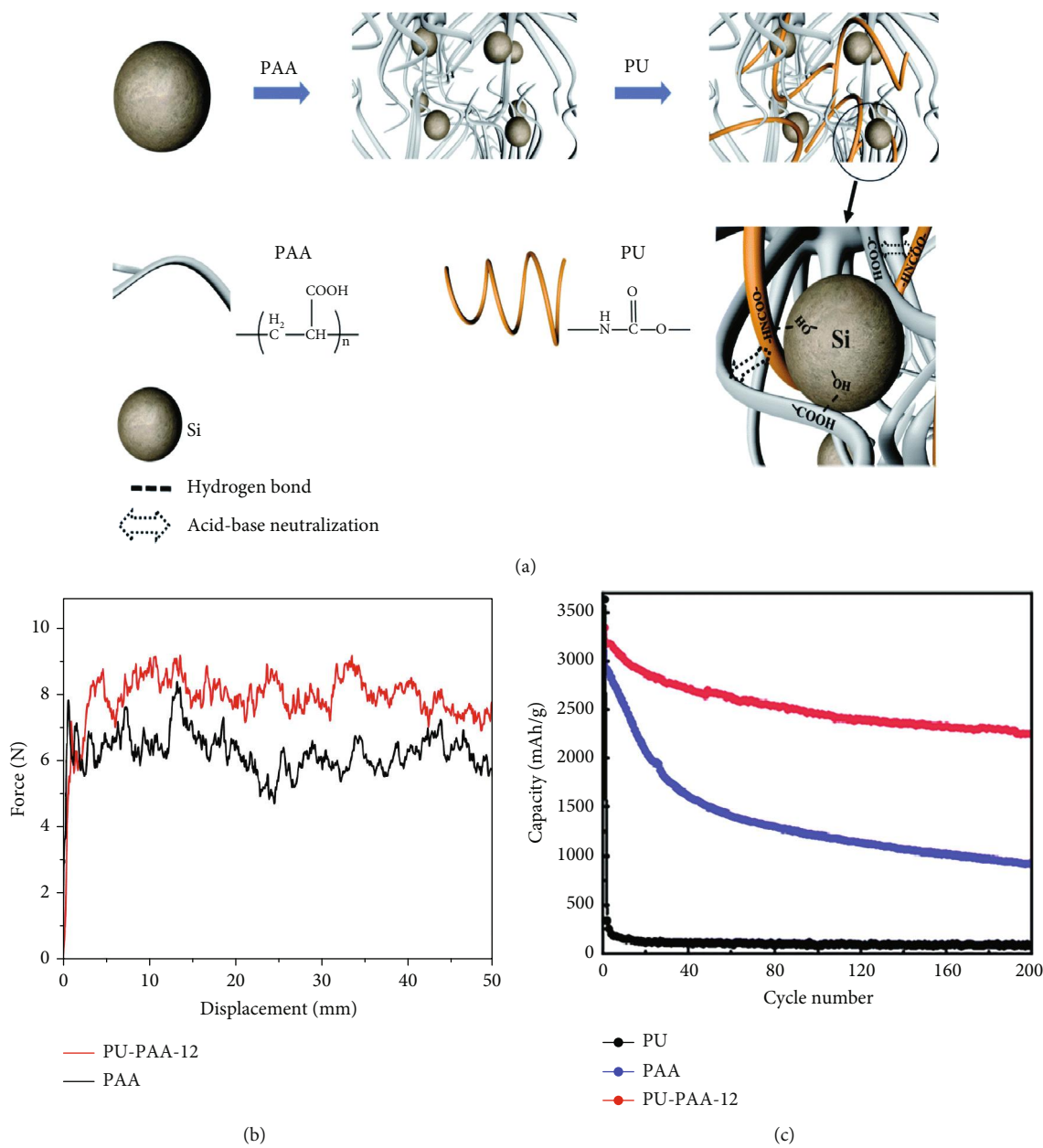


FIGURE 14: Continued.

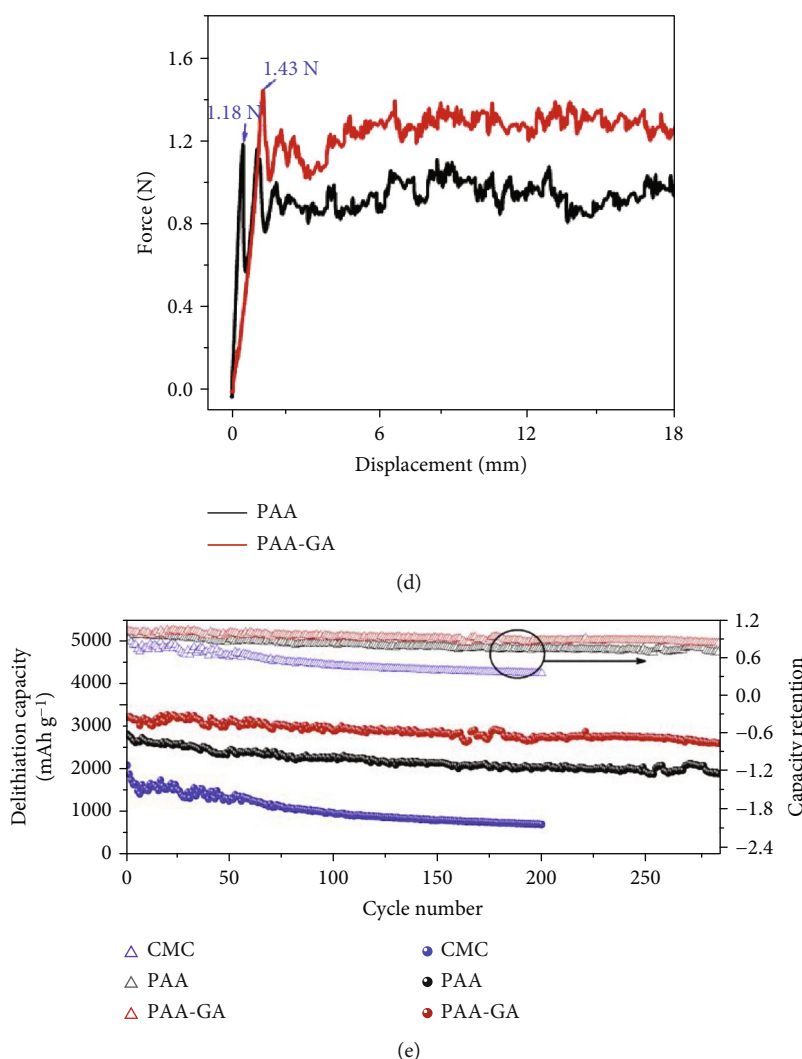


FIGURE 14: (a) Illustration of interactions between Si particles and PU-PAA; (b) the peeling-off test results of PAA and PU-PAA electrodes; (c) cycle performance of the electrodes with PU, PAA, and PU-PAA12 [182]; (d) the adhesion force of the electrodes with PAA and PAA-GA; and (e) cycle performance of the electrodes with CMC, PAA, and PAA-GA [183].

(2.4 N/cm) was higher than that of the electrode with PVDF (0.9 N/cm), because the PVDF bind the active material with weak van der Waals bonding; however, the LiPAA can link the active material and current collector with stronger hydrogen bonding than van der Waals. The long-term cycle stability at 10 C was also enhanced by using LiPAA as a binder compared to the electrode with the PVDF binder. These results clearly indicate that the LiPAA binder is more suitable than the PVDF binder for achieving a higher battery performance (Figure 13(e)). Han et al. [181] reported that the adhesion strength of Si/graphite-based anodes depends on the degree of PAA neutralization. They used different amounts of NaOH to increase the pH of the PAA. The degrees of neutralization were as follows: PAH (PAA in this study), $\text{PAH}_{0.4}\text{Na}_{0.6}$, $\text{PAH}_{0.2}\text{Na}_{0.8}$, and PANa. The results of the peeling test showed that the adhesion strength was proportional to the degree of PAA neutralization (Figure 13(f)). The strength values were approximately 85, 78, and 10 N/cm for PANa, $\text{PAH}_{0.2}\text{Na}_{0.8}$, and PAH, respectively.

In addition to neutralization methods, PAA can be grafted with other types of polymers to enhance the mechanical properties and electrochemical stability of electrodes [182–188]. Niu et al. [182] fabricated a three-dimensional (3D) polyurethane- (PU-) PAA binder via a simple heating and stirring method in DI water and applied a 3D structured binder to a Si-based anode (Figure 14(a)). There was a neutralization interaction between the acid of PAA and the base of PU because PAA has a high density of -COOH groups, and PU has -NH groups. Furthermore, the carboxylic groups of PAA can interact with Si particles via hydrogen bonding, which improves mechanical strength. Depending on the weight ratio of PU to PAA, the binders were named PU-PAA-21, PU-PAA-11, and PU-PAA12. Because the electrode with PU-PAA12 showed the best electrochemical performance in terms of cycling stability, they chose an electrode with the PU-PAA12 binder to compare the adhesion strength and electrochemical stability with those of PAA. As shown in Figure 14(b), the average strength of the electrode with PU-

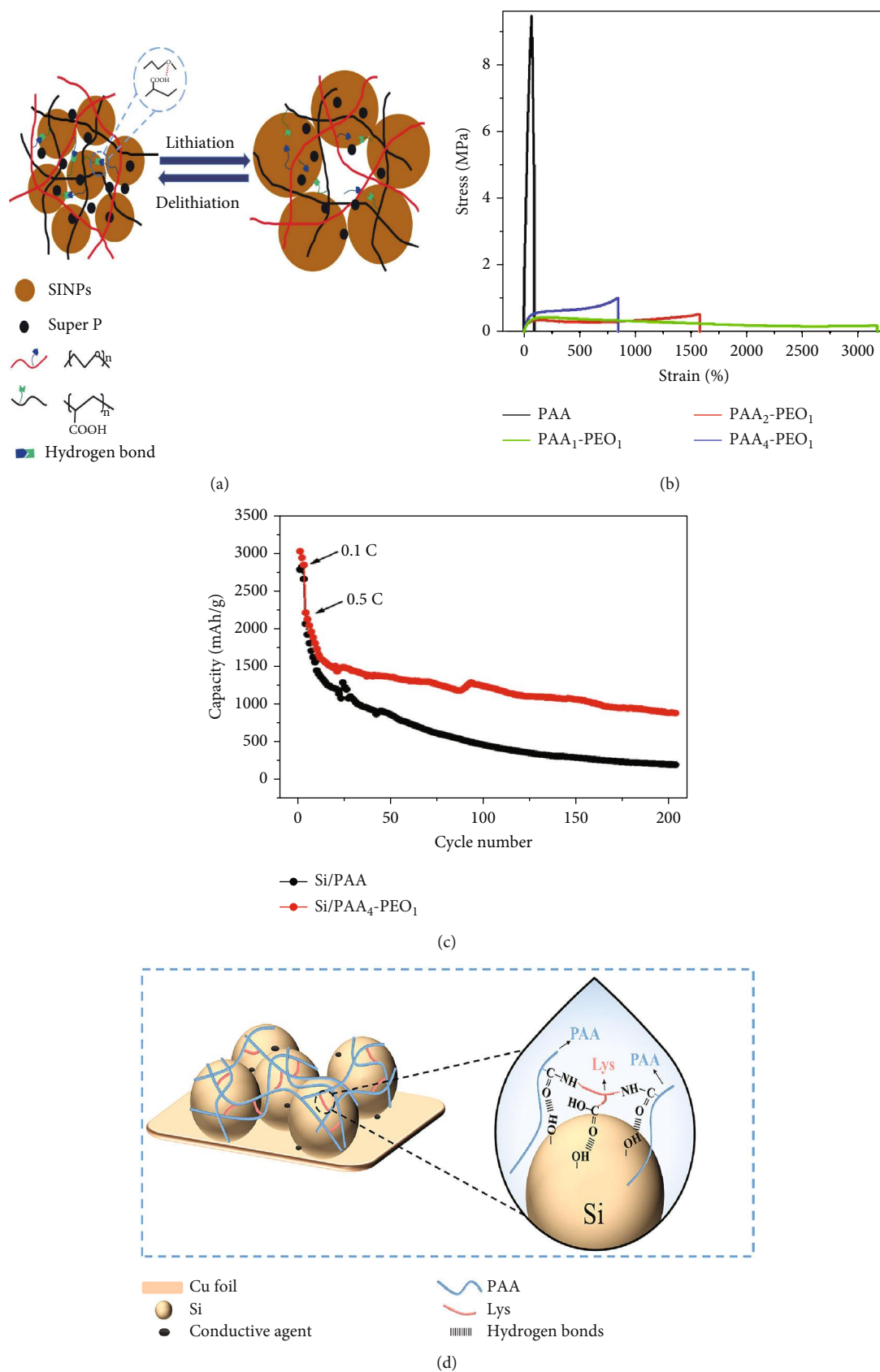


FIGURE 15: Continued.

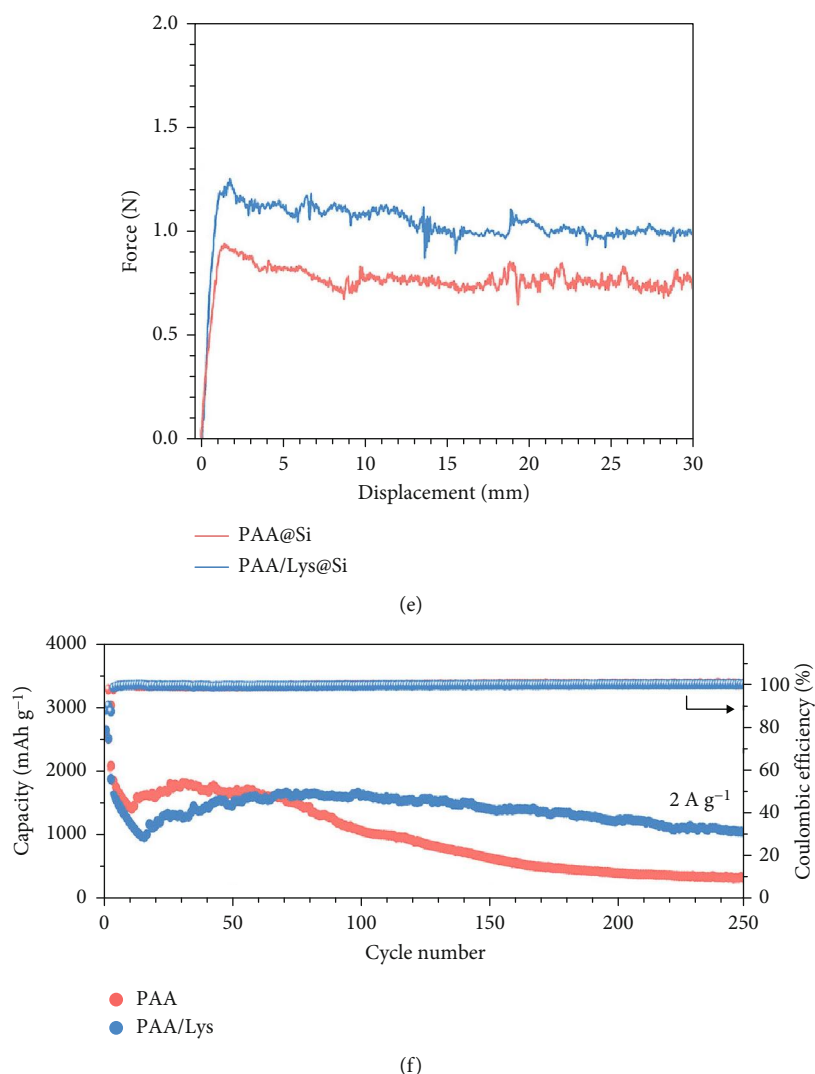


FIGURE 15: (a) Illustration of the binding mechanism of PAA-PEO binder, (b) stress-strain curve of PAA-PEO binder films with different ratios, and (c) cycling stability result of the electrodes with PAA and PAA-PEO binder [184]. (d) Schematic of the binding mechanism of the cross-linked PAA-Lys binder, (e) adhesion profile of the electrodes with PAA and PAA-Lys binder, and (f) cycling performance of the Si-based electrodes with PAA and PAA-Lys binder at 2 A/g [185].

PAA12 was 8.0 N and that of the electrode with only PAA was 6.3 N because the 3D-structured PU-PAA binder can adhere to the components more tightly than the PAA binder. Furthermore, they compared the cycling stability of the electrodes with those of PU, PAA, and PU-PAA12, as shown in Figure 14(c). When PU and PAA were used as binders, the cycling stability decreased dramatically, and the stability of the electrode with PU decreased, indicating that the individual utilization of PU or PAA was insufficient to block the volume expansion of the Si material during the charge/discharge process. In contrast, the electrode with PU-PAA12 showed a significantly improved cycling performance owing to its strong adhesion stability. Li et al. [183] also synthesized a novel binder by modifying PAA with glycinamide (GA). A PAA-GA binder with a number of carboxylic groups and double amide groups was used as the Si-based anode. The

Si particles can be connected to the binder via hydrogen bonding, and the double amide groups of the binder form a double hydrogen bond, causing the binder to behave in a supramolecular manner. They performed a peeling-off test of the electrodes with PAA-GA and PAA. As shown in Figure 14(d), the maximum and average adhesion strengths of the electrode with PAA-GA were 1.43 and 1.3 N, respectively, while those of the electrode with only PAA were 1.18 and 0.9 N. To demonstrate the advantage of PAA-GA in the electrochemical property, they compared the cycling stability of the electrodes with CMC, PAA, and PAA-GA. The electrode with PAA-GA had a capacity retention of 81%, whereas that with PAA was 69.6%. The capacity retention of CMC was more severe than that of PAA and PAA-GA (Figure 14(e)). The results indicated that the binder fabricated by modifying PAA with GA enhanced the adhesion

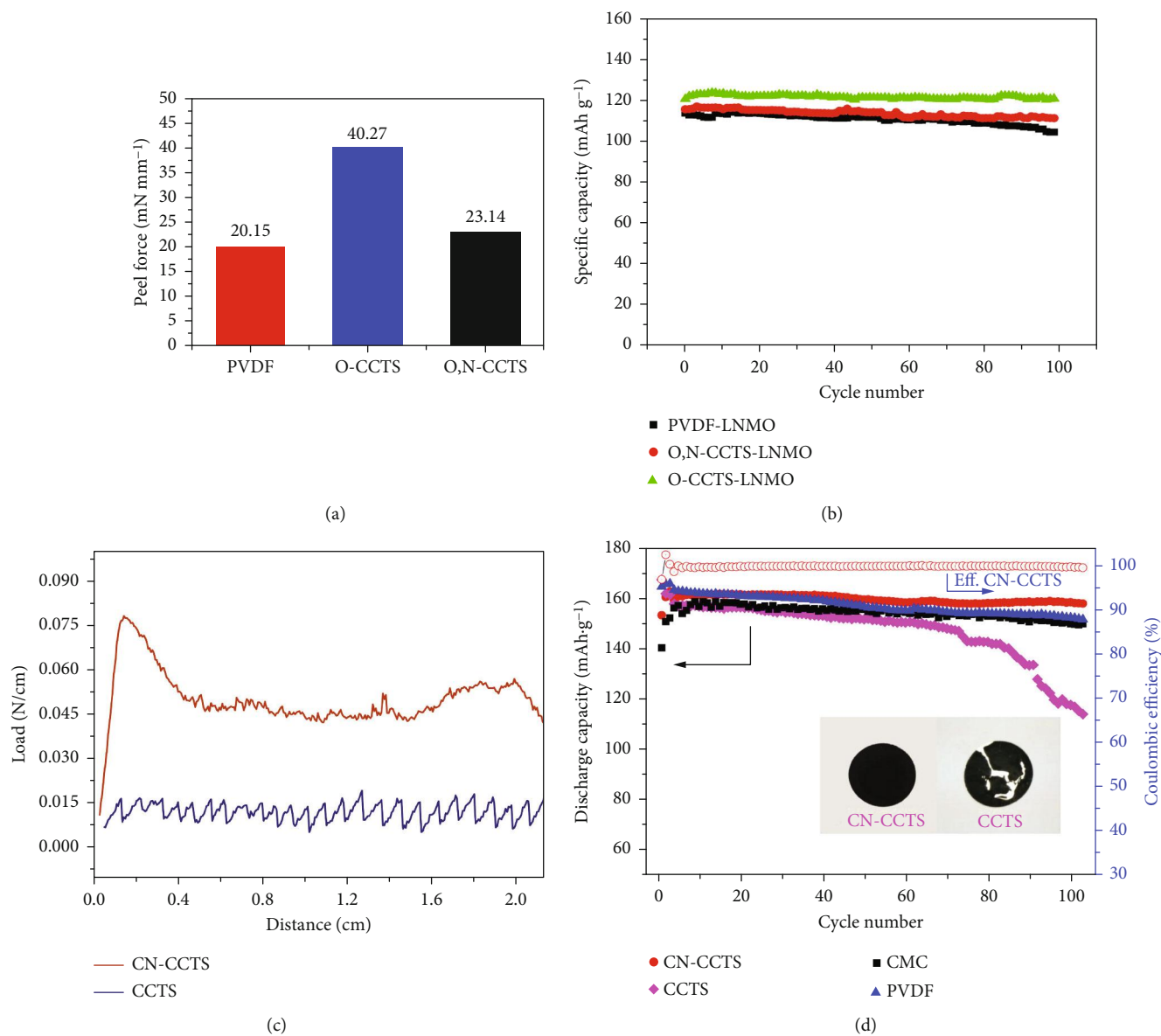


FIGURE 16: Continued.

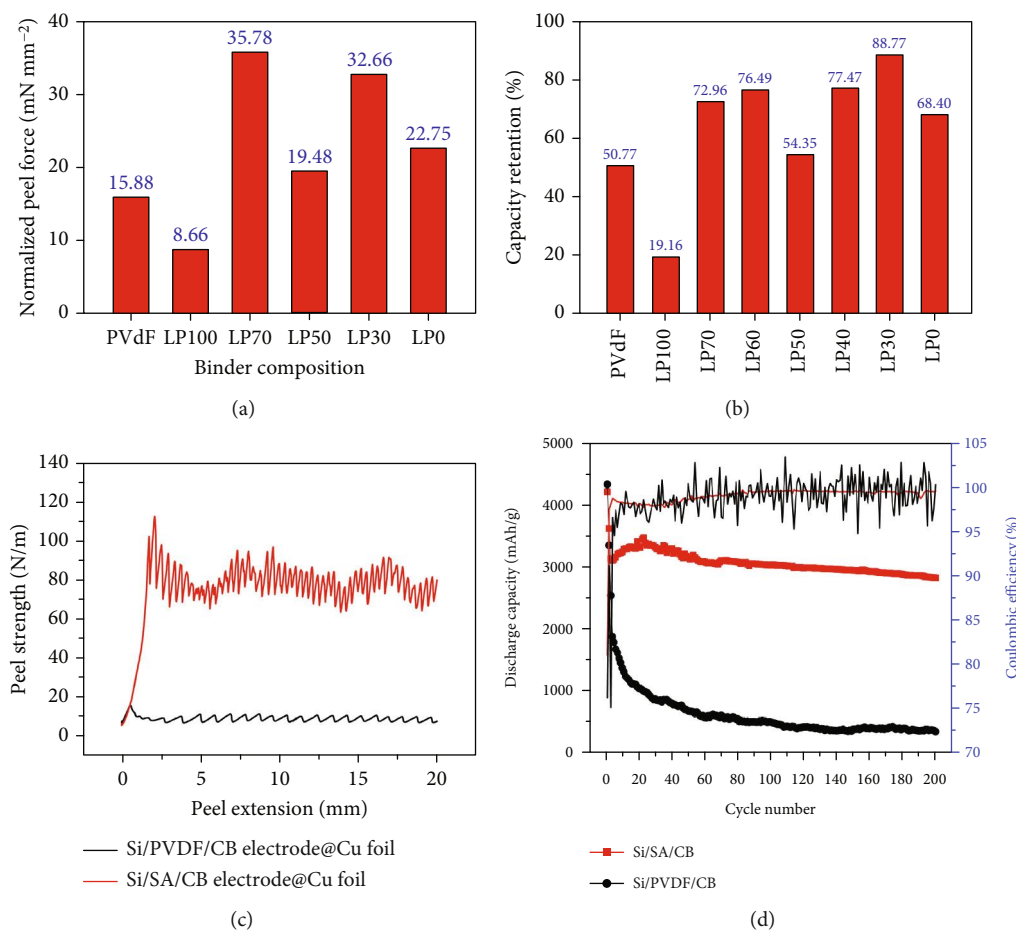


FIGURE 17: (a) Comparison of adhesion force and (b) cycling retention of the electrodes with different types of binder [199]. (c) The profiles of the peeling-off test and (d) cycle stability of the electrodes with PVDF and SA [200].

because of the high density of functional groups, such as hydroxyl and amine groups, in its structure. Therefore, using a binder to enhance the adhesion of the electrode components is possible. Furthermore, because chitosan is a natural polymer, it is considered an ecofriendly and sustainable material for the green system industry. In general, chitosan itself is not soluble in water but can become water-soluble via the carboxymethylation of chitosan, called carboxymethyl chitosan (CCTS) [189, 190]. Yu et al. [191] fabricated a $\text{LiNi}_{0.5}\text{Mn}_{1.5}\text{O}_4$ cathode for LIBs using CCTS. They substituted chitosan by adding a NaOH solution and classified the types of CCTS by the degree of substitution of carboxymethyl groups as O-CCTS and O, N-CCTS. The degree of substitution of O-CCTS was 0.690, and that of O and N-CCTS was 1.413. To investigate the properties of the obtained binder, the adhesion properties of the electrodes with PVDF, O-CCTS, and O, N-CCTS were measured using a peeling-off test, showing the average adhesion strength according to binder type. The average strength decreased in the following order: O-CCTS, O, and PVDF, attributed to the strong hydrogen bonding between the active materials and CCTS (Figure 16(a)). To determine the electrochemical properties, the cycling stabilities of the electrodes with these binders were measured. As shown in Figure 16(b), the cycling

stability of the electrode with O-CCTS was enhanced owing to the -COOH and -OH groups in the O-CCTS binder. The cycle retention of the electrodes after 100 cycles at a 0.2 C rate was 97.7%, 95.5%, and 91.6% of the initial capacity, corresponding to O-CCTS, O, and PVDF, respectively. This trend is the same as that of the mechanical strength of the electrodes. He et al. [190] also investigated water-soluble CCTS for LiFePO_4 cathodes. They synthesized cyanoethylated CCTS (CN-CCTS) by adding NaOH and acrylonitrile and compared the performance of the cathode with that of CN-CCTS and CCTS. As shown in Figure 16(c), the adhesion ability of the electrode using CN-CCTS (0.047 N/cm) was enhanced compared to that of the electrode with CCTS (0.013 N/cm), because -CN is a strong polar group that can tightly adhere to the active materials. Thus, because of the enhanced electrode integrity, the cycling performance of the electrode with CN-CCTS was also enhanced compared to those of CCTS, PVDF, and CMC—all commercial binders in LIBs (Figure 16(d)). Rajeev et al. [192] grafted chitosan and gallic acid (GA) as binders to Si-based anodes. GA is also a natural material that can be extracted from chestnuts and gallnuts [192–194]. They used GA to enhance the water solubility of chitosan and its adhesion to the active materials via hydrogen bonding. The binders were named CS-GA-50

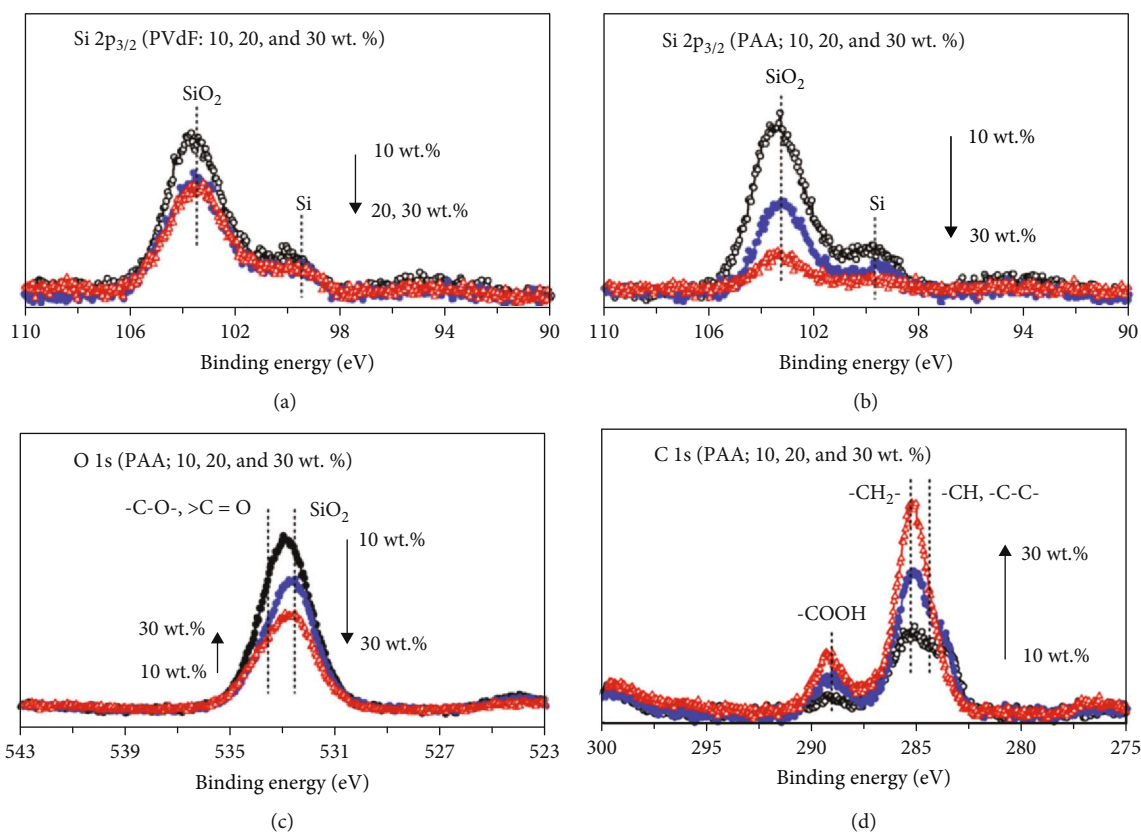


FIGURE 18: XPS spectra of a composite electrode with various polymer binders added: (a) Si 2p_{3/2} of PVDF composite, (b) Si 2p_{3/2}, (c) O 1s, and (d) C 1s of PAA composite, respectively [201].

(1:0.5) and CS-GA-100 (1:1), according to the ratio of repeated units of CS to GA. They also examined the adhesion strength of the electrodes by measuring a 180° peeling-off test at a rate of 30 mm/min. Figure 16(e) compares the average adhesion strengths of the electrodes according to the binders. As shown in Figure 16(e), the Si-based anode with PVDF exhibited the worst performance, and the addition of GA to CS was an effective method to enhance the adhesion property compared to the case with only CS as a binder. To demonstrate the ability of the CS-GA binder to alleviate the volume expansion of Si, they investigated the cycle stability of the electrodes with various binders for 350 cycles at a 0.5 C rate (Figure 16(f)). As a result, CS-GA showed the most stable cycling performance compared to the other binders, indicating that the enhanced mechanical stability of the electrode is important for preventing the volume expansion of Si and for the electrochemical stability of LIBs.

In addition to chitosan-based binders, alginate is a water-soluble and natural polymer extracted from brown seaweeds. This material contains carboxylic groups in its units that enable hydrogen bonding with the components of the electrode. Therefore, alginate is considered a candidate binder for LIBs [60, 149, 195, 196]. Generally, alginate is used as a binder in the form of sodium alginate (SA), a water-soluble material [197, 198]. Rao et al. [199] applied SA as a binder to a thick LiNi_{0.5}Mn_{1.5}O₄ cathode and investigated the effect of SA on the adhesion strength of electrodes with PVDF, LiPAA, and a mixture of LiPAA and

SA at different mass ratios. The binders were labeled LP_x, where *x* is the ratio of LiPAA; thus, LP100 and LP0 were only LiPAA and SA, respectively. A 180° peeling-off test was conducted at the rate of 0.025 ins/s. Consequently, the electrode with LP0 showed a higher peeling force than the electrodes with PVDF and LP100 (Figure 17(a)). Furthermore, the peeling force of the electrode increased with the addition of SA to LiPAA. They explained that these results were due to the hydroxyl groups in SA showing higher adhesion ability to the Al current collector than the carboxylic groups in LiPAA under neutral and mildly acidic conditions. Figure 17(b) shows the capacity retention of the electrodes depending on the type of binder used. As shown in Figure 17(b), the capacity retention trend followed the trend of electrode integrity. These results indicate that the mechanical integrity of the electrodes is an important factor for enhancing electrochemical stability. Hu et al. [200] utilized SA as a binder and applied it to Si-based anodes. They demonstrated the positive effect of SA on the adhesion properties of the electrode via a peeling-off test, as shown in Figure 17(c). The values of the strength were ~8.7 and ~78.3 N/m, corresponding to the electrode with PVDF and SA, respectively. As shown in Figure 17(d), the electrode with the PVDF binder showed a rapid decrease in discharge capacity, whereas the electrode with the SA binder exhibited enhanced cycling stability.

In this section, we introduce various analytical methods for investigating the integrity of electrodes in LIBs, including

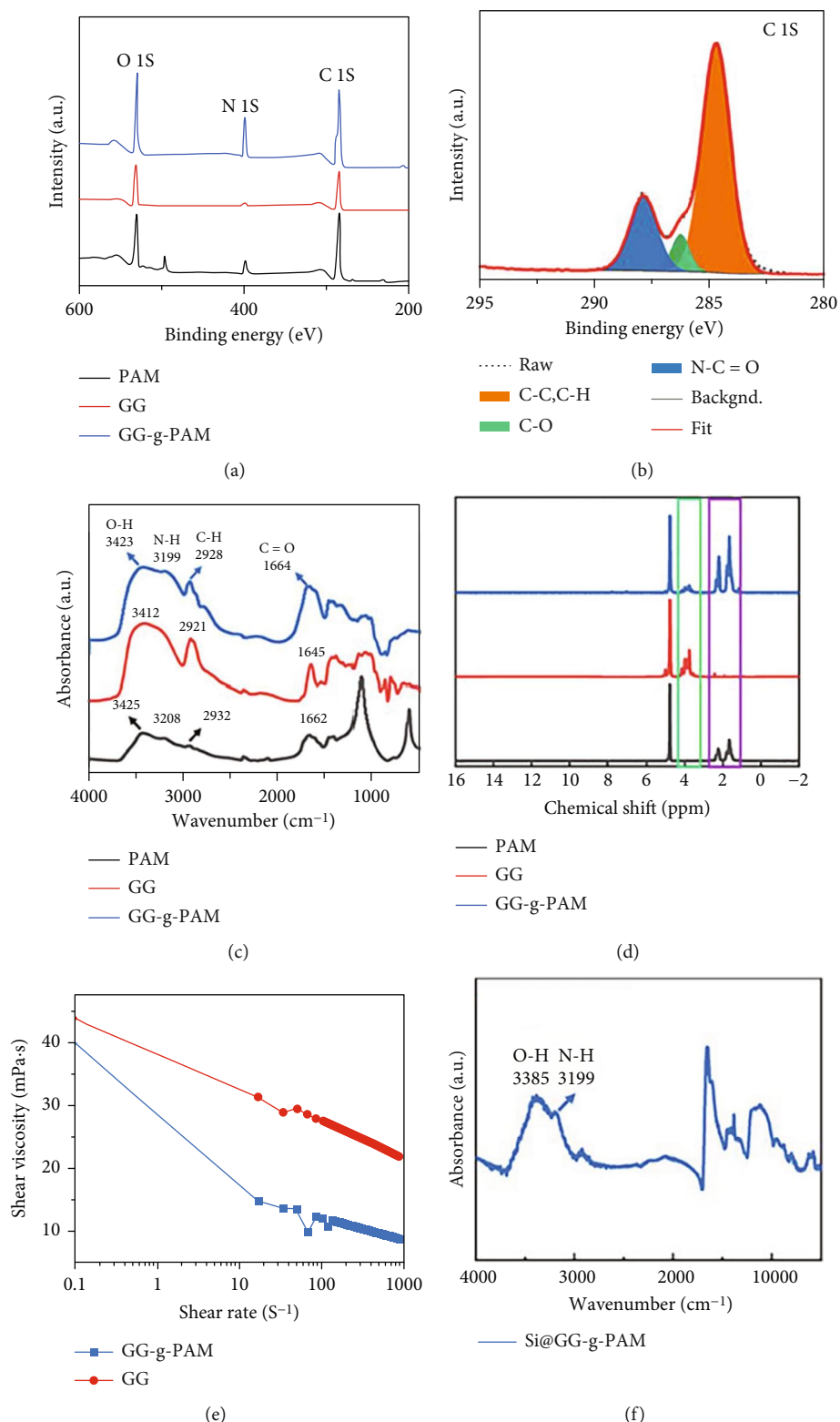


FIGURE 19: (a) X-ray photoelectron spectra of PAM, GG, and GG-g-PAM. (b) C 1s XPS spectrum of GG-g-PAM at high resolution. (c) Spectra of PAM, GG, and GG-g-PAM obtained using Fourier transform infrared spectroscopy. (d) Spectra of PAM, GG, and GG-g-PAM in ^1H NMR from liquid samples. (e) Measurements of the shear viscosity of 1% GG and GG-g-PAM solutions. (f) Infrared (IR) spectra of Si@GG-g-PAM taken with an FTIR spectrometer [204].

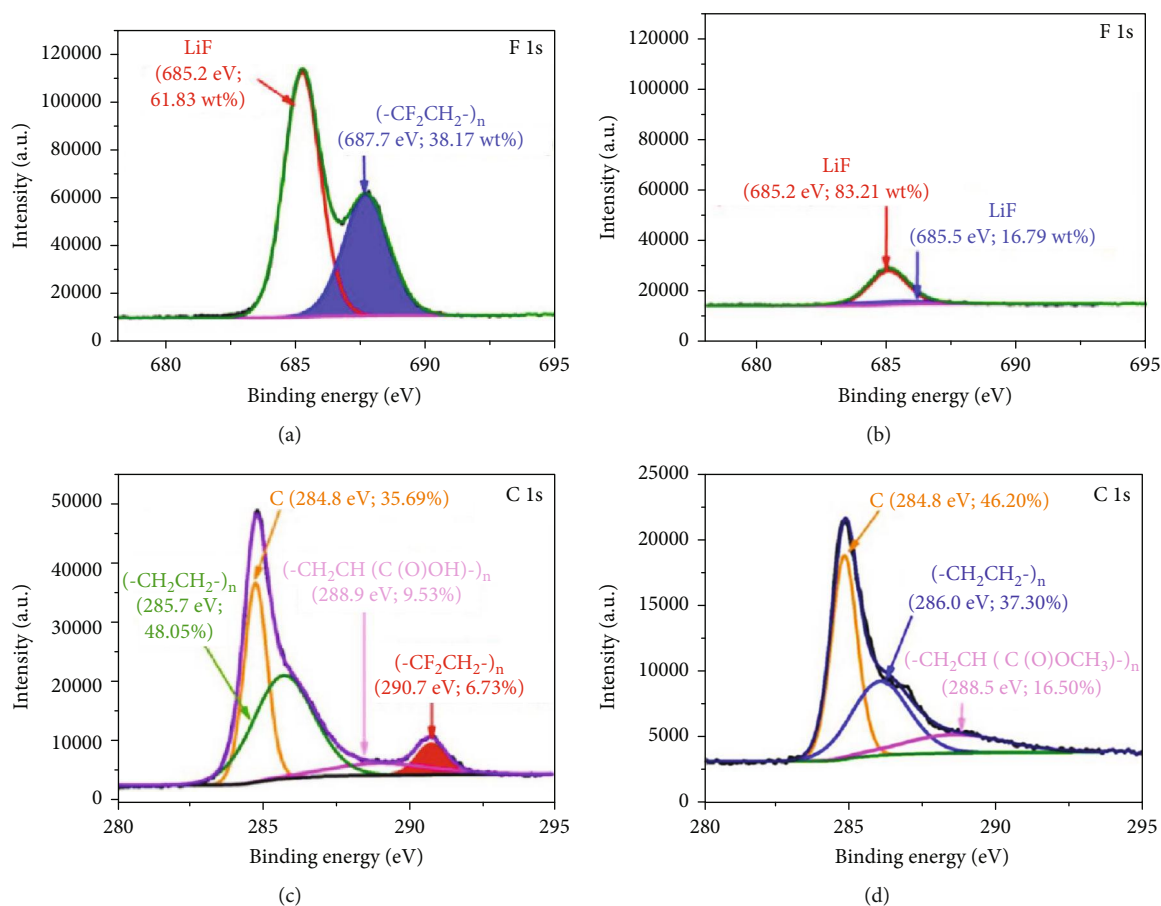


FIGURE 20: High-resolution X-ray photoelectron spectra of various spent LIB samples: (a) preheating F 1s spectra of the cathode electrode, (b) cathode electrode F 1s spectra after 30 minutes of heating in CaO at 300°C, (c) cathode electrode C 1s spectra prior to heating treatment, and (d) the cathode electrode's C 1s spectra after 30 min at 300°C in CaO [206].

peeling-off, scratching, SAICAS, and tensile tests. Various methods can be used to determine the effect of the binder on electrode integrity. However, because different parameters are applied, even if the same measurement is utilized, understanding the trend of the binder effect if the parameters are standardized may be beneficial. In addition, the established parameters are helpful in selecting a suitable binder for LIB electrodes of LIBs, and the advancement of LIBs may be accelerated.

3.3. Compositional Assessment. When comparing traditional PVDF, poly(vinyl alcohol) (PVA), and CMC-Na polymeric binders, Komaba et al. [201] found that a SiO composite electrode made with a polyacrylate binder performed the best. Based on X-ray photoelectron spectroscopy (XPS) analysis, unlike PVDF, the polyacrylate used as a binder completely coats the graphite particles, creating a uniform polyacrylate layer that acts as an artificial solid-electrolyte interphase and functionally modifies the interface between the graphite and electrolyte (SEI) [202, 203]. Figure 18 summarizes the XPS profiles of the SiO-PVDF and SiO-PAA composite electrodes prepared using various binders.

Li et al. [204] created GG-g-PAM by free-radical grafting of acrylamide (AM) onto the guar gum (GG) backbone to

create a stress-distribution binder with high ionic conductivity. A grafted GG-g-PAM binder was created using ceric ammonium nitrate as the initiator and GG and AM as the precursors in a free-radical reaction. X-ray photoelectron spectroscopy (XPS) and Fourier-transform infrared spectrometry (FTIR) (Figure 19) were used to validate GG-g-PAM synthesis. While the XPS spectrum of GG only confirms the presence of C and O, the sharp and powerful 1s peaks in the GG-g-PAM spectrum at 284, 399, and 531 eV provide direct evidence of elemental C, N, and O, respectively (Figure 19(a)). Three peaks of C-C and C-H at 284.7 eV, C-O at 286.3 eV, and N-C=O at 287.9 eV are visible in the deconvoluted high-resolution C 1s spectra of GG-g-PAM (Figure 19(b)).

For the first time, Liu et al. [205] used the biopolymer guar gum (GG) as a binder for a silicon nanoparticle (SiNP) anode of LIB. Fourier transform infrared (FTIR) spectra were obtained to examine the formation of polar hydrogen bonds between the active Si material and GG. Wang et al. [206] suggested using calcium oxide (CaO) as a reaction medium to reduce the thermal decomposition of PVDF in LIB cathodes. The F content was monitored by SEM-EDAX, F species conversion by XPS, and the PVDF decomposition temperature by TG-DSC. The F 1s

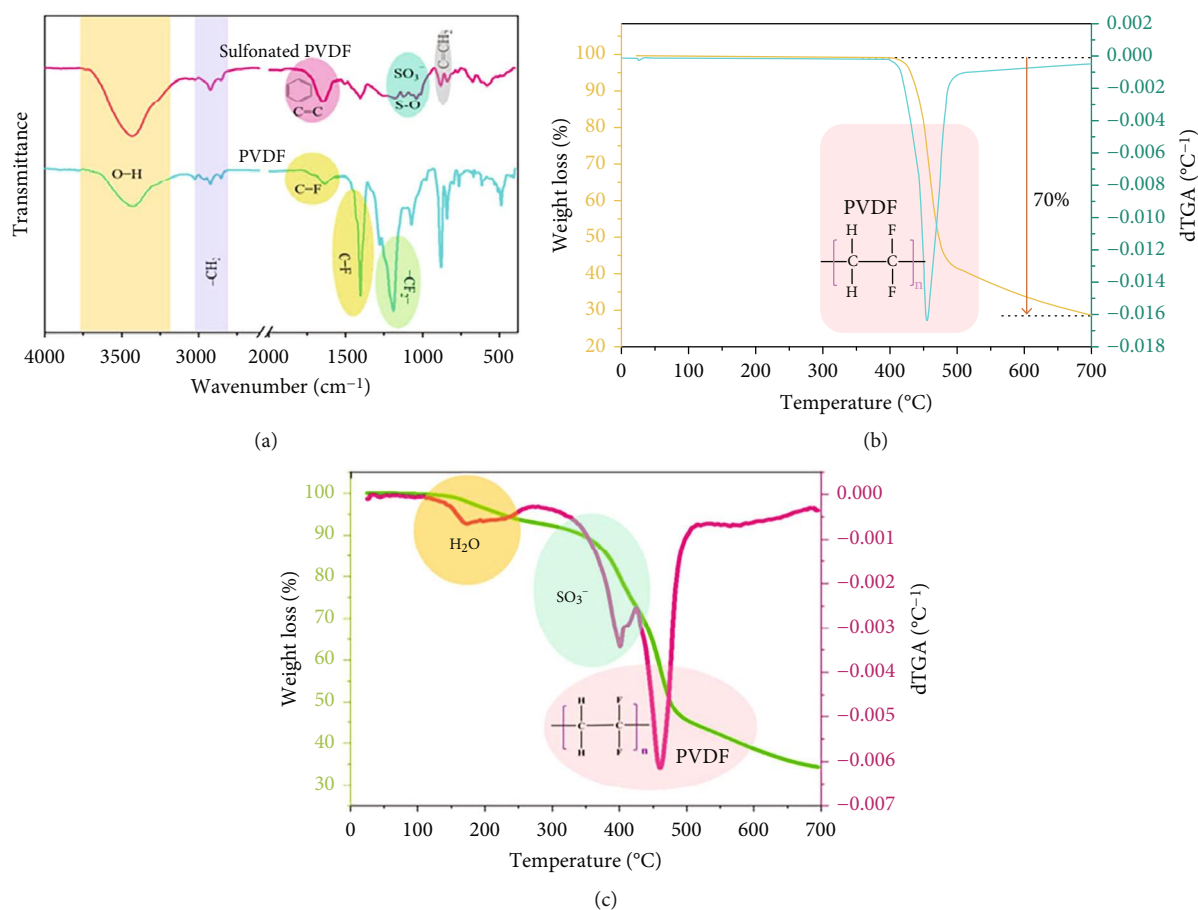


FIGURE 21: (a) PVDF and sulfonated PVDF's Fourier transform infrared (FTIR) spectra. TGA and dTGA curves for (b) polyvinylidene fluoride and (c) sulfonated polyvinylidene fluoride [207].

and C 1s binding energy changes in the spent LIB samples were examined using high-resolution XPS. Figure 20(a) shows that some F reacted with the highly active lithium during battery charging and discharging because the pre-heat treatment XPS high-resolution spectra of F 1s matched the characteristic binding energy peaks of LiF (685.2 eV) and PVDF (687.7 eV). After heating in CaO at 300°C, the binding energy peak intensity of F on the cathode electrode surface was significantly reduced, and the characteristic peaks of PVDF binding disappeared, leaving only a small amount of the characteristic peak of LiF (Figure 20(b)). At 300°C, PVDF decomposes. The high-resolution XPS spectrum (Figure 20(c)) of the cathode before heating showed that PVDF's binding energy peaked at 290.7 eV. The high-resolution XPS spectra (Figure 20(d)) of the cathode electrode after 300°C heating showed that PVDF's binding energy characteristic peak had disappeared.

Müller et al. [101] studied EDS to evaluate its applicability in revealing the binder distribution in LIB electrode films. To better understand the binder distribution in the LIB electrode films, EDS was performed under various conditions. Solvent removal involves subjecting graphite anodes made of carbon black and a PVDF binder to varying degrees of

drying to control the binder distributions. PVDF is detected in the presence of fluorine.

Ghahramani et al. [207] synthesized a sulfonated PVDF copolymer as an ion-conductive binder via an atom transfer radical polymerization (ATRP) procedure. Figure 21(a) shows the FTIR spectra of PVDF and sulfonated PVDF. The C-F family was assigned the peak at 1403 cm⁻¹. According to Qiu et al. [208], the 1187 cm⁻¹ peak is associated with the -CF₂- (stretching) subgroup. The -CH₂ stretching was correlated with the characteristic absorption peaks of PVDF and sulfonated PVDF, located at 2923 and 3023 cm⁻¹, respectively. We detected the unique vibrations of single bond C at 841 cm⁻¹, vinylidene groups at 879 cm⁻¹, and -CH₂ rocking bonds at 1071 cm⁻¹. Following the dehydrofluorination stage, the wide peaks at approximately 1652 cm⁻¹ in sulfonated PVDF were indicative of PSSA grafted.

The strong bonding between C-chitosan and Si nanoparticles, as demonstrated by the XPS measurements (Figure 22), was discussed by Yue et al. [209]. Despite repeated washing, a significant amount of C-chitosan remained on the surfaces of the Si nanoparticles. The authors proposed a strong hydrogen bonding mechanism between the carboxylic and amino groups of C-chitosan and the hydroxylated Si surface.

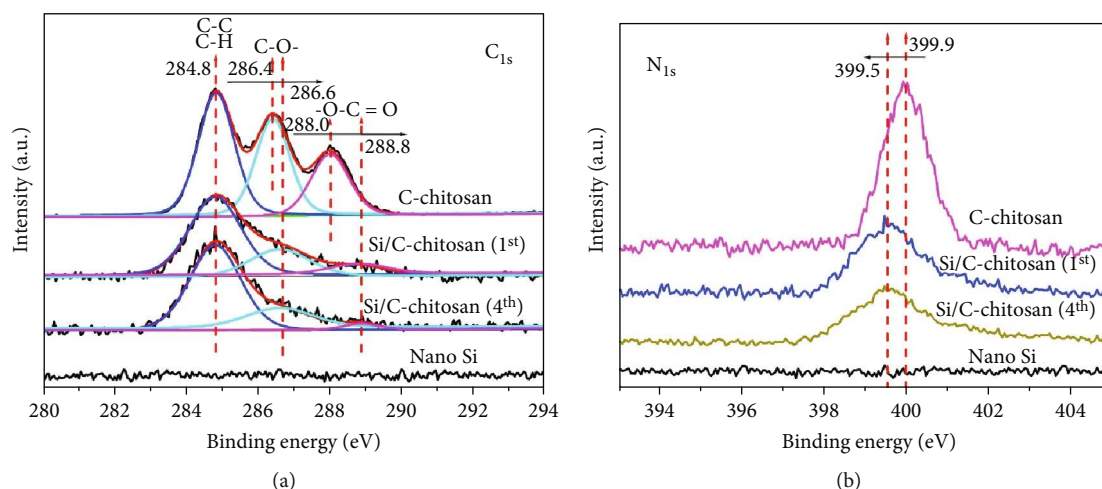


FIGURE 22: XPS spectra of C_{1s} (a) and N_{1s} (b) for C-chitosan, Si/C-chitosan (1st), Si/C-chitosan (4th), and Si nanopowder [209].

Hydrogen bonding between the binder and Si is critical for the cycling performance of Si-based electrodes.

4. Conclusions and Future Perspectives

With at least several decades of development of novel binder materials for LIB electrodes, various structural, morphological, mechanical, and compositional analyses have been performed. Many of these analyses have been employed to investigate the role of binder materials in detail, and significant progress has been made in this regard. For further analyses, the following aspects should be considered to more carefully examine the role of binder materials in electrode materials.

- (1) The combination of various analyses (spectroscopy, microscopy, and mechanical tests) is integral to better understanding novel binder materials in electrode design because each analysis has distinct advantages and disadvantages, thus making careful examination necessary
- (2) Assessment of the role of binder materials in electrodes at elevated temperatures (e.g., 25~55°C) and/or descending temperatures (e.g., -10~25°C) is important because it enables a more comprehensive understanding of binders in practical commercial batteries exposed to actual conditions with varying temperatures
- (3) Real-time (*in situ*) characterization of binder materials in the electrode during the charging and discharging processes, if visualized correctly, can further help to understand the practicality of the binder used for a particular electrode

The above considerations are expected to result in significant advances in binder materials for electrode design, thus leading to the development of more advanced electrode designs in the near future.

Data Availability

Data sharing is not applicable.

Conflicts of Interest

The authors declare that they have no conflicts of interest.

Authors' Contributions

Hyungsub Yoon, Promoda Behera, and Sooman Lim contributed equally to this work.

Acknowledgments

This work was supported by funding from the Bavarian Center for Battery Technology (BayBatt), Bayerisch-Tschechische Hochschulagentur (BTHA) (BTHA-AP-2022-45, BTHA-AP-2023-5, BTHA-AP-2023-12, and BTHA-AP-2023-38); the University of Bayreuth-Deakin University Joint Ph.D. Program, Bayerische Forschungsalianz (BayFOR) (BayIntAn_UBT_2023_84); the BK21 program from the National Research Foundation of Korea; the Erasmus+ program from the European Union, Ministry of Education, Science, and Technology as part of the Higher Education for Economic Transformation (HEET) Project (World Bank); Verband der Chemischen Industrie (Fonds der Chemischen Industrie, No. 661740); and collaboration project funding from Kangwon National University and the LINC 3.0 Research Center. This study was supported by the National Research Foundation of Korea (NRF) (No. NRF-2021K1A3A1A74096164).

References

- [1] Y. Tang, Y. Zhang, W. Li, B. Ma, and X. Chen, "Rational material design for ultrafast rechargeable lithium-ion batteries," *Chemical Society Reviews*, vol. 44, no. 17, pp. 5926–5940, 2015.

- [2] A. Manthiram, Y. Fu, and Y.-S. Su, "Challenges and prospects of lithium-sulfur batteries," *Accounts of Chemical Research*, vol. 46, no. 5, pp. 1125–1134, 2013.
- [3] J. B. Goodenough and K.-S. Park, "The Li-ion rechargeable battery: a perspective," *Journal of the American Chemical Society*, vol. 135, no. 4, pp. 1167–1176, 2013.
- [4] J. Zhao, G. Zhou, K. Yan et al., "Air-stable and freestanding lithium alloy/graphene foil as an alternative to lithium metal anodes," *Nature Nanotechnology*, vol. 12, no. 10, pp. 993–999, 2017.
- [5] A. S. Aricò, P. Bruce, B. Scrosati, J.-M. Tarascon, and W. van Schalkwijk, "Nanostructured materials for advanced energy conversion and storage devices," *Nature Materials*, vol. 4, no. 5, pp. 366–377, 2005.
- [6] M. Armand and J.-M. Tarascon, "Building better batteries," *Nature*, vol. 451, no. 7179, pp. 652–657, 2008.
- [7] V. Etacheri, R. Marom, R. Elazari, G. Salitra, and D. Aurbach, "Challenges in the development of advanced Li-ion batteries: a review," *Energy & Environmental Science*, vol. 4, no. 9, p. 3243, 2011.
- [8] K. Xu, "Electrolytes and interphases in Li-ion batteries and beyond," *Chemical Reviews*, vol. 114, no. 23, pp. 11503–11618, 2014.
- [9] J. Y. Cheong, J. H. Chang, S.-H. Cho et al., "High-rate formation cycle of Co₃O₄ nanoparticle for superior electrochemical performance in lithium-ion batteries," *Electrochimica Acta*, vol. 295, pp. 7–13, 2019.
- [10] M. Stevenson, S. Weiß, G. Cha et al., "Osmotically delaminated silicate nanosheet-coated NCM for ultra-stable Li⁺ storage and chemical stability toward long-term air exposure," *Small*, vol. 19, no. 39, article e2302617, 2023.
- [11] V. V. T. Padil and J. Y. Cheong, "Recent advances in the multifunctional natural gum-based binders for high-performance rechargeable batteries," *Energies*, vol. 15, no. 22, p. 8552, 2022.
- [12] Z. Piao, R. Gao, Y. Liu, G. Zhou, and H. M. Cheng, "A review on regulating Li⁺ solvation structures in carbonate electrolytes for lithium metal batteries," *Advanced Materials*, vol. 35, no. 15, article 2206009, 2023.
- [13] X. Ren, X. Zhang, Z. Shadiker et al., "Designing advanced in situ electrode/electrolyte interphases for wide temperature operation of 4.5 V Li||LiCoO₂ batteries," *Advanced Materials*, vol. 32, no. 49, article 2004898, 2020.
- [14] P. Xiao, X. Yun, Y. Chen et al., "Insights into the solvation chemistry in liquid electrolytes for lithium-based rechargeable batteries," *Chemical Society Reviews*, vol. 52, no. 15, pp. 5255–5316, 2023.
- [15] R. Wang, L. Feng, W. Yang et al., "Effect of different binders on the electrochemical performance of metal oxide anode for lithium-ion batteries," *Nanoscale Research Letters*, vol. 12, no. 1, p. 575, 2017.
- [16] Y. Shi, X. Zhou, and G. Yu, "Material and structural design of novel binder systems for high-energy, high-power lithium-ion batteries," *Accounts of Chemical Research*, vol. 50, no. 11, pp. 2642–2652, 2017.
- [17] N. S. Hochgatterer, M. R. Schweiger, S. Koller et al., "Silicon/graphite composite electrodes for high-capacity anodes: influence of binder chemistry on cycling stability," *Electrochemical and Solid-State Letters*, vol. 11, no. 5, article A76, 2008.
- [18] J. Y. Cheong, J. H. Chang, J. Choe, J. M. Yuk, and I.-D. Kim, "Bias-free graphene solid cell to realize the real-time observation on dynamical changes of electrodes," *Advanced Materials Interfaces*, vol. 10, no. 2, article 2201849, 2023.
- [19] J. Y. Cheong, J.-W. Jung, D.-Y. Youn et al., "Mesoporous orthorhombic Nb₂O₅ nanofibers as pseudocapacitive electrodes with ultra-stable Li storage characteristics," *Journal of Power Sources*, vol. 360, pp. 434–442, 2017.
- [20] J. Y. Cheong, A. Venkateshaiah, T. G. Yun et al., "Transforming gum wastes into high tap density micron-sized carbon with ultra-stable high-rate Li storage," *Electrochimica Acta*, vol. 367, article 137419, 2021.
- [21] J. Kim, J. Choi, K. Park et al., "Host-guest interlocked complex binder for silicon-graphite composite electrodes in lithium ion batteries," *Advanced Energy Materials*, vol. 12, no. 11, article 2103718, 2022.
- [22] T.-C. Kuo, C.-Y. Chiou, C.-C. Li, and J.-T. Lee, "In situ cross-linked poly(ether urethane) elastomer as a binder for high-performance Si anodes of lithium-ion batteries," *Electrochimica Acta*, vol. 327, article 135011, 2019.
- [23] Z. Wang, T. Huang, Z. Liu, and A. Yu, "Dopamine-modified carboxymethyl cellulose as an improved aqueous binder for silicon anodes in lithium-ion batteries," *Electrochimica Acta*, vol. 389, article 138806, 2021.
- [24] W.-C. Li, C.-H. Lin, C.-C. Ho, T.-T. Cheng, P.-H. Wang, and T.-C. Wen, "Superior performances of supercapacitors and lithium-ion batteries with carboxymethyl cellulose bearing zwitterions as binders," *Journal of the Taiwan Institute of Chemical Engineers*, vol. 133, article 104263, 2022.
- [25] X. Li, M. Fortunato, A. M. Cardinale, A. Sarapulova, C. Njel, and S. Dsoke, "Electrochemical study on nickel aluminum layered double hydroxides as high-performance electrode material for lithium-ion batteries based on sodium alginate binder," *Journal of Solid State Electrochemistry*, vol. 26, no. 1, pp. 49–61, 2022.
- [26] H. Aziam, S. Indris, M. Knapp, H. Ehrenberg, and I. Saadoun, "Synthesis, characterization, electrochemistry, and in situ X-ray diffraction investigation of Ni₃(PO₄)₂ as a negative electrode material for lithium-ion batteries," *ChemElectroChem*, vol. 7, no. 18, pp. 3866–3873, 2020.
- [27] L. Zuniga, G. Gonzalez, R. O. Chavez, J. C. Myers, T. P. Lodge, and M. Alcoutlabi, "Centrifugally spun α-Fe₂O₃/TiO₂/carbon composite fibers as anode materials for lithium-ion batteries," *Applied Sciences*, vol. 9, no. 19, p. 4032, 2019.
- [28] Q. Lemarié, E. Maire, H. Idrissi, P.-X. Thivel, F. Alloin, and L. Roué, "Sulfur-based electrode using a polyelectrolyte binder studied via coupled in situ synchrotron X-ray diffraction and tomography," *ACS Applied Energy Materials*, vol. 3, no. 3, pp. 2422–2431, 2020.
- [29] B. Chang, J. Kim, Y. Cho et al., "Highly elastic binder for improved cyclability of nickel-rich layered cathode materials in lithium-ion batteries," *Advanced Energy Materials*, vol. 10, no. 29, article 2001069, 2020.
- [30] D. J. Kirsch, S. D. Lacey, Y. Kuang et al., "Scalable dry processing of binder-free lithium-ion battery electrodes enabled by holey graphene," *ACS Applied Energy Materials*, vol. 2, no. 5, pp. 2990–2997, 2019.
- [31] G. Zhang, Y. He, H. Wang, Y. Feng, W. Xie, and X. Zhu, "Removal of organics by pyrolysis for enhancing liberation and flotation behavior of electrode materials derived from spent lithium-ion batteries," *ACS Sustainable Chemistry & Engineering*, vol. 8, no. 5, pp. 2205–2214, 2020.

- [32] S. Gao, F. Sun, A. Brady et al., "Ultra-efficient polymer binder for silicon anode in high-capacity lithium-ion batteries," *Nano Energy*, vol. 73, article 104804, 2020.
- [33] S. Lee, J. Park, J. Yang, and W. Lu, "Molecular dynamics simulations of the traction-separation response at the interface between PVDF binder and graphite in the electrode of Li-ion batteries," *Journal of The Electrochemical Society*, vol. 161, no. 9, pp. A1218–A1223, 2014.
- [34] G. G. Eshetu and E. Figgemeier, "Confronting the challenges of next-generation silicon anode-based lithium-ion batteries: role of designer electrolyte additives and polymeric binders," *ChemSusChem*, vol. 12, no. 12, pp. 2515–2539, 2019.
- [35] W. Kang, N. Deng, J. Ju et al., "A review of recent developments in rechargeable lithium-sulfur batteries," *Nanoscale*, vol. 8, no. 37, pp. 16541–16588, 2016.
- [36] B. Joshi, E. Samuel, Y.-i. Kim, A. L. Yarin, M. T. Swihart, and S. S. Yoon, "Progress and potential of electrospinning-derived substrate-free and binder-free lithium-ion battery electrodes," *Chemical Engineering Journal*, vol. 430, article 132876, 2022.
- [37] H. Cavers, P. Molaiyan, M. Abdollahifar, U. Lassi, and A. Kwade, "Perspectives on improving the safety and sustainability of high voltage lithium-ion batteries through the electrolyte and separator region," *Advanced Energy Materials*, vol. 12, no. 23, article 2200147, 2022.
- [38] L. Ibing, T. Gallasch, P. Schneider et al., "Towards water based ultra-thick Li ion battery electrodes – a binder approach," *Journal of Power Sources*, vol. 423, pp. 183–191, 2019.
- [39] N. Rey-Raap, M.-L. C. Piedboeuf, A. Arenillas, J. A. Menéndez, A. F. Léonard, and N. Job, "Aqueous and organic inks of carbon xerogels as models for studying the role of porosity in lithium-ion battery electrodes," *Materials & Design*, vol. 109, pp. 282–288, 2016.
- [40] Y. Cui, J. Chen, J. Zhao et al., "Aqueous lithium carboxymethyl cellulose and polyacrylic acid/acrylate copolymer composite binder for the $\text{LiNi}_{0.5}\text{Mn}_{0.3}\text{Co}_{0.2}\text{O}_2$ Cathode of lithium-ion batteries," *Journal of The Electrochemical Society*, vol. 169, no. 1, article 010513, 2022.
- [41] G. D. Salian, J. Højberg, C. Fink Elkjær et al., "Investigation of water-soluble binders for $\text{LiNi}_{0.5}\text{Mn}_{1.5}\text{O}_4$ -Based full cells," *ChemistryOpen*, vol. 11, no. 6, article e202200065, 2022.
- [42] Z. Li, A. Guo, and D. Liu, "Water-soluble conductive composite binder for high-performance silicon anode in lithium-ion batteries," *Batteries*, vol. 8, no. 6, p. 54, 2022.
- [43] J. Li, K. Yang, Y. Zheng et al., "Water-soluble polyamide acid binder with fast Li^+ transfer kinetics for silicon suboxide anodes in lithium-ion batteries," *ACS Applied Materials & Interfaces*, vol. 15, no. 25, pp. 30302–30311, 2023.
- [44] F. Zheng, Z. Tang, Y. Lei, R. Zhong, H. Chen, and R. Hong, "PAAS- β -CDP-PAA as a high-performance easily prepared and water-soluble composite binder for high-capacity silicon anodes in lithium-ion batteries," *Journal of Alloys and Compounds*, vol. 932, article 167666, 2023.
- [45] W. Jang, K. K. Rajeev, G. M. Thorat, S. Kim, Y. Kang, and T. H. Kim, "Lambda carrageenan as a water-soluble binder for silicon anodes in lithium-ion batteries," *ACS Sustainable Chemistry & Engineering*, vol. 10, no. 38, pp. 12620–12629, 2022.
- [46] M. Zheng, C. Wang, Y. Xu, K. Li, and D. Liu, "A water-soluble binary conductive binder for Si anode lithium ion battery," *Electrochimica Acta*, vol. 305, pp. 555–562, 2019.
- [47] S. Yang, Y. Huang, S. Su, G. Han, and J. Liu, "Hybrid humics/sodium carboxymethyl cellulose water-soluble binder for enhancing the electrochemical performance of a Li-ion battery cathode," *Powder Technology*, vol. 351, pp. 203–211, 2019.
- [48] Y. Liu, H. Wang, K. Yang et al., "Enhanced electrochemical performance of Sb_2O_3 as an anode for lithium-ion batteries by a stable cross-linked binder," *Applied Sciences*, vol. 9, no. 13, p. 2677, 2019.
- [49] H. Li, T. Yang, B. Jin et al., "Enhanced reversible capability of a macroporous $\text{ZnMn}_2\text{O}_4/\text{C}$ microsphere anode with a water-soluble binder for long-life and high-rate lithium-ion storage," *Inorganic Chemistry Frontiers*, vol. 6, no. 6, pp. 1535–1545, 2019.
- [50] Y. Yang, S. Wu, Y. Zhang et al., "Towards efficient binders for silicon based lithium-ion battery anodes," *Chemical Engineering Journal*, vol. 406, article 126807, 2021.
- [51] H. Chen, M. Ling, L. Hencz et al., "Exploring chemical, mechanical, and electrical functionalities of binders for advanced energy-storage devices," *Chemical Reviews*, vol. 118, no. 18, pp. 8936–8982, 2018.
- [52] N. Lingappan, L. Kong, and M. Pecht, "The significance of aqueous binders in lithium-ion batteries," *Renewable and Sustainable Energy Reviews*, vol. 147, article 111227, 2021.
- [53] J.-T. Li, Z. Y. Wu, Y. Q. Lu et al., "Water soluble binder, an electrochemical performance booster for electrode materials with high energy density," *Advanced Energy Materials*, vol. 7, no. 24, article 1701185, 2017.
- [54] J. Song, M. Zhou, R. Yi et al., "Interpenetrated gel polymer binder for high-performance silicon anodes in lithium-ion batteries," *Advanced Functional Materials*, vol. 24, no. 37, pp. 5904–5910, 2014.
- [55] P. Mandal, K. Stokes, G. Hernández, D. Brandell, and J. Mindemark, "Influence of binder crystallinity on the performance of Si electrodes with poly(vinyl alcohol) binders," *ACS Applied Energy Materials*, vol. 4, no. 4, pp. 3008–3016, 2021.
- [56] Y.-B. Wang, Q. Yang, X. Guo et al., "Strategies of binder design for high-performance lithium-ion batteries: a mini review," *Rare Metals*, vol. 41, no. 3, pp. 745–761, 2022.
- [57] M. He, L.-X. Yuan, W.-X. Zhang, X.-L. Hu, and Y.-H. Huang, "Enhanced cyclability for sulfur cathode achieved by a water-soluble binder," *The Journal of Physical Chemistry C*, vol. 115, no. 31, pp. 15703–15709, 2011.
- [58] C. Chen, S. H. Lee, M. Cho, J. Kim, and Y. Lee, "Cross-linked chitosan as an efficient binder for Si anode of Li-ion batteries," *ACS Applied Materials & Interfaces*, vol. 8, no. 4, pp. 2658–2665, 2016.
- [59] Y.-M. Zhao, F.-S. Yue, S.-C. Li et al., "Advances of polymer binders for silicon-based anodes in high energy density lithium-ion batteries," *InfoMat*, vol. 3, no. 5, pp. 460–501, 2021.
- [60] Z.-H. Wu, J.-Y. Yang, B. Yu, B.-M. Shi, C.-R. Zhao, and Z.-L. Yu, "Self-healing alginate-carboxymethyl chitosan porous scaffold as an effective binder for silicon anodes in lithium-ion batteries," *Rare Metals*, vol. 38, no. 9, pp. 832–839, 2019.
- [61] J. He, C. Das, F. Yang, and J. Maibach, "Crosslinked poly(acrylic acid) enhances adhesion and electrochemical performance of Si anodes in Li-ion batteries," *Electrochimica Acta*, vol. 411, article 140038, 2022.

- [62] C. Luo, L. Du, W. Wu et al., "Novel lignin-derived water-soluble binder for micro silicon anode in lithium-ion batteries," *ACS Sustainable Chemistry & Engineering*, vol. 6, no. 10, pp. 12621–12629, 2018.
- [63] M. Akhlaq, U. Mushtaq, S. Naz, and M. Uroos, "Carboxymethyl cellulose-based materials as an alternative source for sustainable electrochemical devices: a review," *RSC Advances*, vol. 13, no. 9, pp. 5723–5743, 2023.
- [64] A. Saal, T. Hagemann, and U. S. Schubert, "Polymers for battery applications—active materials, membranes, and binders," *Advanced Energy Materials*, vol. 11, no. 43, article 2001984, 2021.
- [65] T. Rasheed, M. T. Anwar, A. Naveed, and A. Ali, "Biopolymer based materials as alternative greener binders for sustainable electrochemical energy storage applications," *ChemistrySelect*, vol. 7, no. 39, article e202203202, 2022.
- [66] M. T. Musa, N. Shaari, S. K. Kamarudin, and W. Y. Wong, "Recent biopolymers used for membrane fuel cells: characterization analysis perspectives," *International Journal of Energy Research*, vol. 46, no. 12, pp. 16178–16207, 2022.
- [67] Z. A. Sutirman, M. M. Sanagi, and W. I. Wan Aini, "Alginate-based adsorbents for removal of metal ions and radionuclides from aqueous solutions: a review," *International Journal of Biological Macromolecules*, vol. 174, pp. 216–228, 2021.
- [68] C. Wang, N. E. B. Surat'man, J. J. Chang et al., "Polyelectrolyte hydrogels for tissue engineering and regenerative medicine," *Chemistry-An Asian Journal*, vol. 17, no. 18, article e202200604, 2022.
- [69] E. Lizundia and D. Kundu, "Advances in natural biopolymer-based electrolytes and separators for battery applications," *Advanced Functional Materials*, vol. 31, no. 3, article 2005646, 2021.
- [70] X. Li, C. Ding, X. Li et al., "Electronic biopolymers: from molecular engineering to functional devices," *Chemical Engineering Journal*, vol. 397, article 125499, 2020.
- [71] L. Lan, J. Ping, J. Xiong, and Y. Ying, "Sustainable natural bio-origin materials for future flexible devices," *Advanced Science*, vol. 9, no. 15, article e2200560, 2022.
- [72] R. Sahore, M. Wood, A. Kukay et al., "Performance of different water-based binder formulations for Ni-rich cathodes evaluated in $\text{LiNi}_{0.8}\text{Mn}_{0.1}\text{Co}_{0.1}\text{O}_2$ /Graphite pouch cells," *Journal of The Electrochemical Society*, vol. 169, no. 4, article 040567, 2022.
- [73] L. Zhao, C. Hong, C. Wang, J. Li, H. Ren, and C. Zhou, "Enhancement of the adhesion strength of water-based ink binder based on waterborne polyurethane," *Progress in Organic Coatings*, vol. 183, article 107765, 2023.
- [74] S. Zilinskaite, N. Reeves-McLaren, and R. Boston, "Xanthan gum as a water-based binder for $\text{P3-Na}_{2/3}\text{Ni}_{1/3}\text{Mn}_{2/3}\text{O}_2$," *Frontiers in Energy Research*, vol. 10, article 909486, 2022.
- [75] C. D. Reynolds, J. Lam, L. Yang, and E. Kendrick, "Extensional rheology of battery electrode slurries with water-based binders," *Materials & Design*, vol. 222, article 111104, 2022.
- [76] M. E. Bazaldua-Medellin, R. X. Magallanes-Rivera, and J. I. E. Garcia, "Composite hydraulic binders based on fluorgypsum: reactions, properties and sustainability," *Journal of Building Engineering*, vol. 53, article 104590, 2022.
- [77] L. B. Pereira, C. M. S. Sad, E. V. R. Castro, P. R. Filgueiras, and V. Lacerda, "Environmental impacts related to drilling fluid waste and treatment methods: a critical review," *Fuel*, vol. 310, article 122301, Part B, 2022.
- [78] H. Abd El-Wahab, G. El-Meligi, M. G. Hassaan, A. Kazlauciuonas, and L. Lin, "New water-based copolymer nanoparticles and their use as eco-friendly binders for industry of flexographic ink, part I," *Pigment & Resin Technology*, vol. 49, no. 3, pp. 239–248, 2020.
- [79] S. M. Koch, M. Pillon, T. Keplinger, C. H. Dreimol, S. Weinkötz, and I. Burgert, "Intercellular matrix infiltration improves the wet strength of delignified wood composites," *ACS Applied Materials & Interfaces*, vol. 14, no. 27, pp. 31216–31224, 2022.
- [80] S. Sudhakaran and T. K. Bijoy, "A comprehensive review of current and emerging binder technologies for energy storage applications," *ACS Applied Energy Materials*, vol. 6, no. 23, pp. 11773–11794, 2023.
- [81] N. M. Shinde, P. V. Shinde, R. S. Mane, and K. H. Kim, "Solution-method processed Bi-type nanoelectrode materials for supercapacitor applications: a review," *Renewable and Sustainable Energy Reviews*, vol. 135, article 110084, 2021.
- [82] N. Su, L. Lou, A. Amirkhanian, S. N. Amirkhanian, and F. Xiao, "Assessment of effective patching material for concrete bridge deck - a review," *Construction and Building Materials*, vol. 293, article 123520, 2021.
- [83] N.-S. Oh, D.-J. Kim, J. L. Ong, H.-Y. Lee, and K.-W. Lee, "Properties and cyclic fatigue of glass infiltrated tape cast alumina cores produced using a water-based solvent," *Dental Materials*, vol. 23, no. 4, pp. 442–449, 2007.
- [84] M. Enekvist, X. Liang, X. Zhang, K. Dam-Johansen, and G. M. Kontogeorgis, "Computer-aided design and solvent selection for organic paint and coating formulations," *Progress in Organic Coatings*, vol. 162, article 106568, 2022.
- [85] F. Fei, L. Kirby, A. Gralczyk, and X. Song, "Binder-free additive manufacturing of ceramics using hydrothermal-assisted jet fusion," *Journal of the European Ceramic Society*, vol. 43, no. 14, pp. 6308–6320, 2023.
- [86] C. G. Kolb, A. Sommer, M. Lehmann et al., "The role of binders for water-based anode dispersions in inkjet printing," *Batteries*, vol. 9, no. 11, p. 557, 2023.
- [87] M. Kurniawan and S. Ivanov, "Electrochemically structured copper current collectors for application in energy conversion and storage: a review," *Energies*, vol. 16, no. 13, p. 4933, 2023.
- [88] K. Shen, Q. Zhai, Y. Gu et al., "Life cycle assessment of lithium ion battery from water-based manufacturing for electric vehicles," *Resources, Conservation and Recycling*, vol. 198, article 107152, 2023.
- [89] D. Cheng, P. Ni, D. Qin et al., "A water-based binder with 3D network enabling long-cycle-life silicon/graphite composite anode materials for lithium ion batteries," *Solid State Ionics*, vol. 399, article 116289, 2023.
- [90] L. Qiu, Z. Shao, D. Wang, F. Wang, W. Wang, and J. Wang, "Novel polymer Li-ion binder carboxymethyl cellulose derivative enhanced electrochemical performance for Li-ion batteries," *Carbohydrate Polymers*, vol. 112, pp. 532–538, 2014.
- [91] Y. Zhang, A. Grant, A. Carroll et al., "Water-soluble binders that improve electrochemical sodium-ion storage properties in a $\text{NaTi}_2(\text{PO}_4)_3$ Anode," *Journal of The Electrochemical Society*, vol. 170, no. 5, article 050529, 2023.

- [92] D. Kasprzak and M. Galiński, "Chitin as a universal and sustainable electrode binder for electrochemical capacitors," *Journal of Power Sources*, vol. 553, article 232300, 2023.
- [93] L. Qiu, W. Yang, X. B. Hu, and W. S. Li, "High performance study of lithium carboxymethylcellulose as water-soluble binder for lithium supplementation in lithium batteries," *Starch - Stärke*, vol. 74, no. 7-8, article 2200049, 2022.
- [94] D. L. Wood, J. Li, and C. Daniel, "Prospects for reducing the processing cost of lithium ion batteries," *Journal of Power Sources*, vol. 275, pp. 234–242, 2015.
- [95] L. Airoidi, R. Bruculeri, P. Baldini et al., "3D printing of copper using water-based colloids and reductive sintering," *3D Printing and Additive Manufacturing*, vol. 10, no. 3, pp. 559–568, 2023.
- [96] M. Zackrisson, L. Avellán, and J. Orlenius, "Life cycle assessment of lithium-ion batteries for plug-in hybrid electric vehicles – critical issues," *Journal of Cleaner Production*, vol. 18, no. 15, pp. 1519–1529, 2010.
- [97] J. M. Kim, V. Guccini, K. Seong, J. Oh, G. Salazar-Alvarez, and Y. Piao, "Extensively interconnected silicon nanoparticles via carbon network derived from ultrathin cellulose nanofibers as high performance lithium ion battery anodes," *Carbon*, vol. 118, pp. 8–17, 2017.
- [98] A. Magasinski, B. Zdyrko, I. Kovalenko et al., "Toward efficient binders for Li-ion battery Si-based anodes: polyacrylic acid," *ACS Applied Materials & Interfaces*, vol. 2, no. 11, pp. 3004–3010, 2010.
- [99] J. Li, R. B. Lewis, and J. R. Dahn, "Sodium carboxymethyl cellulose," *Electrochemical and Solid-State Letters*, vol. 10, no. 2, article A17, 2007.
- [100] W. J. Chang, G. H. Lee, Y. J. Cheon et al., "Direct observation of carboxymethyl cellulose and styrene-butadiene rubber binder distribution in practical graphite anodes for Li-ion batteries," *ACS Applied Materials & Interfaces*, vol. 11, no. 44, pp. 41330–41337, 2019.
- [101] M. Müller, L. Pfaffmann, S. Jaiser et al., "Investigation of binder distribution in graphite anodes for lithium-ion batteries," *Journal of Power Sources*, vol. 340, pp. 1–5, 2017.
- [102] J.-N. Wu, H.-X. Chen, C. Chen, H.-D. Li, H.-W. Zhang, and B. Wang, "Construction of dual crosslinked network binder via sequential ionic crosslinking for high-performance silicon anodes," *Rare Metals*, vol. 42, no. 7, pp. 2238–2249, 2023.
- [103] X. Zeng, H. Yue, J. Wu, C. Chen, and L. Liu, "Hybrid ionically covalently cross-linked network binder for high-performance silicon anodes in lithium-ion batteries," *Batteries*, vol. 9, no. 5, p. 276, 2023.
- [104] S. Hu, Z. Cai, T. Huang, H. Zhang, and A. Yu, "A modified natural polysaccharide as a high-performance binder for silicon anodes in lithium-ion batteries," *ACS Applied Materials & Interfaces*, vol. 11, no. 4, pp. 4311–4317, 2019.
- [105] S. Wang, Q. Liu, C. Zhao et al., "Advances in understanding materials for rechargeable lithium batteries by atomic force microscopy," *Energy & Environmental Materials*, vol. 1, no. 1, pp. 28–40, 2018.
- [106] A. Oishi, R. Tatara, E. Togo, H. Inoue, S. Yasuno, and S. Komaba, "Sulfated alginate as an effective polymer binder for high-voltage $\text{LiNi}_{0.5}\text{Mn}_{1.5}\text{O}_4$ electrodes in lithium-ion batteries," *ACS Applied Materials & Interfaces*, vol. 14, no. 46, pp. 51808–51818, 2022.
- [107] M. Akshay, K. Subramanyan, M. L. Divya, Y. S. Lee, and V. Aravindan, "Choice of binder on conversion type CuO nanoparticles toward building high energy Li-ion capacitors: an approach beyond intercalation," *Advanced Materials Technologies*, vol. 7, no. 9, article 2200423, 2022.
- [108] H. Zheng, L. Zhang, G. Liu, X. Song, and V. S. Battaglia, "Correlation between electrode mechanics and long-term cycling performance for graphite anode in lithium ion cells," *Journal of Power Sources*, vol. 217, pp. 530–537, 2012.
- [109] Y. Wang, D. Dang, D. Li, J. Hu, and Y.-T. Cheng, "Influence of polymeric binders on mechanical properties and microstructure evolution of silicon composite electrodes during electrochemical cycling," *Journal of Power Sources*, vol. 425, pp. 170–178, 2019.
- [110] Y. Ma, K. Chen, J. Ma et al., "A biomass based free radical scavenger binder endowing a compatible cathode interface for 5 V lithium-ion batteries," *Energy & Environmental Science*, vol. 12, no. 1, pp. 273–280, 2019.
- [111] N. P. W. Pieczonka, V. Borgel, B. Ziv et al., "Lithium polyacrylate (LiPAA) as an advanced binder and a passivating agent for high-voltage Li-ion batteries," *Advanced Energy Materials*, vol. 5, no. 23, article 1501008, 2015.
- [112] Z. Li, Y. Zhang, T. Liu et al., "Silicon anode with high initial coulombic efficiency by modulated trifunctional binder for high-areal-capacity lithium-ion batteries," *Advanced Energy Materials*, vol. 10, no. 20, article 1903110, 2020.
- [113] D. Munao, J. W. M. van Erven, M. Valvo, E. Garcia-Tamayo, and E. M. Kelder, "Role of the binder on the failure mechanism of Si nano-composite electrodes for Li-ion batteries," *Journal of Power Sources*, vol. 196, no. 16, pp. 6695–6702, 2011.
- [114] C. Toigo, M. Singh, B. Gmeiner, M. Biso, and K. H. Pettinger, "A method to measure the swelling of water-soluble PVDF binder system and its electrochemical performance for lithium ion batteries," *Journal of The Electrochemical Society*, vol. 167, no. 2, article 020514, 2020.
- [115] J.-. T. Wang, C.-. C. Wan, and J.-. L. Hong, "Polymer blends of pectin/poly(acrylic acid) as efficient binders for silicon anodes in lithium-ion batteries," *ChemElectroChem*, vol. 7, no. 14, pp. 3106–3115, 2020.
- [116] M.-H. Ryou, J. Kim, I. Lee et al., "Mussel-inspired adhesive binders for high-performance silicon nanoparticle anodes in lithium-ion batteries," *Advanced Materials*, vol. 25, no. 11, pp. 1571–1576, 2013.
- [117] G. Zhang, Y. Yang, Y. Chen et al., "A quadruple-hydrogen-bonded supramolecular binder for high-performance silicon anodes in lithium-ion batteries," *Small*, vol. 14, no. 29, article 1801189, 2018.
- [118] N. Yuca, H. Zhao, X. Song et al., "A systematic investigation of polymer binder flexibility on the electrode performance of lithium-ion batteries," *ACS Applied Materials & Interfaces*, vol. 6, no. 19, pp. 17111–17118, 2014.
- [119] J. Chen, J. Liu, Y. Qi, T. Sun, and X. Li, "Unveiling the roles of binder in the mechanical integrity of electrodes for lithium-ion batteries," *Journal of The Electrochemical Society*, vol. 160, no. 9, pp. A1502–A1509, 2013.
- [120] S. N. S. Hapuarachchi, K. C. Wasalathilake, J. Y. Nerkar, E. Jaatinen, A. P. O'Mullane, and C. Yan, "Mechanically robust tapioca starch composite binder with improved ionic conductivity for sustainable lithium-ion batteries," *ACS Sustainable Chemistry & Engineering*, vol. 8, no. 26, pp. 9857–9865, 2020.
- [121] M. Yoo, C. W. Frank, S. Mori, and S. Yamaguchi, "Effect of poly(vinylidene fluoride) binder crystallinity and graphite

- structure on the mechanical strength of the composite anode in a lithium ion battery,” *Polymer*, vol. 44, no. 15, pp. 4197–4204, 2003.
- [122] S. Byun, J. Choi, Y. Roh, D. Song, M.-H. Ryou, and Y. M. Lee, “Mechanical robustness of composite electrode for lithium ion battery: insight into entanglement & crystallinity of polymeric binder,” *Electrochimica Acta*, vol. 332, article 135471, 2020.
- [123] B. Son, M.-H. Ryou, J. Choi et al., “Measurement and analysis of adhesion property of lithium-ion battery electrodes with SAICAS,” *ACS Applied Materials & Interfaces*, vol. 6, no. 1, pp. 526–531, 2014.
- [124] K. Kim, S. Byun, J. Choi, S. Hong, M.-H. Ryou, and Y. M. Lee, “Elucidating the polymeric binder distribution within lithium-ion battery electrodes using SAICAS,” *ChemPhysChem*, vol. 19, no. 13, pp. 1627–1634, 2018.
- [125] R. Tang, X. Zheng, Y. Zhang et al., “Highly adhesive and stretchable binder for silicon-based anodes in Li-ion batteries,” *Ionics*, vol. 26, no. 12, pp. 5889–5896, 2020.
- [126] Z. H. Xie, M. Z. Rong, and M. Q. Zhang, “Dynamically cross-linked polymeric binder-made durable silicon anode of a wide operating temperature Li-ion battery,” *ACS Applied Materials & Interfaces*, vol. 13, no. 24, pp. 28737–28748, 2021.
- [127] Q. Huang, C. Wan, M. Loveridge, and R. Bhagat, “Partially neutralized polyacrylic acid/poly(vinyl alcohol) blends as effective binders for high-performance silicon anodes in lithium-ion batteries,” *ACS Applied Energy Materials*, vol. 1, no. 12, pp. 6890–6898, 2018.
- [128] X. Zhu, F. Zhang, L. Zhang et al., “A highly stretchable cross-linked polyacrylamide hydrogel as an effective binder for silicon and sulfur electrodes toward durable lithium-ion storage,” *Advanced Functional Materials*, vol. 28, no. 11, article 1705015, 2018.
- [129] S. H. Lee, J. H. Lee, D. H. Nam et al., “Epoxidized natural rubber/chitosan network binder for silicon anode in lithium-ion battery,” *ACS Applied Materials & Interfaces*, vol. 10, no. 19, pp. 16449–16457, 2018.
- [130] Y. Wen and H. Zhang, “Highly stretchable polymer binder engineered with polysaccharides for silicon microparticles as high-performance anodes,” *ChemSusChem*, vol. 13, no. 15, pp. 3887–3892, 2020.
- [131] M. Jia, X. Qin, X. Zhang et al., “Novel rigid-flexible hydrogenated carboxyl nitrile rubber-guar gum binder for ultra-long cycle silicon anodes in lithium-ion batteries,” *Journal of Power Sources*, vol. 561, article 232759, 2023.
- [132] D. Chen, Z. Lou, K. Jiang, and G. Shen, “Device configurations and future prospects of flexible/stretchable lithium-ion batteries,” *Advanced Functional Materials*, vol. 28, no. 51, article 1805596, 2018.
- [133] H. Li, H. Wang, D. Chan et al., “Nature-inspired materials and designs for flexible lithium-ion batteries,” *Carbon Energy*, vol. 4, no. 5, pp. 878–900, 2022.
- [134] Y.-F. Zhang, M.-M. Guo, Y. Zhang et al., “Flexible, stretchable and conductive PVA/PEDOT:PSS composite hydrogels prepared by SIPN strategy,” *Polymer Testing*, vol. 81, article 106213, 2020.
- [135] P. Niu, N. Bao, H. Zhao et al., “Room-temperature self-healing elastomer-graphene composite conducting wires with superior strength for stretchable electronics,” *Composites Science and Technology*, vol. 219, article 109261, 2022.
- [136] L. Liang, C. Gao, G. Chen, and C.-Y. Guo, “Large-area, stretchable, super flexible and mechanically stable thermoelectric films of polymer/carbon nanotube composites,” *Journal of Materials Chemistry C*, vol. 4, no. 3, pp. 526–532, 2016.
- [137] D. Rodriguez, J.-H. Kim, S. E. Root et al., “Comparison of methods for determining the mechanical properties of semi-conducting polymer films for stretchable electronics,” *ACS Applied Materials & Interfaces*, vol. 9, no. 10, pp. 8855–8862, 2017.
- [138] D. Dang, Y. Wang, M. Wang, J. Hu, C. Ban, and Y.-T. Cheng, “Lithium substituted poly(acrylic acid) as a mechanically robust binder for low-cost silicon microparticle electrodes,” *ACS Applied Energy Materials*, vol. 3, no. 11, pp. 10940–10949, 2020.
- [139] D. S. Shin, Y. S. Kim, and E. S. Jeon, “Approximation of non-linear stress-strain curve for GFRP tensile specimens by inverse method,” *Applied Sciences*, vol. 9, no. 17, p. 3474, 2019.
- [140] X. Zhong, J. Han, L. Chen et al., “Binding mechanisms of PVDF in lithium ion batteries,” *Applied Surface Science*, vol. 553, article 149564, 2021.
- [141] E. Markevich, G. Salitra, and D. Aurbach, “Influence of the PVDF binder on the stability of LiCoO₂ electrodes,” *Electrochemistry Communications*, vol. 7, no. 12, pp. 1298–1304, 2005.
- [142] N. Iqbal and S. Lee, “Mechanical failure analysis of graphite anode particles with PVDF binders in Li-ion batteries,” *Journal of The Electrochemical Society*, vol. 165, no. 9, pp. A1961–A1970, 2018.
- [143] Z. Chen, L. Christensen, and J. R. Dahn, “Comparison of PVDF and PVDF-TFE-P as binders for electrode materials showing large volume changes in lithium-ion batteries,” *Journal of The Electrochemical Society*, vol. 150, no. 8, article A1073, 2003.
- [144] Z. Wang, N. Dupré, A.-C. Gaillot et al., “CMC as a binder in LiNi_{0.4}Mn_{1.6}O₄ 5V cathodes and their electrochemical performance for Li-ion batteries,” *Electrochimica Acta*, vol. 62, pp. 77–83, 2012.
- [145] L. Qiu, Z. Shao, D. Wang, F. Wang, W. Wang, and J. Wang, “Carboxymethyl cellulose lithium (CMC-Li) as a novel binder and its electrochemical performance in lithium-ion batteries,” *Cellulose*, vol. 21, no. 4, pp. 2789–2796, 2014.
- [146] L. Qiu, Z. Shao, D. Wang, W. Wang, F. Wang, and J. Wang, “Enhanced electrochemical properties of LiFePO₄ (LFP) cathode using the carboxymethyl cellulose lithium (CMC-Li) as novel binder in lithium-ion battery,” *Carbohydrate Polymers*, vol. 111, pp. 588–591, 2014.
- [147] B. Hu, I. A. Shkrob, S. Zhang et al., “The existence of optimal molecular weight for poly(acrylic acid) binders in silicon/graphite composite anode for lithium-ion batteries,” *Journal of Power Sources*, vol. 378, pp. 671–676, 2018.
- [148] B. Hu, S. Jiang, I. A. Shkrob et al., “Understanding of pre-lithiation of poly(acrylic acid) binder: striking the balances between the cycling performance and slurry stability for silicon-graphite composite electrodes in Li-ion batteries,” *Journal of Power Sources*, vol. 416, pp. 125–131, 2019.
- [149] B. Gendensuren and E.-S. Oh, “Dual-crosslinked network binder of alginate with polyacrylamide for silicon/graphite anodes of lithium ion battery,” *Journal of Power Sources*, vol. 384, pp. 379–386, 2018.

- [150] S. Zhang, S. Ren, D. Han, M. Xiao, S. Wang, and Y. Meng, "Aqueous sodium alginate as binder: dramatically improving the performance of dilithium terephthalate-based organic lithium ion batteries," *Journal of Power Sources*, vol. 438, article 227007, 2019.
- [151] M. M. Loghavi, S. Bahadorikhalili, N. Lari, M. H. Moghim, M. Babaiee, and R. Eqra, "The effect of crystalline microstructure of PVDF binder on mechanical and electrochemical performance of lithium-ion batteries cathode," *Zeitschrift für Physikalische Chemie*, vol. 234, no. 3, pp. 381–397, 2020.
- [152] M. Benz and W. B. Euler, "Determination of the crystalline phases of poly(vinylidene fluoride) under different preparation conditions using differential scanning calorimetry and infrared spectroscopy," *Journal of Applied Polymer Science*, vol. 89, no. 4, pp. 1093–1100, 2003.
- [153] D. W. Chae and S. M. Hong, "Rheology, crystallization behavior under shear, and resultant morphology of PVDF/multiwalled carbon nanotube composites," *Macromolecular Research*, vol. 19, no. 4, pp. 326–331, 2011.
- [154] W. Haselrieder, B. Westphal, H. Bockholt, A. Diener, S. Höft, and A. Kwade, "Measuring the coating adhesion strength of electrodes for lithium-ion batteries," *International Journal of Adhesion and Adhesives*, vol. 60, pp. 1–8, 2015.
- [155] S. Zhang, H. Gu, H. Pan et al., "A novel strategy to suppress capacity and voltage fading of Li- and Mn-rich layered oxide cathode material for lithium-ion batteries," *Advanced Energy Materials*, vol. 7, no. 6, article 1601066, 2017.
- [156] R. Gordon, R. Orias, and N. Willenbacher, "Effect of carboxymethyl cellulose on the flow behavior of lithium-ion battery anode slurries and the electrical as well as mechanical properties of corresponding dry layers," *Journal of Materials Science*, vol. 55, no. 33, pp. 15867–15881, 2020.
- [157] H. Buqa, M. Holzapfel, F. Krumeich, C. Veit, and P. Novák, "Study of styrene butadiene rubber and sodium methyl cellulose as binder for negative electrodes in lithium-ion batteries," *Journal of Power Sources*, vol. 161, no. 1, pp. 617–622, 2006.
- [158] R. Zhang, X. Yang, D. Zhang et al., "Water soluble styrene butadiene rubber and sodium carboxyl methyl cellulose binder for ZnFe_2O_4 anode electrodes in lithium ion batteries," *Journal of Power Sources*, vol. 285, pp. 227–234, 2015.
- [159] R. Jagau, F. Huttner, J. K. Mayer et al., "Influence of different alginate and carboxymethyl cellulose binders on moisture content, electrode structure, and electrochemical properties of graphite-based anodes for lithium-ion batteries," *Energy Technology*, vol. 11, no. 5, article 2200871, 2023.
- [160] F. Ma, Y. Fu, V. Battaglia, and R. Prasher, "Microrheological modeling of lithium ion battery anode slurry," *Journal of Power Sources*, vol. 438, article 226994, 2019.
- [161] J. M. Torres, C. M. Stafford, and B. D. Vogt, "Impact of molecular mass on the elastic modulus of thin polystyrene films," *Polymer*, vol. 51, no. 18, pp. 4211–4217, 2010.
- [162] L. Ma, X. Fu, F. Zhao et al., "High-performance carboxymethyl cellulose integrating polydopamine binder for silicon microparticle anodes in lithium-ion batteries," *ACS Applied Energy Materials*, vol. 6, no. 3, pp. 1714–1722, 2023.
- [163] D. Lee, H. Park, A. Goliaszewski, Y. Byeun, T. Song, and U. Paik, "In situ cross-linked carboxymethyl cellulose-polyethylene glycol binder for improving the long-term cycle life of silicon anodes in Li ion batteries," *Industrial & Engineering Chemistry Research*, vol. 58, no. 19, pp. 8123–8130, 2019.
- [164] L. Wei, C. Chen, Z. Hou, and H. Wei, "Poly (acrylic acid sodium) grafted carboxymethyl cellulose as a high performance polymer binder for silicon anode in lithium ion batteries," *Scientific Reports*, vol. 6, no. 1, article 19583, 2016.
- [165] W. Luo, X. Chen, Y. Xia et al., "Surface and interface engineering of silicon-based anode materials for lithium-ion batteries," *Advanced Energy Materials*, vol. 7, no. 24, article 1701083, 2017.
- [166] K. Feng, M. Li, W. Liu et al., "Silicon-based anodes for lithium-ion batteries: from fundamentals to practical applications," *Small*, vol. 14, no. 8, article 1702737, 2018.
- [167] Z. Karkar, D. Guyomard, L. Roué, and B. Lestriez, "A comparative study of polyacrylic acid (PAA) and carboxymethyl cellulose (CMC) binders for Si-based electrodes," *Electrochimica Acta*, vol. 258, pp. 453–466, 2017.
- [168] J. Zhang, N. Wang, W. Zhang et al., "A cycling robust network binder for high performance Si-based negative electrodes for lithium-ion batteries," *Journal of Colloid and Interface Science*, vol. 578, pp. 452–460, 2020.
- [169] C. Zhang, F. Wang, J. Han et al., "Challenges and recent progress on silicon-based anode materials for next-generation lithium-ion batteries," *Small Structures*, vol. 2, no. 6, article 2170015, 2021.
- [170] Y. Domi, H. Usui, K. Yamaguchi, S. Yodoya, and H. Sakaguchi, "Silicon-based anodes with long cycle life for lithium-ion batteries achieved by significant suppression of their volume expansion in ionic-liquid electrolyte," *ACS Applied Materials & Interfaces*, vol. 11, no. 3, pp. 2950–2960, 2019.
- [171] Y. Ma, P. Guo, M. Liu et al., "To achieve controlled specific capacities of silicon-based anodes for high-performance lithium-ion batteries," *Journal of Alloys and Compounds*, vol. 905, article 164189, 2022.
- [172] A. Casimir, H. Zhang, O. Ogoke, J. C. Amine, J. Lu, and G. Wu, "Silicon-based anodes for lithium-ion batteries: effectiveness of materials synthesis and electrode preparation," *Nano Energy*, vol. 27, pp. 359–376, 2016.
- [173] Z. Zhang, T. Zeng, C. Qu et al., "Cycle performance improvement of LiFePO_4 cathode with polyacrylic acid as binder," *Electrochimica Acta*, vol. 80, pp. 440–444, 2012.
- [174] Z. Zhang, T. Zeng, Y. Lai, M. Jia, and J. Li, "A comparative study of different binders and their effects on electrochemical properties of LiMn_2O_4 cathode in lithium ion batteries," *Journal of Power Sources*, vol. 247, pp. 1–8, 2014.
- [175] J. Sun, X. Ren, Z. Li et al., "Effect of poly (acrylic acid)/poly (vinyl alcohol) blending binder on electrochemical performance for lithium iron phosphate cathodes," *Journal of Alloys and Compounds*, vol. 783, pp. 379–386, 2019.
- [176] D. Shin, H. Park, and U. Paik, "Cross-linked poly(acrylic acid)-carboxymethyl cellulose and styrene-butadiene rubber as an efficient binder system and its physicochemical effects on a high energy density graphite anode for Li-ion batteries," *Electrochemistry Communications*, vol. 77, pp. 103–106, 2017.
- [177] J.-H. Lee, U. Paik, V. A. Hackley, and Y.-M. Choi, "Effect of poly(acrylic acid) on adhesion strength and electrochemical performance of natural graphite negative electrode for lithium-ion batteries," *Journal of Power Sources*, vol. 161, no. 1, pp. 612–616, 2006.
- [178] S. Niu, S. heng, G. Zhu et al., "Analysis on the effect of external press force on the performance of $\text{LiNi}_{0.8}\text{Co}_{0.1}\text{Mn}_{0.1}\text{O}_2$ /graphite large pouch cells," *Journal of Energy Storage*, vol. 44, article 103425, Part B, 2021.

- [179] S. Li, Y.-M. Liu, Y.-C. Zhang et al., "A review of rational design and investigation of binders applied in silicon-based anodes for lithium-ion batteries," *Journal of Power Sources*, vol. 485, article 229331, 2021.
- [180] A. Su, Q. Pang, X. Chen et al., "Lithium poly-acrylic acid as a fast Li⁺ transport media and a highly stable aqueous binder for Li₃V₂(PO₄)₃ cathode electrodes," *Journal of Materials Chemistry A*, vol. 6, no. 46, pp. 23357–23365, 2018.
- [181] Z.-J. Han, N. Yabuuchi, K. Shimomura, M. Murase, H. Yui, and S. Komaba, "High-capacity Si-graphite composite electrodes with a self-formed porous structure by a partially neutralized polyacrylate for Li-ion batteries," *Energy & Environmental Science*, vol. 5, no. 10, p. 9014, 2012.
- [182] S. Niu, M. Zhao, L. Ma et al., "High performance polyurethane-polyacrylic acid polymer binders for silicon microparticle anodes in lithium-ion batteries," *Sustainable Energy & Fuels*, vol. 6, no. 5, pp. 1301–1311, 2022.
- [183] J. Li, G. Zhang, Y. Yang et al., "Glycinamide modified polyacrylic acid as high-performance binder for silicon anodes in lithium-ion batteries," *Journal of Power Sources*, vol. 406, pp. 102–109, 2018.
- [184] P. Luo, P. Lai, Y. Huang et al., "A highly stretchable and self-healing composite binder based on the hydrogen-bond network for silicon anodes in high-energy-density lithium-ion batteries," *ChemElectroChem*, vol. 9, no. 12, article e202200155, 2022.
- [185] S. Zhang, K. Liu, J. Xie et al., "An elastic cross-linked binder for silicon anodes in lithium-ion batteries with a high mass loading," *ACS Applied Materials & Interfaces*, vol. 15, no. 5, pp. 6594–6602, 2023.
- [186] M. J. Jolley, T. S. Pathan, A. M. Wemyss et al., "Development and application of a poly(acrylic acid)-grafted styrene-butadiene rubber as a binder system for silicon-graphite anodes in Li-ion batteries," *ACS Applied Energy Materials*, vol. 6, no. 1, pp. 496–507, 2023.
- [187] J. He and L. Zhang, "Polyvinyl alcohol grafted poly (acrylic acid) as water-soluble binder with enhanced adhesion capability and electrochemical performances for Si anode," *Journal of Alloys and Compounds*, vol. 763, pp. 228–240, 2018.
- [188] J. He, L. Zhang, and H. Zhong, "Enhanced adhesion and electrochemical performance of Si anodes with gum arabic grafted poly(acrylic acid) as a water-soluble binder," *Polymer International*, vol. 70, no. 12, pp. 1668–1679, 2021.
- [189] M. Sun, H. Zhong, S. Jiao, H. Shao, and L. Zhang, "Investigation on carboxymethyl chitosan as new water soluble binder for LiFePO₄ cathode in Li-ion batteries," *Electrochimica Acta*, vol. 127, pp. 239–244, 2014.
- [190] J. He, J. Wang, H. Zhong, J. Ding, and L. Zhang, "Cyanoethylated carboxymethyl chitosan as water soluble binder with enhanced adhesion capability and electrochemical performances for LiFePO₄ cathode," *Electrochimica Acta*, vol. 182, pp. 900–907, 2015.
- [191] N. Yu, J. Ke, L. Li, and Y. Bi, "Encapsulating carboxymethyl substituted chitosan on LiNi_{0.5}Mn_{1.5}O₄ cathode for enhanced charge/discharge performances," *Electrochimica Acta*, vol. 443, article 141903, 2023.
- [192] K. K. Rajeev, W. Jang, S. Kim, and T.-H. Kim, "Chitosan-grafted gallic acid as a nature-inspired multifunctional binder for high-performance silicon anodes in lithium-ion batteries," *ACS Applied Energy Materials*, vol. 5, no. 3, pp. 3166–3178, 2022.
- [193] P. Tang, T. Zheng, L. Shen, and G. Li, "Properties of bovine type I collagen hydrogels cross-linked with laccase-catalyzed gallic acid," *Polymer Degradation and Stability*, vol. 189, article 109614, 2021.
- [194] S. Dhiman and G. Mukherjee, "Prospects of bacterial tannase catalyzed biotransformation of agro and industrial tannin waste to high value gallic acid," in *Biorefinery Production Technologies for Chemicals and Energy*, pp. 129–143, Wiley, 2020.
- [195] M.-H. Ryou, S. Hong, M. Winter, H. Lee, and J. W. Choi, "Improved cycle lives of LiMn₂O₄ cathodes in lithium ion batteries by an alginate biopolymer from seaweed," *Journal of Materials Chemistry A*, vol. 1, no. 48, article 15224, 2013.
- [196] Y. Gu, S. Yang, G. Zhu et al., "The effects of cross-linking cations on the electrochemical behavior of silicon anodes with alginate binder," *Electrochimica Acta*, vol. 269, pp. 405–414, 2018.
- [197] R. Ahmad Raus, W. M. F. Wan Nawawi, and R. R. Nasaruddin, "Alginate and alginate composites for biomedical applications," *Asian Journal of Pharmaceutical Sciences*, vol. 16, no. 3, pp. 280–306, 2021.
- [198] I. Kovalenko, B. Zdyrko, A. Magasinski et al., "A major constituent of brown algae for use in high-capacity Li-ion batteries," *Science*, vol. 334, no. 6052, pp. 75–79, 2011.
- [199] L. Rao, X. Jiao, C.-Y. Yu et al., "Multifunctional composite binder for thick high-voltage cathodes in lithium-ion batteries," *ACS Applied Materials & Interfaces*, vol. 14, no. 1, pp. 861–872, 2022.
- [200] J. Hu, Y. Wang, D. Li, and Y.-T. Cheng, "Effects of adhesion and cohesion on the electrochemical performance and durability of silicon composite electrodes," *Journal of Power Sources*, vol. 397, pp. 223–230, 2018.
- [201] S. Komaba, K. Shimomura, N. Yabuuchi, T. Ozeki, H. Yui, and K. Konno, "Study on polymer binders for high-capacity SiO negative electrode of Li-ion batteries," *The Journal of Physical Chemistry C*, vol. 115, no. 27, pp. 13487–13495, 2011.
- [202] S. Komaba, T. Ozeki, and K. Okushi, "Functional interface of polymer modified graphite anode," *Journal of Power Sources*, vol. 189, no. 1, pp. 197–203, 2009.
- [203] S. Komaba, K. Okushi, T. Ozeki et al., "Polyacrylate modifier for graphite anode of lithium-ion batteries," *Electrochemical and Solid-State Letters*, vol. 12, no. 5, article A107, 2009.
- [204] Z. Li, G. Wu, Y. Yang et al., "An ion-conductive grafted polymeric binder with practical loading for silicon anode with high interfacial stability in lithium-ion batteries," *Advanced Energy Materials*, vol. 12, no. 29, article 2201197, 2022.
- [205] J. Liu, Q. Zhang, T. Zhang, J.-T. Li, L. Huang, and S.-G. Sun, "A robust ion-conductive biopolymer as a binder for Si anodes of lithium-ion batteries," *Advanced Functional Materials*, vol. 25, no. 23, pp. 3599–3605, 2015.
- [206] M. Wang, Q. Tan, L. Liu, and J. Li, "A facile, environmentally friendly, and low-temperature approach for decomposition of polyvinylidene fluoride from the cathode electrode of spent lithium-ion batteries," *ACS Sustainable Chemistry & Engineering*, vol. 7, no. 15, pp. 12799–12806, 2019.
- [207] M. Ghahramani, S. Hamidi, M. Mohammad, M. Javanbakht, and P. Gorji, "The effect of sulfonated copolymer as a binder on the electrochemical performance of LiFePO₄ cathode for

- lithium-ion batteries,” *Journal of Electroanalytical Chemistry*, vol. 936, article 117342, 2023.
- [208] X. Qiu, W. Li, S. Zhang, H. Liang, and W. Zhu, “The microstructure and character of the PVDF-g-PSSA membrane prepared by solution grafting,” *Journal of The Electrochemical Society*, vol. 150, no. 7, article A917, 2003.
- [209] L. Yue, L. Zhang, and H. Zhong, “Carboxymethyl chitosan: a new water soluble binder for Si anode of Li-ion batteries,” *Journal of Power Sources*, vol. 247, pp. 327–331, 2014.